ALMA MATER STUDIORUM - UNIVERSITÀ DI BOLOGNA

SCHOOL OF ENGINEERING AND ARCHITECTURE

DEPARTMENT OF CIVIL, CHEMICAL, ENVIRONMENTAL AND MATERIALS ENGINEERING

MASTER'S DEGREE IN CHEMICAL AND PROCESS ENGINEERING SUSTAINABLE TECHNOLOGIES AND BIOTECHNOLOGIES FOR ENERGY AND MATERIALS

THESIS

In
Materials Chemistry M

EXTRACTION OF ANTIOXIDANTS FROM CORN BY-PRODUCTS FOR APPLICATIONS IN BIO-BASED POLYMER MATRICES

CANDIDATE
Lorenzo Boscolo

SUPERVISOR:
Prof.ssa Annamaria Celli

CO-SUPERVISORS:
Prof.ssa Laura Sisti
Prof. Haroutioun Askanian

Academic Year 2019/2020

Session III

EXTRACTION OF ANTIOXIDANTS FROM CORN BY-PRODUCTS FOR APPLICATIONS IN BIO-BASED POLYMER MATRICES

Introduction

Corn, also known as maize, is a grain plant, mainly cultivated for food, and it is one of the largest and most important crops in the world. Over the last years, corn farmers experienced a noticeable increase in annual revenues. As it stands nowadays, United States are the largest producers and exporters of corn, with a production in $2019/2020$ of $3.46 \times 10^8\ tons$, and European Union assessing the fourth place, with over 66 million tons[1].

Corn is mostly processed via a wet milling technique, to produce several important goods. The most abundant of these is starch, but also oil can be obtained. At the end of the processing, from one hundred pounds of dry corn, about 67 pounds of starch are produced, as well as 3.6 pounds of oil and 29.4 pounds of by-products. Considering overall production, this 30% of discarded by-products makes up to a considerable amount. Until now, there are no relevant developed routes to exploit these by-products, even if on literature some studies are done concerning their antimicrobial and antioxidant activities[2], the opportunity to extract amorphous silica[3], as well as the possibility to produce bio-composites[4].

Therefore, the corn processing by-products could be exploited in a better way.

The most promising process seems the extraction of antioxidants, so the focus of this project is to identify their content in corn cobs and corn leaves. Once the antioxidants have been extracted, they can be inserted in bio-based polymer matrices, such as polybutylene succinate (PBS), polybutylene succinate–co–adipate (PBSA) and polybutylene adipate terephthalate (PBAT), with the aim to enhance their performances by decreasing degrading effects due to external agents. In this way, bio-based polymers can be improved in their characteristics and keeping the fundamental quality of being fully composed by natural and bio-derived materials.

---

[1] https://www.statista.com/statistics/254292/global-corn-production-by-country/

[2] Cruz, J. M. *et al.* (2001) 'Antioxidant and antimicrobial effects of extracts from hydrolysates of lignocellulosic materials', *Journal of Agricultural and Food Chemistry*, 49 (5), pp. 2459–2464.

[3] Okoronkwo, E. A. *et al.* (2016) 'Development of Silica Nanoparticle from Corn Cob Ash', *Advances in Nanoparticles*, 5 (2), pp. 135–139.

[4] Yeng, C. M., Husseinsyah, S. and Ting, S. S. (2013) 'Chitosan/corn cob biocomposite films by cross-linking with glutaraldehyde', *BioResources*, 8 (2), pp. 2910–2923.

SUMMARY

1. Overview of possible uses of corn by-products

In recent times, an increasing interest has been shown concerning the ways of reuse and recycle of corn by-products, which form an incredibly high amount of wastes. There are two main parts of corn which are discarded:

- corn cob, which is the central portion of the corn, and is composed by cellulose ($40-45\ wt\%$), hemicellulose ($30-35\ wt\%$) and lignin ($10-20\ wt\%$);
- corn stover, made by the ensemble of roots, leaves and stalks, and is composed again by cellulose ($40-45\ wt\%$), hemicellulose ($20-25\ wt\%$) and lignin ($10-15\ wt\%$).

Several approaches have been considered, regarding the possibility to extract different materials and stabilisers from the by-products themselves, as well as the opportunity to use them for the production of bio-based polymers or composites. The most promising directions are the following:

- extraction of antioxidants, which can subsequently be used to stabilise biopolymers;
- extraction of xylan, which is the third most abundant biopolymer on Earth and shows promising characteristics for drug delivery and many other applications;
- extraction of silica, obtained by a sol-gel process in the form of amorphous nanoparticles;
- formation of bio-composites, both using xylan and corn cobs themselves;
- introduction in bio-based agricultural mulch films.

1.1. Antioxidants[5]

1.1.1. Antioxidant compounds and their mechanism

An antioxidant is defined as a substance that, at low concentrations, delays or prevents the oxidation of a substrate. Antioxidants act through three fundamental mechanisms:

a) hydrogen atom transfer (HAT);
b) single electron transfer (SET);
c) ability to chelate metals.

HAT[6] is a chemical transformation consisting in the concerted movement of two elementary particles, a proton and an electron, between two substrates in a single kinetic step, as reported in Scheme 1.

[5] Francenia Santos-Sánchez, N. *et al.* (2019) 'Antioxidant Compounds and Their Antioxidant Mechanism', *Antioxidants*, IntechOpen, chap. 2, pp. 1-20.

[6] Capaldo, L. and Ravelli, D. (2017) 'Hydrogen Atom Transfer (HAT): A Versatile Strategy for Substrate Activation in Photocatalyzed Organic Synthesis', *European Journal of Organic Chemistry*, 2017 (15), pp. 2056–2071.

$$A_1 - H + A_2^{\cdot} \rightarrow A_1^{\cdot} + A_2 - H$$

Scheme 1: *HAT mechanism*

Several research groups are developing suitable models to explain HAT mechanism, as well as to predict the rates at which these processes occur. HAT is relevant in many different fields, being a key step in a wide variety of chemical reactions, such as aerobic oxidations and combustion of hydrocarbons. In biology, several enzymes are known to operate through a HAT process, fundamental for the decomposition of reactive oxygen species.

An SET[7] reaction is imitated by single-electron transfer from the nucleophile to the substrate, producing a radical intermediate, as reported in Scheme 2. In this mechanism, the antioxidant provides an electron to the free radical and itself becomes a radical cation.

$$A^{\cdot} + B{:}H \xrightarrow{-e^-} A{:}^- + B \cdot H^+$$

Scheme 2: *SET mechanism*

In biological systems, an oxidative stress may occur. This happens when there is an imbalance between the production of free radicals and the ability of the body to eliminate these highly reactive species through antioxidants. During metabolic reactions, a relevant amount of reactive oxygen species (ROS) is formed, and an excess of these may cause severe problems, such as cardiovascular diseases or even the promotion of cancer. Biological systems have an important resource of endogenous antioxidants, mostly enzymes, to reduce the concentration of ROS. If this is no longer possible, the organism must rely on external sources of antioxidants, supplied through food or pharmaceuticals. Some of the main antioxidants will be analysed in the following paragraphs.

[7] Liang, N. and Kitts, D. D. (2014) 'Antioxidant property of coffee components: Assessment of methods that define mechanism of action', *Molecules*, 19 (11), pp. 19180–19208.

Phenolic compounds

The phenolic compounds constitute a wide group of chemical substances, more than 8000 compounds, which have the capacity to act as hydrogen donors or to chelate metal ions, such as copper and iron. These characteristics are associated with a decrease in risks of neurodegenerative diseases and cardiovascular diseases. Phenolic compounds reduce or inhibit free radicals by transfer of a hydrogen atom from its hydroxyl group. The reaction mechanism with a peroxyl radical ($ROO^{\cdot}$) involves a transfer of the hydrogen cation from the phenol to the radical, forming a transition state of an $O-H$ bond with one electron. Their antioxidant capacity is strongly reduced when the reaction medium consists of a solvent prone to the formation of hydrogen bonds with the phenolic compounds. For example, alcohols have a double effect: on one hand, they act as acceptors of hydrogen bond, on the other hand they favour the ionisation of phenols into phenoxides, which can react rapidly with the peroxide radicals, through an electron transfer. From a study of Leopoldini *et al.*[8], it was possible to demonstrate that different phenolic compounds act with different mechanisms. The compounds most likely to undergo a HAT are reported in Figure 1. They were found to be tocopherol, hydroxytyrosol, gallic acid, caffeic acid and epicatechin, while the phenolic compounds better able to perform an SET mechanism, reported in Figure 2, were kaempferol and resveratrol.

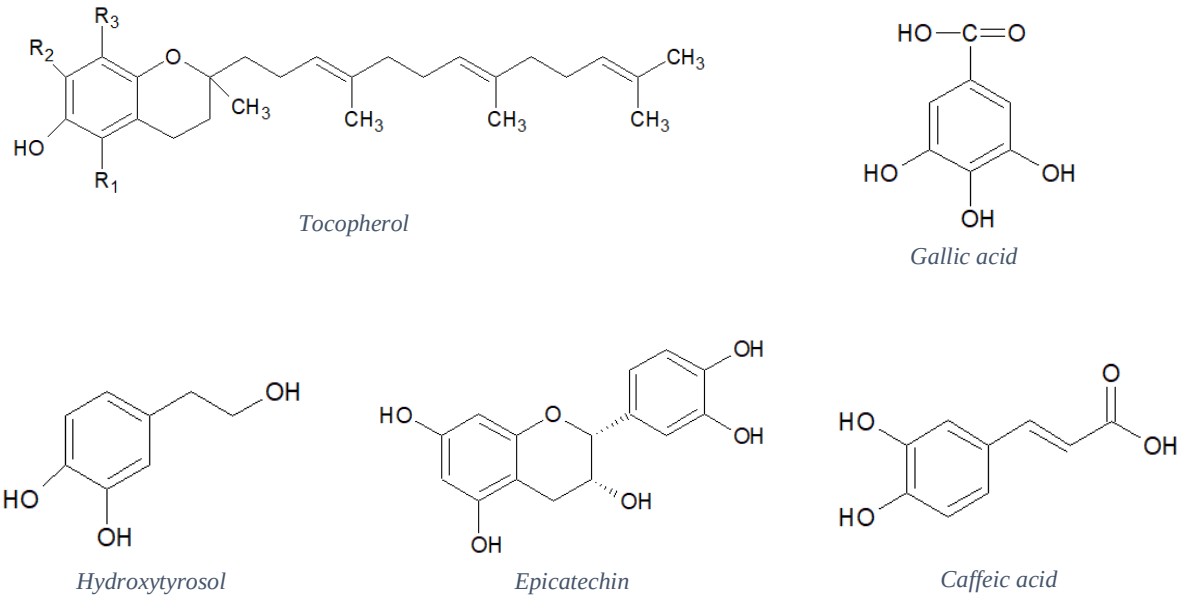

Figure 1: *Phenols undergoing HAT mechanism*

[8] Leopoldini, M. *et al.* (2004) 'Antioxidant properties of phenolic compounds: H-atom versus electron transfer mechanism', *Journal of Physical Chemistry A*, 108 (22), pp. 4916–4922.

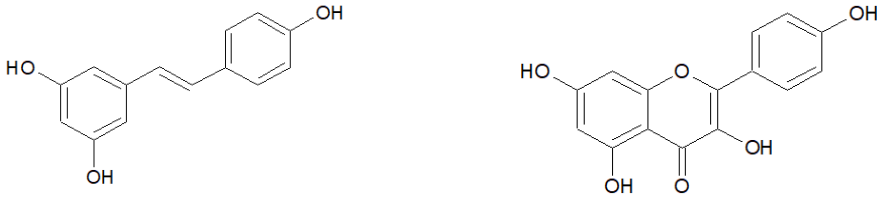

Resveratrol *Kaempferol*

Figure 2: *Phenols undergoing SET mechanism*

Carotenoids

Carotenoids are found virtually in all plants, animals, and microorganisms, and more than 700 compounds have been identified. An example of carotenoid is β −carotene, reported in Figure 3. They are characterised by a general base fragment, known as tetraterpene, with the presence of conjugated double bonds. These insaturations are responsible for the absorption of specific wavelengths, giving them a yellow – red colouration. These compounds, other than conferring pigmentation, fulfil other important functions, mainly as antioxidants. Carotenoids react as antioxidant through three mechanisms: by SET, by formation of one adduct, and by HAT. In general, their antioxidant properties are related to the high capacity for electron donations.

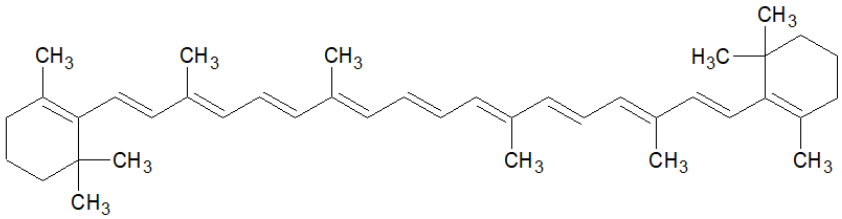

Figure 3: β *−carotene*

Vitamin C

Vitamin C refers to a group of analogues of the ascorbic acid, that can be both natural and synthetically produced. Ascorbic acid is mostly present as anion ascorbate at physiological pH, and ascorbate is a powerful reducing agent undergoing two subsequent losses of an electron. The radical is relatively stable, due to the resonance of the electron (see Scheme 3). Vitamin C is chemically capable of reacting with most of the relevant ROS and acts as a hydrosoluble antioxidant. The reaction mechanism is based on the HAT to peroxyl radicals, the inactivation of the singlet oxygen, and the elimination of molecular oxygen. It has also been proven that ascorbate can produce reactions with oxidising agents through SET or a concerted transfer of electrons/protons (SET/HAT).

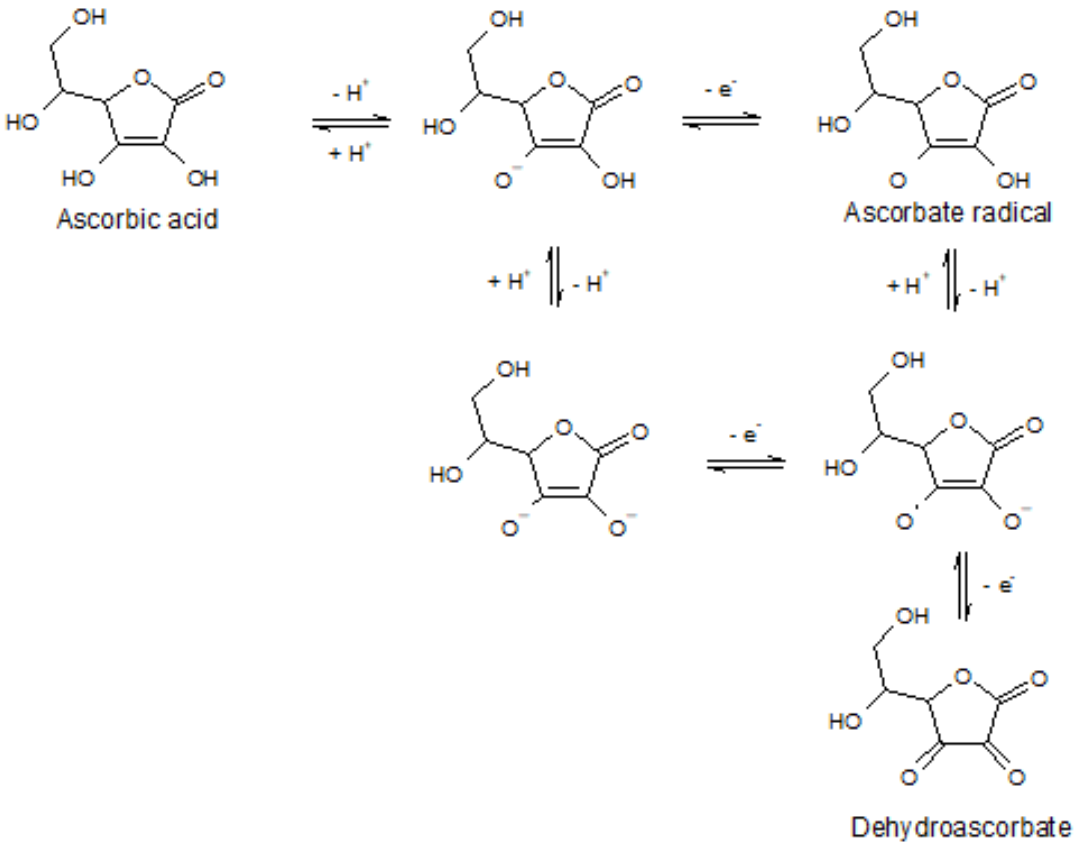

Scheme 3: *Ascorbic acid and formation of its stable radicals*

1.1.2. Main methods to evaluate antioxidant activity

Antioxidant activity cannot be measured directly, but it is determined by the effects of the antioxidant to control the degree of oxidation. The most used tests are:

- inhibition of $2,2-diphenyl-1-picrylhydrazyl\ radical$ (DPPH) (Figure 4) → this is a colorimetric method, operating both with SET and HAT mechanisms. It is based on the measurement of the scavenging capacity of antioxidants towards DPPH.

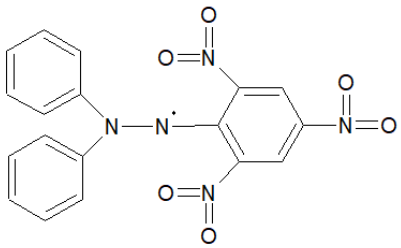

Figure 4: *DPPH radical*

The DPPH radical is characterised as a stable free radical due to the fact that π electrons of the aromatic system can compensate for the lack of an electron. The delocalisation also gives rise to a deep violet colour, characterised by absorption at around $\lambda_{MAX} = 517\ nm$. When a solution of DPPH radical is in contact with a substance that can donate a hydrogen atom, the reduced form is produced, with subsequent colour loss.

Consequently, the reduction of DPPH provides an index to estimate the ability of the test compound to trap radicals. The experimental models use the percentage of DPPH remaining to obtain the necessary quantities that are required to reduce the initial concentration to 50 % (EC_{50}). This method is generally fast, simple, inexpensive, and widely used to measure the ability of compounds to act as free radical scavengers or as hydrogen donors. It can also be used to quantify the antioxidants in complex biological systems, for solid or liquid samples. The method allows for a reaction with almost any type of antioxidant due to the stability of DPPH itself, even for weak antioxidants, and it can be used with both polar and nonpolar organic solvents. It still has some disadvantages, among which is that DPPH can react with other radicals and consequently the time needed to reach steady state is not linear with the concentration of the antioxidant. The stability of DPPH radical can be decreased by solvents with the properties of a Lewis base, as well as the presence of dissolved oxygen. Moreover, the absorbance of DPPH is lower in methanol and acetone than with other solvents.

- total phenols assay by Folin – Ciocalteu reagent → useful for SET mechanism, the test is realised by a mixture of phosphomolybdate and phosphotungstate in a highly basic medium.

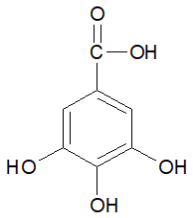

Figure 5: *Gallic acid*

This technique is useful to evaluate the content of phenolic and polyphenolic compounds in the sample analysed. A calibration curve is needed, and gallic acid, reported in Figure 5, is used as a reference. Given this, the result is obtained as gallic acid equivalents (GAE), with a final value expressed as mg_{GAE}/g_{SAMPLE}. The calibration curve is obtained by analysing standard solutions of gallic acid at different concentrations, at a wavelength of $\lambda_{MAX} = 765\ nm$. The samples can then be observed at the same wavelength, relating the absorbance retrieved to the concentration of gallic acid.

- ferric-reducing antioxidant power (FRAP) → this assay deals with SET reaction mechanism, and it is a colorimetric method that evaluates the reduction of $Fe^{3+} - tripyridyltriazine$ complex (Figure 6) to a ferrous form (Fe^{2+}).

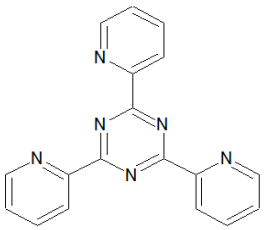

Figure 6: *2, 4, 6 – tripyridyl – s – triazine*

The FRAP analysis was introduced to measure total antioxidant activity, and it is based on the ability of samples to reduce ferric ions to ferrous ions, forming a blue complex. A high absorption wavelength of $700\ nm$ indicates a high reduction power of the chemical compound under analysis. The most used method regards the reduction of the complex to $2{,}4{,}6 - tripyridyl - s - triazine - Fe^{2+}$ ($TPTZ - Fe^{2+}$). An antioxidant reduces the ferric compound to the ferrous one, forming a complex which absorbs at $\lambda_{MAX} = 590\ nm$. The reducing power is related to the degree of hydroxylation and the conjugation in phenols.

- total antioxidant capacity → this test too deals with SET reactions. It is used to measure the peroxide level during the initial stage of lipid oxidation. Peroxides are formed during the linoleic acid oxidation, which reacts with Fe^{2+} to form Fe^{3+} and later these ions form a complex with thiocyanate.

TAC is defined as the ability of a compound to inhibit the oxidative degradation of lipids. This peroxidation, called initiation process, begins with the formation of conjugated dienes and trienes, known as primary oxidation products. Subsequently, a propagation process is carried out: it consists in the reaction of deprotonated species from the lipids with molecular oxygen, leading to the formation of peroxyl radicals. The high energy of free radicals promotes the abstraction of hydrogen from neighbouring fatty acids. This gives the formation of hydroperoxides, which promotes the formation of new radicals. To encourage the antioxidant activity, it is necessary to inhibit the peroxidation of a fatty acid emulsion. Linoleic acid, reported in Figure 7, is generally used as a model. The hydroperoxides derived from linoleic acid react with Fe^{2+}, causing the oxidation to Fe^{3+}.

The ferric ion forms a complex with thiocyanate, which has a maximum absorbance at $\lambda_{MAX} = 500\ nm$. This complex is then used to measure the peroxide value.

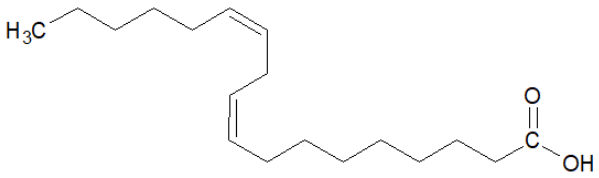

Figure 7: *Linoleic acid*

1.1.3. Effect of antioxidants in polymer matrices

When exposed to radiation, excessive heat and corrosive environment, polymers' structure will change. These changes are the result of oxidative degradation caused by free radicals, which form through hydrogen abstraction or homolytic scission of carbon – carbon bonds when polymers are exposed to heat, oxygen, ozone, or light.

To prevent slow degradation, antioxidants and UV stabilisers are often added. The two main classes of antioxidants are free-radical scavengers (primary antioxidants) and peroxide scavengers (secondary antioxidants).

- *Primary antioxidants*

This class of antioxidants react with chain-propagating radicals, such as peroxyl, alkoxy and hydroxy radicals in a chain-terminating reaction. More in detail, these antioxidants donate hydrogen to the above-mentioned radicals, converting them into non-reacting species (water, alcohols, …).

Typical primary antioxidants are hindered phenols, which may come in a wide range of molecular weights, structures, and functionalities. The most widely used antioxidants are sterically hindered phenols, which are every effective radical scavengers during both processing and long-term thermal ageing. These compounds are able to convert peroxyl radicals to hydroperoxides, thus inhibiting the autooxidation of organic polymers by reducing the amount of peroxyl radicals. An example of the mechanism, considering $butylated\ hydroxytoluene\ (BHT)$, is shown in Scheme 4.

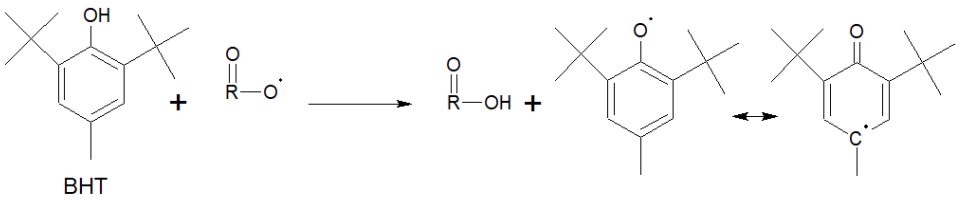

Scheme 4: *Antioxidative mechanism of BHT*

The resulting oxytoluene radicals are stabilised by electron delocalisation, as well as by the cumbersome substituents, increasing the steric hindrance. These two factors greatly reduce the reactivity of these radicals, preventing them from further reactions with the polymeric chains. Instead, the oxytoluene radicals are able to undergo a bimolecular reaction that produces another BHT molecule and a $para-quinomethane$, or can undergo an irreversible reaction with a second peroxyl radical which thermally decomposes to $para-quinone$ (Scheme 5).

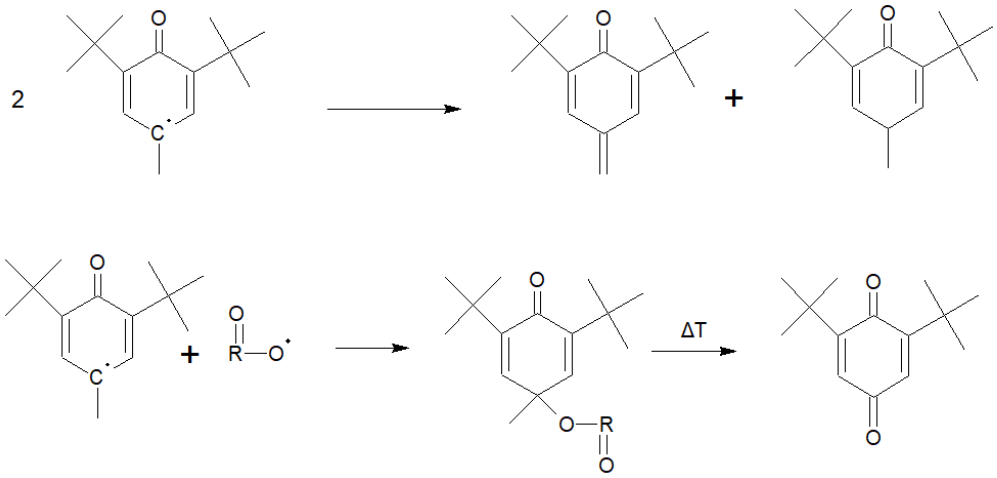

Scheme 5: *Oxytoluene bimolecular reactions*

Thus, each BHT molecule can react with two peroxyl radicals to form products which are much more stable to further reactions. Recombination of two oxytoluene radicals is also possible, giving rise to a quinonoid structure. Actually, BHT is only one among the many sterically hindered phenols. Other relevant molecules include those reported in Figure 8.

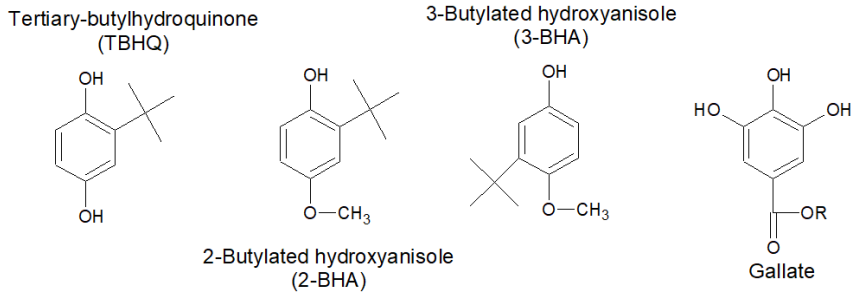

Figure 8: *Most relevant sterically hindered phenols*

The most effective primary antioxidants are secondary aromatic amines, but they cause noticeable discolouration, and can only be used if this is not an issue. They also function as antiozonants and metal ion deactivators.

- *Secondary antioxidants*

This family of compounds, also known as peroxide scavengers, decompose hydroperoxides ($ROOH$) into nonreactive products before they are able to decompose into alkoxy or hydroxy radicals. They are often used in combination with primary antioxidants, to achieve a synergistic inhibition effect. The most common secondary antioxidants are trivalent phosphorus compounds, which reduce hydroperoxides to the corresponding alcohol and are transformed themselves into phosphates. The general mechanism is shown in Scheme 6.

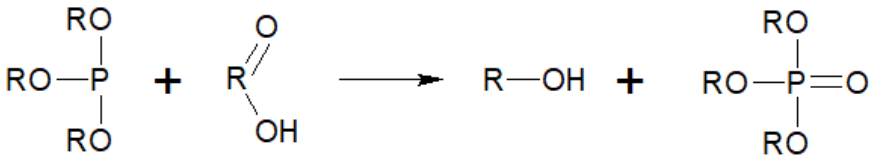

Scheme 6: *Antioxidative effect of trivalent phosphorus compounds*

Another class of secondary antioxidants is represented by thioethers, or organic sulphides. They are able to decompose two molecules of hydroperoxide into the corresponding alcohols, and are transformed to sulphoxides and sulphones, as demonstrated in Scheme 7.

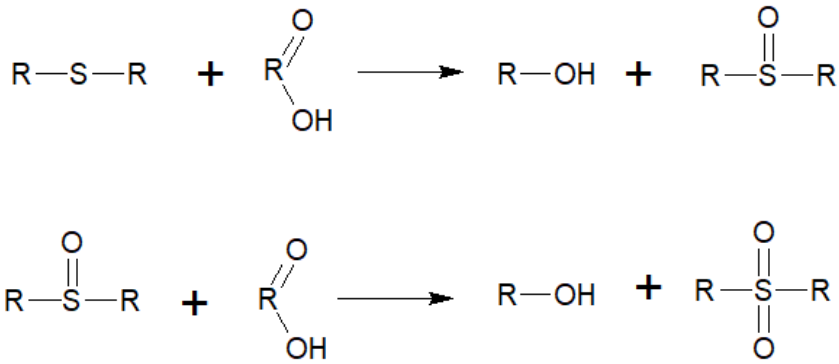

Scheme 7: *Antioxidative effect of thioethers*

Organic sulphides are very effective hydrogen peroxide decomposers during long-term thermal ageing and are often used in combination with other antioxidants that provide good protection during processing. In general, a good stabiliser package should protect the plastic during both processing, where high temperatures might be reached, especially during the melting step, and during lifetime, when exposed to their upper service temperature.

1.2. Antioxidant activity in corn by-products

The most promising application for corn by-products regards the extraction of antioxidants and phenolic compounds, representing the most important secondary metabolites. These products can be used to decrease diseases linked to the presence of reactive oxygen species, such as cardiovascular diseases, cancer, and immune system decline, as well as the possibility to introduce them in bio-based polymer matrices to enhance their performances against thermal and UV degradation, slowing down these disruptive processes.

The main obstacle to overcome is to find an efficient way of extraction of these compounds, utilising different solvents or extraction methods (microwave-assisted extraction, Soxhlet apparatus, …). Once the antioxidants are retrieved, the subsequent step is to quantify and characterise them, in order to assess the possibility of using them as bio-based additives in polymer matrices. Several studies have been performed to understand the antioxidant, antiproliferative and antimicrobial capacities of corn by-products, and the most relevant will be reported in the following paragraphs.

1.2.1. Evaluation of antioxidant activity and phenolic content of corn by-products

The first step in all the procedures is to find a suitable way to extract these components from the corn by-product. This means both selecting a solvent and choosing an appropriate method, able to consent a noticeable yield without damaging the natural components. The main used solvents are ethanol and methanol, in different ratios with water (generally $50\%\ v/v$ and $80\%\ v/v$), but some literature can be found in which ethyl acetate, acetone and n-hexane are used.

Regarding the extraction method, several approaches have been used. The most common[9] concerns the soaking of powdered samples in a certain amount of the selected solvent for 24 hours, with subsequent filtration and concentration under a rotary evaporator. On the so-obtained extracts, different tests and assays are performed, to assess the content of phenolic compounds (TPC, through the Folin-Ciocalteu method), flavonoid and ketosteroid compounds, and to test the DPPH antioxidant activity. The antioxidant activity can be established also with the tests reported in Paragraph 1.1.2, but the DPPH assay is found to be the most efficient, fast, and inexpensive of them all.

With the above-mentioned procedure, the best results are obtained with $50\%\ v/v$ and $80\%\ v/v$ of ethanol-water as solvent.

[9] Dong, J. *et al.* (2014) 'Antioxidant activities and phenolic compounds of cornhusk, corncob and stigma maydis', *Journal of the Brazilian Chemical Society*, 25(11), pp. 1956–1964.

1.2.2. Anticoagulant and antimicrobial effect of xylan[10]

Xylan is a group of hemicelluloses that represents the third most abundant biopolymer on Earth. It can be virtually found in any plant and is composed by polysaccharides made up of $\beta - 1{,}4 -$linked xylose, with residual side branches of $\alpha - arabinofuranose$ and $\alpha - glucaronic\ acids$. The general structure is reported in Figure 9.

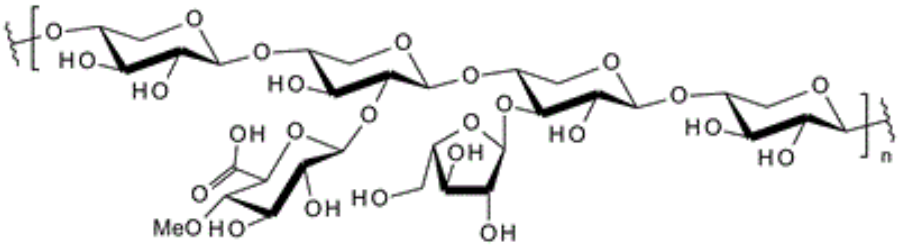

Figure 9: *Xylan chemical structure*

Corn cobs contain a considerable reservoir of xylan-type hemicelluloses, in two different types:

- low-branched arabinoglucuronoxylan, which is water insoluble;
- high-branched heteroxylan, which is water soluble.

Using a methodology that combines alkaline extraction and ultrasonication, water-soluble xylan is obtained, with a yield of $40 \pm 5\%\ (w/w)$. The ultrasonic bath consents to enhance the extraction yield by a mechanical disruption of the cell walls, as well as the rupture of inter- and intramolecular xylan bonds.

Melo-Silveira *et al*. reported the use of xylan as antiproliferative additive. In fact, recent studies regard the development of compounds able to inhibit or delay tumour cells proliferation without affecting normal cells. Xylan proved to be effective against *HeLa* tumour cells, in concentration-dependant way, while it showed no effect on *3T3* fibroblast cells. *HeLa* cells are part of an immortalised line, which is the oldest and most commonly used human cell, since they were found to be remarkably durable and prolific, thus very keen to be used in laboratory studies. *3T3* are fibroblast cells, and their name refers to "3-days transfer, inoculum 3×10^5 cells", originally established from the primary mouse embryonic fibroblast cells.

[10] Melo-Silveira, R. F. *et al.* (2012) 'In vitro antioxidant, anticoagulant and antimicrobial activity and in inhibition of cancer cell proliferation by xylan extracted from corn cobs', *International Journal of Molecular Sciences*, 13 (1), pp. 409–426.

As reported in Figure 10, the proliferation of *HeLa* cells (dashed line) decreases with the increment of xylan concentration, while *3T3* proliferation (continuous line) is unaffected by the presence of the biopolymer.

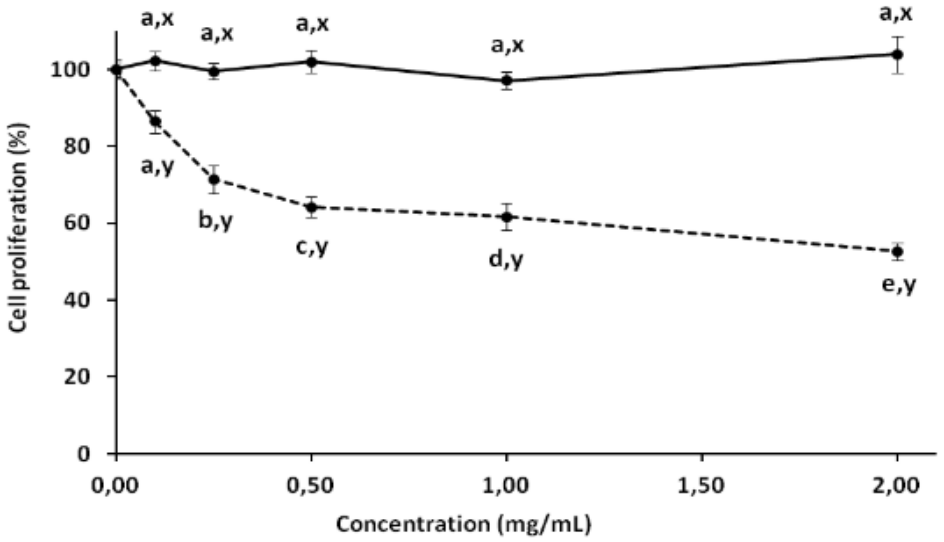

Figure 10: *Effect of xylan concentration on HELA tumoral cells (dashed line) and on fibroblast 3T3 cells (continuous line)*

1.2.3. New ways of xylan exploiting

Colon-specific drug delivery system[11]

An important characteristic of the water-insoluble xylan is the ability to maintain its structure in the physiological stomach environment, as well as in the intestine. This property makes xylan a suitable material for medical applications, in particular for colon-related drug delivery systems.

This possibility is of fundamental importance, since the location of colon requires a specific approach for drug delivery, which should avoid the release in the stomach and the intestine.

Oliveira *et al*. studied the recovery of insoluble xylan, and they reported that first samples are grinded and soaked in water for 24 hours. Subsequently, they are treated with a 1.3 % (v/v) solution of sodium hypochlorite, to remove the impurities, and then again with an alkaline solution (4% (v/v) $NaOH$). The extract is neutralised with acetic acid, then xylan is separated by precipitation after

[11] Oliveira, E. E. *et al.* (2010) 'Xylan from corn cobs, a promising polymer for drug delivery: Production and characterization', *Bioresource Technology*, 101 (14), pp. 5402–5406.

methanol addition. Several washing steps are needed, then the samples are filtered, dried at $50\ °C$ and characterised through particle size analysis, NMR spectroscopy, FT-IR, and flow analysis.

***Wound management aid*[12]**

In these last years, a relevant complex polysaccharide has gained relevance: branan ferulate. This polymer can be seen as a highly substituted xylan, which can still be obtained from an alkaline extraction of corn brans. In presence of water, this biopolymer forms a hydrogel, making it suitable as a wound management aid.

Hydrogels/xerogels are defined as a three-dimensional network of hydrophilic polymer chains, where at least 20% of weight is retained by water. Hydrogels swell and shrink as water level changes, but if water is completely removed the structure collapses, giving rise to a xerogel. This process is reversible, so the hydrogel can be formed again. To maintain its structure, polymer chains are cross-linked, either by covalent bonds or by electrostatic, hydrophilic or Van der Waals forces. These materials can be manufactured in a way to make them flexible, durable, non-antigenic and permeable to water vapour and metabolites, whilst covering the wound from bacteria.

Another type of wound management aid are hydrocolloids. These materials are produced with a multilayer structure, consisting of a protective outer layer and a backing material which may be a film, foam, or fibre, onto which is laminated a composite consisting of an adhesive and some hydrophilic particles. Generally, the backing material is made by non-woven polyester fibres and semipermeable polyurethan films, while the hydrophilic particles may contain polyurethan gels and polysaccharides, such as cellulose derivatives.

[12] Lloyd, L. L. *et al.* (1998) 'Carbohydrate polymers as wound management aids', *Carbohydrate Polymers*, 37 (3), pp. 315–322.

Flocculant for dyes[13]

As investigated by Liu *et al.* phosphorylated xylan can be employed for isolating cationic dyes. They extracted the xylans from birchwood in alkali conditions, the influence of time, temperature, and molar ratio of trisodium trimetaphosphate (STMP) to xylan on the degree of substitution (DS) and on charge density were also studied. Then, the characteristics of the so-produced phosphorylated biopolymer was evaluated by assessing its performances as a flocculant in isolating cationic dye segments from an ethyl violet dye.

They produced solutions at different concentrations by dissolving the dye in deionised water, and adjusting the pH as needed by adding HCl or $NaOH$. Then, different amounts of phosphorylated xylan solution were added to the dyes, subsequently subjected to stirring, centrifugation and filtering. The concentrations before and after xylan addition were measured via a UV spectrophotometer at $\lambda_{MAX} = 596\ nm$, evaluating the dye removal as reported in Equation 1, where C_0 is the initial concentration of the dye and C is the concentration of the dye at different times.

$$Dye\ removal\ (\%) = \frac{C_0 - C}{C_0} \times 100$$

Equation 1: *Evaluation of dye removal percentage*

[13] Liu, Z. *et al.* (2018) 'Preparation and application of phosphorylated xylan as a flocculant for cationic ethyl violet dye', *Polymers*, 10 (3), 317.

Both the time, the temperature, and the molar ratio of xylan/STMP showed similar effects on the analysed properties.

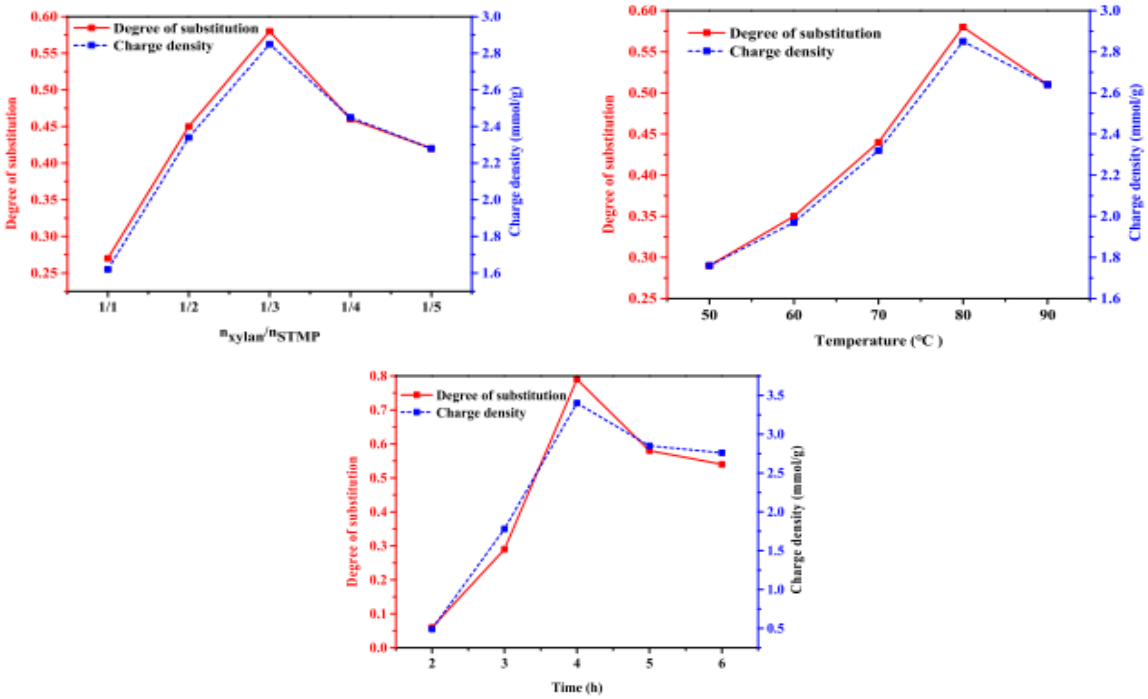

Figure 11: *Effects of molar ratio, temperature and time*

As shown in Figure 11, increasing each one of these variables brings an increase on the degree of substitution and on the charge density, until a peak is reached.

The initial concentration of the violet dye varies between 40 mg/L and 120 mg/L, and a rise of the initial content of dye results in an increased optimal xylan concentration, as shown in Figure 12.

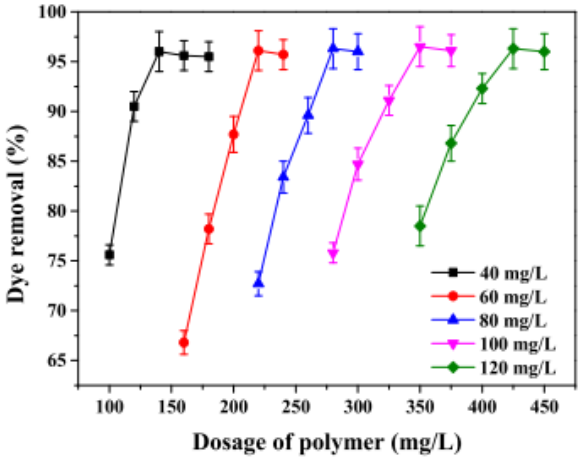

Figure 12: *Optimal concentration of xylan for different concentrations of violet dye*

Formation of biobased films[14]

Peng *et al.* demonstrated that xylan could be employed also as a biobased film. In their study, xylan was isolated from bamboo plants, through a suspension in $NaOH$ 10%. After filtration, dialysis, concentration and freeze-drying, polypropylene oxide was grafted on the xylan chain via a ring-opening polymerisation, initiated by aluminium iso-propoxide $(Al(O-i-Pr)_3)$. Then, the biopolymer was subjected to a carboxymethylation, by formation of a suspension with $50\,mL$ of isopropanol-water $(70-30\ v/v)$, sodium chloroacetate and sodium hydroxide. The final product was dissolved with chitosan, a linear polysaccharide composed of randomly distributed $\beta-1,4-$linked $D-glucosamine$ and $N-acetyl-D-glucosamine$, generally obtained by treatment of chitin deriving from crustaceans' shells in alkaline conditions.

Then, the blends with different weight percent ratios were vacuum-dried overnight.

The films produced were characterised through Gel Permeation Chromatography to evaluate the molecular weight, FT-IR and NMR spectroscopy, Atomic Force Microscopy, and tensile tests. Results indicated that films possessed a relatively smooth surface, hydrophobic properties, and a noticeable thermal stability. Mechanical testing demonstrated a decreased in tensile strength, strain at break, and Young's modulus with increasing grafted xylan concentration. These results showed a good potential for film coating and packaging applications.

1.3. Extraction of Silica from corn cobs

Silica is another name for the chemical compound composed of silicon and oxygen, with formula SiO_2. There are many forms of silica, each of which having the same composition, but with atoms arranged in different manner. The most relevant distinction is between crystalline silica, having repetitive patterns of silicon and oxygen, and amorphous silica, characterised by a random disposition of its components.

All the silica that can be extracted from corn cobs is amorphous[15] and obtained via a sol-gel method. Given this, the final product is generally achieved as a xerogel. Okoronkwo *et al.* studied the extraction of amorphous nano-silica through a sol-gel technique from corn cob previously

[14] Peng, P. *et al.* (2015) 'Synthesis and characterization of carboxymethyl xylan-g-poly(propylene oxide) and its application in films', *Carbohydrate Polymers*, 133, pp. 117–125.

[15] Okoronkwo, E. A. *et al.* (2016) 'Development of Silica Nanoparticle from Corn Cob Ash', *Advances in Nanoparticles*, 5 (2), pp. 135–139.

transformed into ash by combustion in a muffle furnace. The sol-gel technique consisted in the addition of the sample in a solution of hexadecyl trimethyl ammonium bromide, distilled water and $NaOH$. Final samples were calcinated in a furnace at $550\ °C$.

Nano-silica particles were analysed with X-Ray diffraction (XRD), X-Ray fluorescence (XRF), FT-IR, and scanning electron microscopy, to identify its chemical composition and properties. From XRF, an important amount of silica was identified: $47.8\ wt.\%$ in corn cob ash and $98.8\ wt.\%$ after extraction. The average particle size of silica was evaluated by applying Debye-Scherrer's formula to the X-Ray diffractogram (Equation 2).

$$D = 0.89\frac{\lambda}{\beta \times \cos\theta}$$

Equation 2: *Debye-Scherrer's formula*

where:

- D is the average particle size;
- λ is the wavelength of the incident X-Ray beam;
- β is the full width at half maximum of the X-Ray peak;
- θ is the Bragg angle of X-Ray diffraction peak.

Solving the equation, the average particle size was found to be $54\ nm$.

This study indeed revealed that amorphous silica can be produced from corn cobs using a sol-gel method, with the possibility to produce nanoparticles.

This product can be relevant for many different markets in which nanohybrids[16] are employed. Following, the description of some silica nanohybrids is reported.

Molecule-silica nanohybrids

A wide variety of functional molecules have been doped into silica to form nanohybrids. The main linking force is an electrostatic interaction between the negatively charged silica matrix and the positively charged doping molecules. Covalent bonding is frequent as well, but its application requires additional reactions. These nanohybrids generally have a more extensive array of applications than the molecules themselves, including bioimaging, biosensing, drug delivery and

[16] Jin, Y. *et al.* (2009) 'Amorphous silica nanohybrids: Synthesis, properties and applications', *Coordination Chemistry Reviews*, 253 (23–24), pp. 2998–3014.

cancer therapy. The three most relevant hybrids, described below, are fluorescent nanohybrids, chemiluminescent nanohybrids, and drug transporting nanohybrids.

- *Fluorescent nanohybrids* are found to be extremely useful in tracing amounts of biological analytes and their processes. The most common fluorophore molecules have two major drawbacks: low fluorescent intensity and poor photostability. To overcome these problems, silica nanoparticles have been exploited as a matrix to carry thousands of fluorophore molecules. In this way, both the intensity and the photostability of the luminescent molecules improved extensively.

  Generally, fluorescent molecules are doped into silica matrices by electrostatic interaction, but fluorophores can also be immobilised onto the surface of the matrix through chemical reactions.
- *Chemiluminescent nanohybrids* technology is highly attractive due to the inexpensive instrumentation required and the presence of a very low background signal, since it does not require an external radiation source. However, an enhancement of the chemiluminescent signal is needed to fully exploit this technique, and a solution is reached by concentrating a high number of chemiluminescent species in the domain of a silica nanoparticle. There are two main pathways to produce silica chemiluminescent nanohybrids, and they regard the doping with either luminol or tris(bipyridine) ruthenium (II), also written as $[Ru(bpy)_3]^{2+}$ (Figure 13).

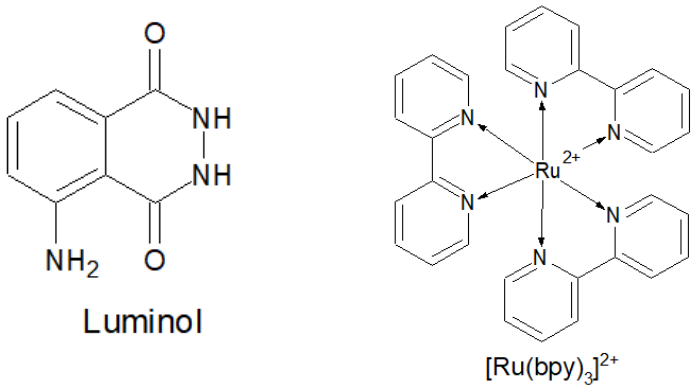

Figure 13: *Molecules employed for silica chemiluminescent nanohybrids*

- *Drug transporting nanohybrids* are required to have a quick target delivery and to have a controllable release rate. To be effective, a drug carrier must have a low toxicity, must be biodegradable and finally must have specific surface functionalities. Amorphous silica has

been proven to be nontoxic and to have an easily modified surface, so it has been increasingly scrutinised for drug-transporting systems.

The doping of silica nanoparticles can be achieved through a reverse microemulsion process, but doping molecules, differently from fluorescent and chemiluminescent ones, must be trapped only temporarily, in order to be released once the target is reached. Therefore, drug molecules are doped by means of physical trapping, such as an electrostatic interaction, which can be easily dissociated compared to chemical bonds.

Functional nanomaterial-silica nanohybrids

Silica nanoparticles are increasingly being used as matrices in which other functional materials are doped. The hybridisation of these two types of nanomaterials is able to overcome some limitations of the individual components, helping the transition of nanotechnology from a laboratory scale to practical applications.

Many different functional nanohybrids are currently under study, with the most relevant being quantum dots, magnetic nanoparticles, gold nanomaterials and catalysts.

- *Quantum dots nanohybrids* are known to have unique luminescent properties and a great potential for biological applications. These materials show a narrow emission peak in their luminescence spectrum, resulting from the quantum size confinement effect, which can be precisely adjusted by modifying their size. Moreover, their luminosity is strong and resistant to bleaching.

  The main drawback comes from their biocompatibility, since, due to the noticeable presence of heavy metals, unmodified quantum dots demonstrate severe toxicity. An easier and safer use can be achieved by shielding them with silica layers, which confer them three main advantages: reduction of toxicity, improved stability against degradation and possibility to be modified with functional molecules or biomacromolecules.
- *Magnetic nanoparticle nanohybrids* have a great number of utilisations in medical treatments as well as for the separation of target molecules from a matrix. The doping of magnetic nanoparticles into a silica matrix is able to prevent the major drawback of these materials: self-aggregation. As for quantum dots, the silica layer serves also as a medium for a possible subsequent insertion of functional molecules.
- *Gold nanomaterial nanohybrids*, thanks to their photoactivity, are used as photosensitive probes, enhancers of detection signal, and occasionally also for photothermal therapy. Silica

nanomaterials are able to adjust the optical properties of gold particles when the hybrid is formed. Many factors affect the property of the nanohybrid, such as the shape, the structure, and the size of both silica and gold nanoparticles. In fact, these nanohybrids can be produced in different forms to be used in different applications.

- *Catalytic nanohybrids*, in which amorphous silica is used as a support due to its highly porous structure, high thermal stability, optical transparency and chemical inertness. Silica supports are able to increase the stability, the reactivity and the selectivity of the catalyst itself, honing the product in all its fundamental characteristics.

  There are two types of catalytic hybrids:

  - *silica-based metal catalysts*, in which silica was first suspended in a metal salt solution and successively improved by employing covalent and hydrogen bonds. This system demonstrated promising characteristics for a further development, with increased reactivity and selectivity;
  - *silica-based titania nanohybrids*, which combine the photocatalytic characteristics of titania (TiO_2), with the capability of silica support to increase the general thermal stability and the dispersion of titania, as well as the catalytic activity itself.

1.4. Formation of biocomposites

By definition, a biocomposite is a material composed by two or more distinct constituent materials, at least one of which being naturally derived, which are combined to yield a new material with enhanced performances. Exploiting the characteristics of xylan and corn by-products, several combinations are possible. The most relevant regard the formation of a xylan – Montmorillonite composite, the honing of a thermoplastic starch film and the realisation of a chitosan – corn cob composite film.

1.4.1. Xylan – Montmorillonite composite[17]

The use of naturally occurring xylan in combination with a montmorillonite-type clay (NaMt), to synthetise a biopolymer – clay biocomposite was investigated by Ünlü *et al*. Xylan was first extracted

[17] Ünlü, C. H. *et al.* (2009) 'Synthesis and characterization of NaMt biocomposites with corn cob xylan in aqueous media', *Carbohydrate Polymers*, 76 (4), pp. 585–592.

from grinded corn cobs with an alkaline process, using a solution of $NaOH$ 10% (w/v) and H_2O_2 35% (w/v), and a subsequent precipitation of xylan with the addition of isopropanol.

The synthesis of the biocomposite was performed by dispersion of the clay onto the xylan, following two different routes: first, montmorillonite concentration was kept constant at $0.02\ g/mL$, with xylan concentration varying between $7.81 \times 10^{-5}\ g/mL$ and $0.02\ g/mL$, then, xylan concentration was kept constant at $0.01\ g/mL$ and clay concentration was varied between $1.25 \times 10^{-3}\ g/mL$ and $0.02\ g/mL$.

All the samples were characterised by rheological measurements, FT-IR, thermal, and morphological analyses. An increasing xylan concentration showed a better intercalation, giving improved mechanical properties, increased thermal and rheological characteristics.

1.4.2. Reinforcement of a thermoplastic starch film[18]

Starch is a polymeric carbohydrate, mostly produced by green plants as energy storage, and contained in large amounts in potatoes, corn, rice, and wheat. Starch is formed by two different molecules: a linear chain of amylose and branched amylopectin, as shown in Figure 14.

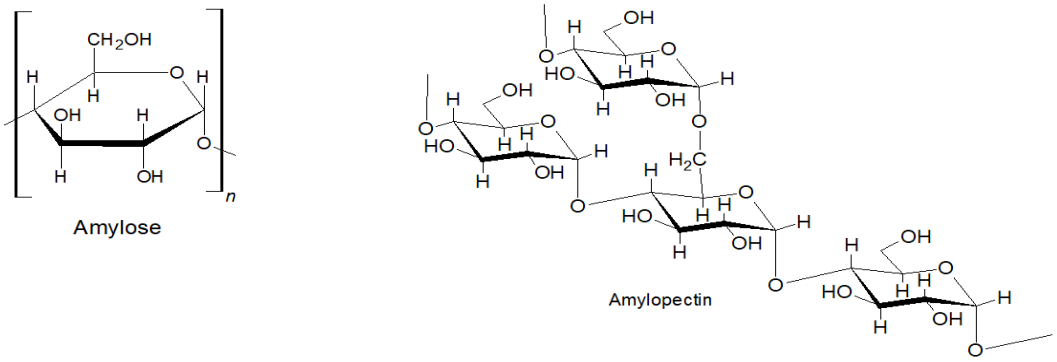

Figure 14: *Starch components*

Starch has many different industrial applications, such as the conversion into sugars by malting, the fermentation to produce ethanol in beer, whisky, biofuel manufacturing, and as an adhesive in papermaking process. In addition, the development of a biodegradable film based on starch has become a very attractive option, since starch can be processed as a synthetic thermoplastic polymer through the addition of plasticisers at high temperature and in conditions of high shear. However, the

[18] Mondragón, M., Arroyo, K. and Romero-García, J. (2008) 'Biocomposites of thermoplastic starch with surfactant', *Carbohydrate Polymers*, 74 (2), pp. 201–208.

mechanical properties of the so-formed thermoplastic starch (TPS) are poor, and extremely sensitive to humidity. To overcome these drawbacks, TPS has been blended with other natural polymers and fibres used as fillers and reinforcements. For example, natural cellulose fibres have been extensively used due their low price and low abrasive nature, coupled with an extremely high abundance and renewability.

Cornstalks and cornhusks were also largely investigated[19] due to their high surface area, which can be exploited by using microfibrillated cellulose obtained from these materials as a reinforcing compound. Mondragon *et al*. reported the preparation of starch biocomposites film in water at different concentration, also using glycerol monostearate (GMS) (Figure 15) as a surfactant. As reinforcing agent, they used cellulose microfibrils, obtained from husks of corn cobs by milling and suspension in a water solution of H_2SO_4 at 90 $°C$.

The films were characterised through XRD analysis, tensile properties measurement, scanning electron microscopy, thermal analysis, and equilibrium water uptake experiment.

These analyses showed an increase in Young's modulus and tensile strength of TPS films, due to the interactions between starch matrix and corn cob microfibrils. These properties can be furtherly improved by the formation of amylose-GMS complexes, which have demonstrated to increase the crystallinity of the film. GMS-modified films also showed a significant reduction in water uptake.

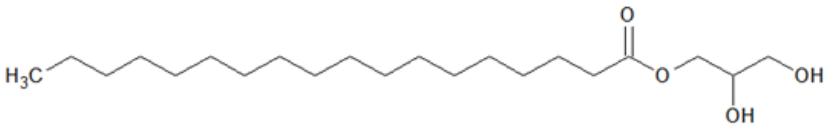

Figure 15: *1-glycerol monostearate*

[19] Reddy, N. and Yang, Y. (2005) 'Structure and properties of high quality natural cellulose fibers from cornstalks', *Polymer*, 46 (15), pp. 5494–5500.

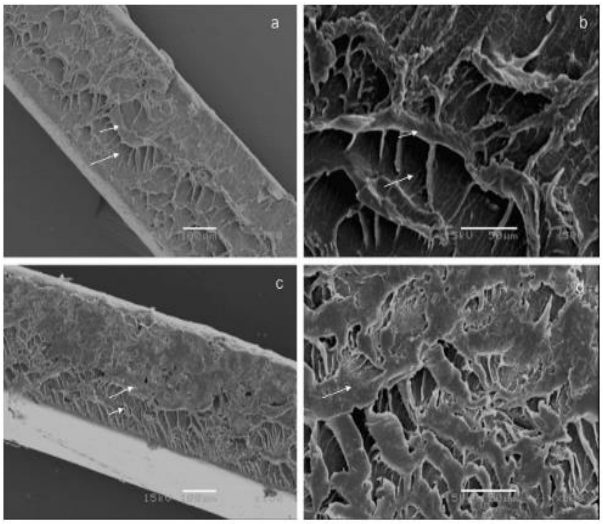

Figure 16: *SEM micrographs of TPS fractured surface without GMS (a and b) and with GMS (c and d)*

1.4.3. Chitosan – corn cob biocomposite[20]

Chitosan, reported in Figure 17, is a linear polysaccharide composed of randomly distributed $\beta -$ 1,4 −linked $D - glucosamine$ and $N - acetyl - D - glucosamine$.

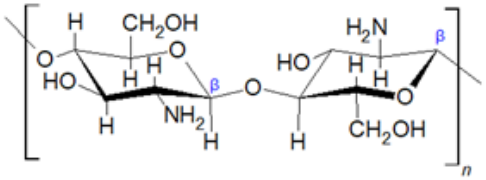

Figure 17: *Chitosan*

This biopolymer is the most abundant natural polysaccharide after cellulose and hemicellulose. It is a semicrystalline polymer, with a noticeable amorphous fraction and a glass transition temperature ranging from $30\ °C$ to $222\ °C$.

Chitosan is considered one of the most promising materials for future applications, based on its outstanding biocompatibility, biodegradability, antimicrobial activity, non-toxicity, and low production costs. Through a reaction with a crosslinking agent, chitosan may get hydrogel-like properties, which expands its range of applications to food packaging and drug delivery systems. In

[20] Yeng, C. M., Husseinsyah, S. and Ting, S. S. (2013) 'Chitosan/corn cob biocomposite films by cross-linking with glutaraldehyde', *BioResources*, 8 (2), pp. 2910–2923.

fact, crosslinking is a chemical modification through which the properties of chitosan may be enhanced. It generally occurs between the active groups of the crosslinking agent (aldehyde groups, acid groups, and epoxy groups) and the amino groups of chitosan.

Glutaraldehyde (GLA) is the most common crosslinking agent for chitosan improvement, since it is able to increase tensile and thermal properties by formation of a three-dimensional network, which also reduces the mobility of the polymer chains. The reaction of the aldehydic groups of GLA with the amino groups occurs through a Schiff base reaction, forming imine bonds.

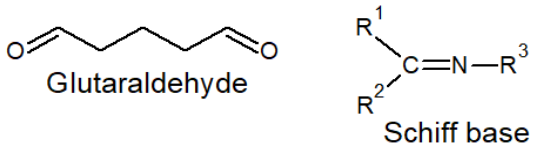

Figure 18: *Components of the crosslinking reaction: glutaraldehyde and a general Schiff base*

A Schiff base is a compound with the general formula showed in Figure 18, characterised by the presence of an imine bond ($C = N$), where R^3 is an alkyl or an aryl group, but cannot be a hydrogen, while R^1 and R^2 could be hydrogens. This molecule is the one responsible for the formation of the crosslinking between the glutaraldehyde and the chitosan, shown in Figure 19.

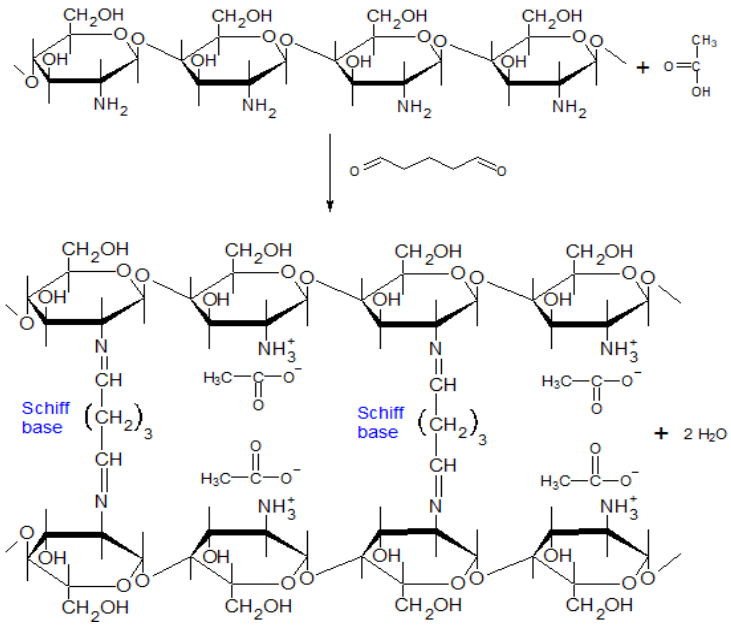

Figure 19: *Schematic reaction between glutaraldehyde and Chitosan*

The effect of corn cob content on mechanical, thermal, and morphological characteristics of chitosan – corn cob biocomposite, with also the evaluation of glutaraldehyde efficiency as crosslinking agent was studied by Yeng *et al*. Unmodified and modified films were prepared via a solvent casting method, with chitosan powder dissolved in acetic acid 1% v/v and corn cob powder added and stirred until a homogenous solution is formed. After that, the solution was poured into a mould and dried at room temperature, with subsequent casting in an acrylic mould. For the crosslinked film, glutaraldehyde was dissolved in distilled water to produce a 1% v/v solution, which was then mixed with chitosan and corn cob. Both types of film were prepared with different compositions.

Several analyses were performed on the films, such as FT-IR, tensile testing, and thermogravimetric analysis (TGA).

The results of tensile tests, reported in Figure 20, demonstrated that the use of corn cob in chitosan films enhances the modulus of elasticity, while decreases the tensile strength and elongation at break at increasing corn cob content. Furthermore, the GLA-modified film showed improved tensile properties (tensile strength, modulus of elasticity), with a consequent decrease in elongation at break. Finally, the modified chitosan/corn cob (CS/CC) biocomposites displayed better thermal stability, as visible in Figure 21, probably due to the presence of imine bonds, as well as improved CC dispersion, improved wettability, and increased interfacial interaction.

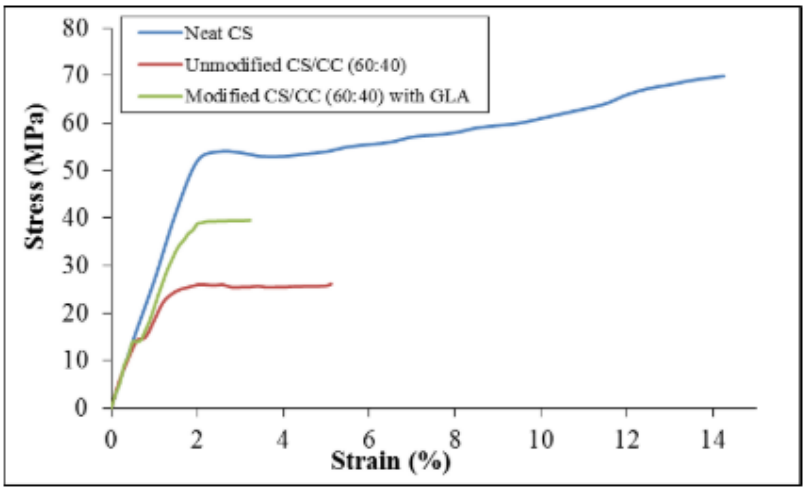

Figure 20: *Stress-strain curves of neat chitosan (CS), unmodified and modified biocomposite chitosan/corn cob films (CS/CC)*

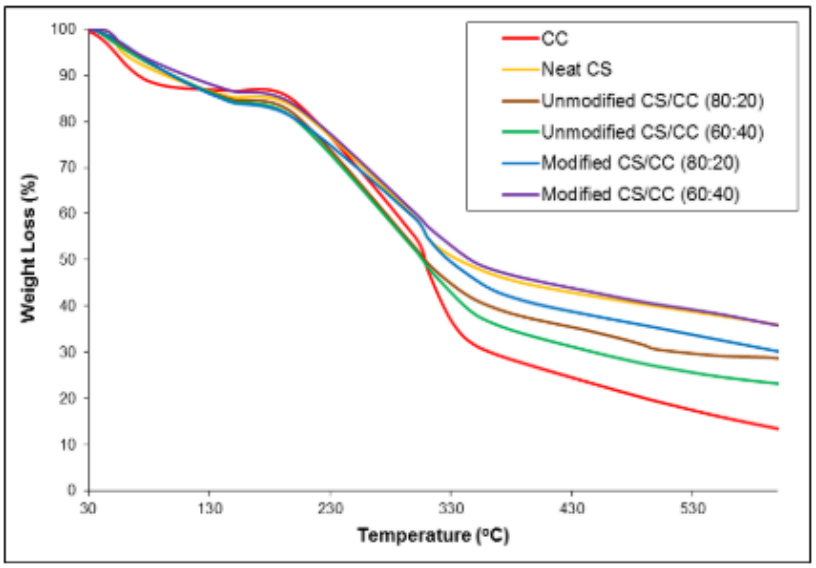

Figure 21: *TGA curves of modified and unmodified chitosan/corn cob (CS/CC) biocomposite films*

After having analysed all the different applications in which corn cobs and corn by-products can be exploited, the next chapter will focalise on the tests performed in laboratory to identify the content of phenolic compounds and antioxidants in corn cobs and corn leaves, verifying the possibility to insert them in polymeric matrices.

1.5. Polymeric matrices

1.5.1. Polyethylene (PE)[21]

Ethylene is the simplest olefin and may be polymerised (Scheme 8) through the action of initiators and catalysts, mostly organic peroxides, which generate free radicals. Polyethylene is the cheapest of the major synthetic polymers, it shows excellent chemical resistance and can be processed through numerous methods (blown film, pipe extrusion, blow moulding, …) into a wide variety of shapes.

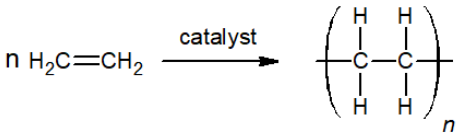

Scheme 8: *Polyethylene polymerisation*

This polymer, defined as thermoplastic, is produced in a wide range of densities and molecular weight, depending on the degree of crosslinking and on the linearity of the chain. The most common products are low-density polyethylene (LDPE, $\rho = 0.910 - 0.925\, g/cm^3$), linear low-density polyethylene (LLDPE, $\rho = 0.919 - 0.925\ g/cm^3$), and high-density polyethylene (HDPE, $\rho = 0.941 - 0.960\ g/cm^3$).

Concerning its mechanical and thermal properties, polyethylene is characterised by good processability, good toughness, and outstanding film clarity, but it also presents some drawbacks: high thermal expansion, difficult to bond, flammability, and poor temperature resistance capability.

Low-density polyethylene (LDPE)

Low-density polyethylene is characterised by an extensive chain branching, which extent and length depend primarily on the polymerisation mechanism and comonomers incorporation.

Branching is classified as short chain branching (by convention six or fewer carbon atoms) and long chain branching. LDPE contains extensive long chain branching, with side chains containing up to hundreds of carbon atoms. This increases the amorphous content of the polymer, contributing to an increased film clarity and ease of processing. Given this, its main application is for food packaging[22].

---

[21] Malpass, D. B. (2010) *Introduction to Industrial Polyethylene: Properties, Catalysts, and Processes*, Wiley, chap. 1, pp. 1-8.

[22] Malpass, D. B. (2010) *Introduction to Industrial Polyethylene: Properties, Catalysts, and Processes*, Wiley, chap. 2, pp. 25-27.

LDPE is produced exclusively in high pressure or autoclave processes, using free radical initiators. Generally, organic peroxides are employed, though other compounds that are able to undergo homolytic scission to generate free radicals may be used as well.

The high-pressure process relies on extreme conditions, such as temperatures higher than $200\ °C$ and pressures in the order of $15000 - 45000\ psig$. Free radical polymerisations are thus conducted adiabatically, in autoclaves or thick-walled tubes. At such high temperatures, polymerisation occurs in solution of polymer in excess monomer. PE particles then precipitate from the solution upon cooling.

The original process for high pressure polyethylene was based on the use of an autoclave and used air to introduce free radicals in a sufficient quantity to initiate the polymerisation reaction. Nowadays, air has been supplanted by organic peroxides, which are injected at several point in the autoclave.

Reactor residence times are very short (seconds or fractions of a second), and excess ethylene is used as aid in heat removal. For this kind of process, subsequent purification is not necessary.

Tubular process is considered to be an evolution of the original design: long and narrow tubes are employed ($l = 1000 - 2000\ m, \emptyset = 25 - 50\ mm$), with organic peroxide initiator injected at several points. Products from this technique are typically higher in molecular weight and have a higher quantity of short branches[23].

Key features of both processes are summarised in Table 1.

Table 1: *Summary of typical LDPE operating features*

Process type	Operating temperature (°C)	Operating pressure (psig)
Autoclave process	180 - 300	15000 - 30000
Tubular process	150 - 300	30000 - 45000

[23] Malpass, D. B. (2010) *Introduction to Industrial Polyethylene: Properties, Catalysts, and Processes*, Wiley, chap. 7, pp. 88-91.

1.5.2. Poly (butylene succinate – co – adipate) (PBSA)[24]

PBSA is a biodegradable, aliphatic, semi-crystalline polyester, obtained by co-condensation of succinic acid and adipic acid with 1, 4 – butanediol (Scheme 9). All three monomers can be produced either from fermentation of renewable feedstock, such as glucose and sucrose, or from oil-based raw materials. PBSA is mostly produced by the Japanese company *Showa Highpolymer Co., Ltd.*, distributed under the trade name of *Bionolle*. PBSA materials come in two different grades, and it is suitable for films, filaments, textiles, foams, and injection moulding products[25].

PBSA shows melting temperatures lower than those of widely used biodegradable polymers ($95\ °C\ PBSA - 155\ °C\ PLA - 115\ °C\ PBS$), making it easier to be processed.

Also concerning the mechanical properties, PBSA shows a lower Young's Modulus with respect to polybutylene succinate, PBS ($323\ MPa\ PBSA - 690\ MPa\ PBS$), but a much higher strain at break ($900\%\ PBSA - 50\%\ PBS$)[26].

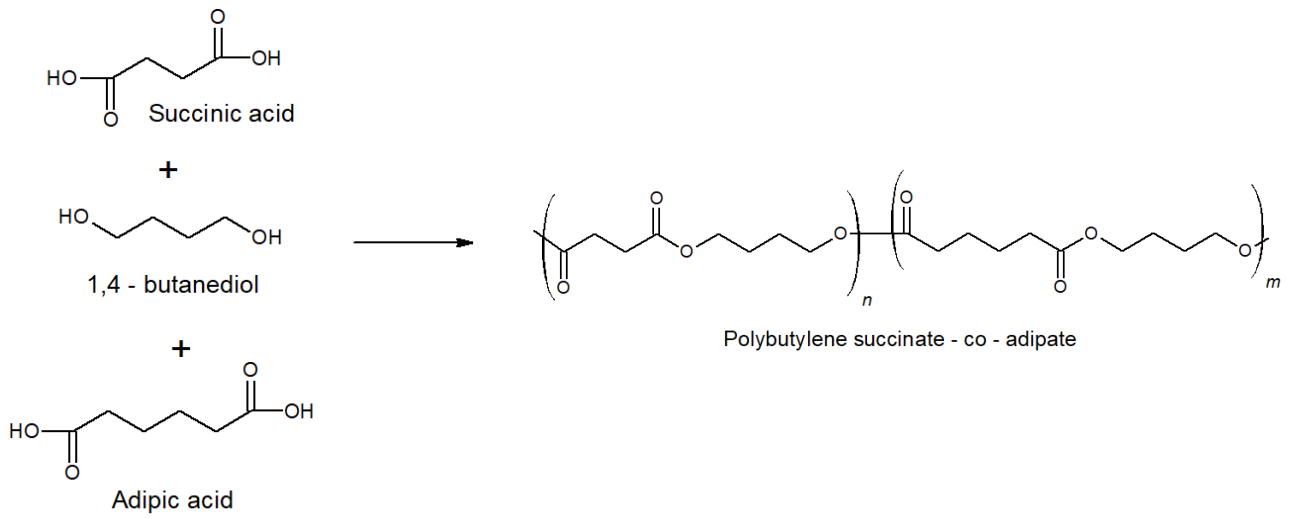

Scheme 9: *Polymerisation reactions of PBSA*

---

[24] Endres, H. and Siebert-Raths, A. (2011), *Engineering Biopolymers: Markets, Manufacturing, Properties and Applications*, Hanser, chap. 4, p. 141.

[25] Endres, H. and Siebert-Raths, A. (2011), *Engineering Biopolymers: Markets, Manufacturing, Properties and Applications*, Hanser, chap. 8, pp. 357-358.

[26] Endres, H. and Siebert-Raths, A. (2011), *Engineering Biopolymers: Markets, Manufacturing, Properties and Applications*, Hanser, Appendix A, pp. 630-631.

Biobased butanediol production

A sustainable bioprocess for the production of 1,4-butanediol (BDO) from carbohydrate feedstocks has been analysed in the article from Burgard *et al*[27]. This review highlights the development of an *E. coli* strain and an overall successful process for direct production of bio-BDO. A schematic pathway is represented in Figure 22.

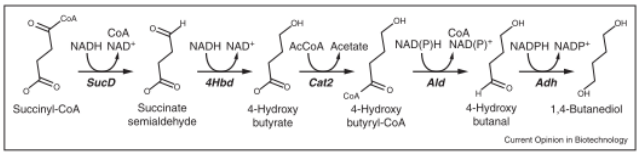

Figure 22: *Schematic pathway of 1,4-butanediol production*

BDO is currently produced from fossil feedstocks, such as coal, oil, and natural gas, through processes that are highly energy intensive. Growing concerns opened a way for the development of a more sustainable process for BDO production from renewable feedstocks with lower costs and energy consumption. To this aim, *E. coli* has been engineered for direct production of BDO from a variety of different carbohydrate feedstocks. In addition, a downstream recovery and purification process was developed, to provide bio-BDO that meets industry specifications and performance requirements. Being BDO a non-natural chemical, a new biosynthetic pathway was needed for the conversion of the primary metabolite to into the desired product.

As reported in Figure 22, multiple heterogeneous steps were required, then separation and purification stages were employed. The separation of BDO is energy intensive, due to its high boiling point ($\sim 235\ °C$) and its complete miscibility with water.

Following fermentation, the broth is sterilised through a heated coil, then cells are removed by centrifugation or microfiltration. The cell-free broth is then ultra-filtrated to remove large biomolecules and some of the salts. Remaining salts are removed by ion exchange chromatography, followed by water evaporation. The crude 1,4-BDO is finally purified by distillation, to achieve industrial specification (purity > 99.5 %).

Subsequent life cycle analyses of the bio-BDO process reported a decrease up to 83% of total emissions of $CO_{2,eq}/kg_{BDO}$ and up to 67% lower fossil energy usage, with respect to traditional petrol-based processes.

[27] Burgard, A. *et al.* (2016) 'Development of a commercial scale process for production of 1,4-butanediol from sugar', *Current Opinion in Biotechnology*, 42, pp. 118–125.

***Biobased succinic acid production*[28]**

Currently, succinic acid is mostly produced by chemical process from n-butane to maleic anhydride. Succinic acid is obtained by hydrogenation of maleic anhydride followed by hydration, as displayed in Scheme 10.

Scheme 10: *Succinic acid production process*

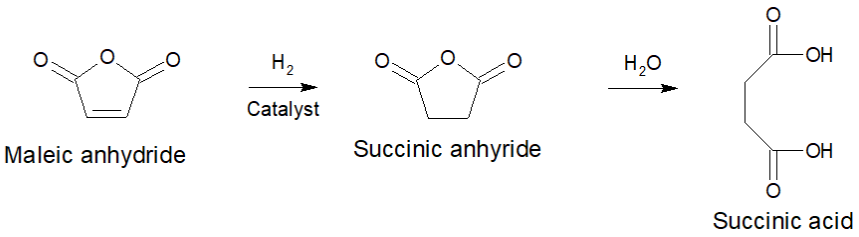

Another important process regards the production of biobased succinate, achieved from the most abundant sugars in plant biomass (glucose, fructose, arabinose, and xylose). Glucose is the most commonly used substrate for relevant fermentations, and theoretically 1.71 mol of succinate can be produced per mol of glucose, with the reaction shown in Scheme 11.

$$C_6H_{12}O_6 + 0.86\ HCO_3^- \rightarrow 1.71\ Succinate^{2-} + 1.74\ H_2O + 2.58\ H^+$$

Scheme 11: *Succinate production from glucose*

In the presence of CO_2 and additional reducing power, the theoretical yield increases to 2 mol of succinate per mol of glucose, as shown in Scheme 12.

$$C_6H_{12}O_6 + 2\ HCO_3^- + 2\ H_2 \rightarrow 2\ Succinate^{2-} + 2\ H_2O + 2\ H^+$$

Scheme 12: *Succinate production from glucose with added* CO_2

The market of succinic acid is constantly increasing in value, with the aim to produce it with a cheaper and biobased technology. The most relevant potential markets are:

- replacement for maleic anhydride → a primary use of succinic acid is as a replacement for selective reduction, to give butanediols, tetrahydrofuran (THF) and γ −butyrolactone (GBL) family of products;

[28] Vaswani, S. (2010) 'Process Economics Program Review: Bio-based succinic acid', *Process Economics Program*, (December), p. 42.

- polymers → PBS can be obtained through the combination with butanediol, and it can be used in biodegradable packaging films and disposable cutlery;
- pyrrolidinones → this family of products is used to make green solvents and eco-friendly chemicals for water treatment.

Biobased succinic acid production consists in a fermentation step, followed by recovery and purification, although many companies rely on the use of genetically modified *E. coli*.

The process shown in Figure 23 is the metabolic pathway of *E. coli*, with a few gene alterations. To improve the overall yield of succinate production, a number of genes are deleted from the pathway.

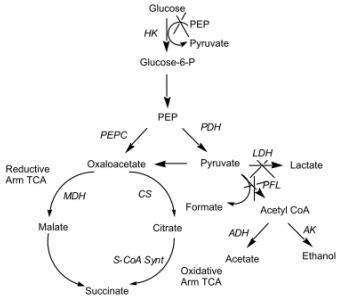

Figure 23: *Methabolic pathway of altered* E. coli

Biobased adipic acid production

In addition to the production of biobased succinic acid and butanediol, also adipic acid has a pathway starting from renewable resources. Adipic acid has traditionally been produced from various oil-based feedstocks, such as phenol, benzene, and cyclohexane, with the last one being responsible for 93% of global production capacity.

The most promising biobased process is the *Rennovia* process (Scheme 13), which uses air oxidation to convert glucose to glucaric acid, followed by hydrodeoxygenation to convert glucaric acid into adipic acid. This process has a high potential to be cost competitive with the conventional cyclohexane oxidation technology.

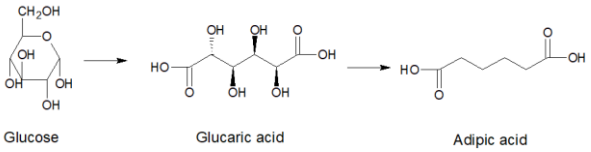

Scheme 13: *Production of adipic acid via* Rennovia *process*

2. Experimental part

Pretreatment – grinding of corn cobs

Corn cobs represent the central core of the corn, and they are characterised by a high stiffness and rigidity. To try to extract any useful molecule which could be present inside the cobs, they must be grinded and reduced to smaller parts. Several equipment could be used, since the main goal is to decrease their size, and different attempts were made with an industrial pulveriser (*Fritsch Pulverisette 14*). All the samples were grinded at $15000\ rpm$, to get extremely fine particles.

The major issue was the high temperatures reached during the pulverising step, in fact some particles, even humidified, were partially burned, thus possible decomposition of the organic molecules, such as the antioxidants, may have occurred.

Then a new approach, consisting in a pre-grinding in a two-blades machine and a subsequent grinding in a four-blades machine, was employed. The grinding was less efficient in terms of dimensions reached, but the corn particles were small enough for antioxidant evaluation and were not burnt. Corn leaves were treated too, but their grinding was much easier.

Types of grinded samples and their retrieved amounts are shown in Table 2.

Table 2: *Types and amounts of grinded corn cobs*

Sample	Amount obtained (g)
Red corn cob	24.6
Yellow corn cob	20.4
Mixed corn cob	23.6
Corn leaves	13.4

2.1. Extraction methods

2.1.1. Microwave-Assisted Extraction method

2.1.1.1. Description of the method[29]

The microwave-assisted extraction (MAE) is an efficient technique to derive natural compounds from plants. It allows organic compounds to be extracted more rapidly, with similar or better yield when compared to traditional extraction methods. For example, MAE has several advantages over Soxhlet method:

- reduction in extraction time;
- improved yield;
- better accuracy;
- higher suitability for thermolabile substances.

Microwaves are a form of electromagnetic radiation with wavelengths ranging between $\sim 1\ m$ and $1\ mm$. They are widely used in modern technology, mostly in communication links, radio astronomy, particle accelerators and for microwave ovens.

Microwaves heat up the molecules by a dual mechanism of ionic conduction and dipole rotation. When the radiation interacts with the solvent, heating of the substance may occur due to any one of the above-mentioned phenomena, individually or simultaneously. The electrophoretic migration of ions under the influence of the changing electric field is defined as ionic conduction, and if the solution offers a resistance to this migration, a friction is generated, and the solution is heated. The realignment of the dipoles of the molecule with the rapid change of the electric field is called dipole rotation. At a frequency of $2450\ MHz$, the process of heating occurs: microwaves show a change in the electric component at a speed of $4.9 \times 10^4\ times/second$, and the heat generation happens when molecules try to realign themselves with the changing field, failing to do so and thus creating frictional energy. No heating occurs when the frequency is higher than $2450\ MHz$ and the electrical component changes at a much higher speed, or when the frequency is lower than $2450\ MHz$ and the electrical component changes at a much lower speed. The outcome from these phenomena is that only dielectric materials or solvents with permanent dipoles get heated up in the microwave oven.

[29] Tatke, P. and Jaiswal, Y. (2011) 'An overview of microwave assisted extraction and its applications in herbal drug research', *Research Journal of Medicinal Plant*, pp. 21–31.

The value of dissipation factor ($\tan\delta$) is a measure of the efficiency with which different solvents heat up, and the formula is given by Equation 3, where ε'' and ε' are, respectively, the dielectric loss factor and the dielectric constant.

$$\tan\delta = \frac{\varepsilon''}{\varepsilon'}$$

Equation 3: *Dissipation factor*

Due to their lower ε' value, polar solvents like ethanol and methanol undergo lesser microwave absorption compared to water, but as the $\tan\delta$ value remains high, the overall heating efficiency is higher. Some solvents, such as hexane and chloroform, produce no heat, as they are transparent to microwave.

In MAE, heating occurs in a targeted and selective manner, with practically no heat being lost to the environment, as the heating occurs in a closed system.

The extraction principle relies on the content of moisture in plants, which serves as target for the heating. As moisture evaporates, an enormous pressure generates on cell walls, which eventually break, releasing phytoconstituents. The phenomenon can be intensified if the plant matrix is impregnated with solvents, having higher heating efficiency under microwave.

There are two types of commercially available MAE systems:

- closed extraction vessel, which performs extraction under controlled pressure and temperature;
- focused microwave ovens, where only the part of the extraction vessel containing the sample is irradiated with microwaves.

Both systems comprise the following components:

- a microwave generator, generally a magnetron which generates energy;
- a wave guide, useful to propagate microwave to the cavity;
- an applicator, where the samples are placed;
- a circulator, allowing the microwave to move in forward direction.

With closed-vessel extraction, pressurised MAE is performed: the higher pressure allows temperature above boiling points of the solvents to be reached more efficiently, increasing the speed and the efficiency of the extraction itself. When dealing with thermolabile compounds, high temperature may cause the degradation of the analytes, so an open system is chosen. Closed-vessel systems have some advantages and disadvantages, as shown in Table 3.

Table 3: *Positive and negative features of closed-vessel systems*

PROS	CONS
Decreased extraction time	High pressure may involve risks
Avoidance of volatile substances loss	The usual constituent material of the apparatus does not allow high solution temperatures
Minor solvent quantity required	Addition of reagent during treatment is impossible
No hazardous fumes are produced	Vessel must be cooled down before opening

With an open-vessel system, extraction is performed at atmospheric pressure, and the maximum available temperature is determined by the boiling point of the solvent. Vapour losses are prevented by a cooling system operating on the top of the vessel, which causes condensation of solvent gases. Open-vessel systems have some positive and some negative features, as shown in Table 4.

Table 4: *Positive and negative features of open-vessel systems*

PROS	CONS
Increased safety	The method is less precise than the close-vessel system
Addition of reagents during treatment is possible	The sample throughput is lower, since many samples cannot be processed simultaneously
Different materials can be used to realise the vessel	Longer times are required to achieve the same results as for closed system
Excess solvent can be removed easily	
Large samples can be processed	
The need of a cooling step is removed	
Lower cost of the equipment	
Suitable for thermolabile products	

MAE is affected by different factors:

- *microwave power*, which must be correctly chosen to minimise the extraction time, although increased power may cause solvent loss by evaporation. For closed systems, maximum power ranges between $600\ W$ and $1000\ W$, while for open system it is around $250\ W$;

- *matrix characteristics*, such as the plant particle size and the status in which it is treated can affect the recovery yield of the needed compounds. Particle sizes of extracted materials are generally between $100\ \mu m - 2\ mm$, with smaller particles enhancing the extraction, since they provide a higher surface area;

- *temperature*, which should be sufficiently high to ensure good solubility of the compounds and a good penetration of the solvent in the plant matrix, to increase the yield. However, it should be always below the degradation temperature of targeted compounds.

2.1.1.2. Microwave-Assisted Extraction of corn by-products

The first extraction has been performed on red corn cobs only, using a mixture of $ethanol{:}\,water\ 50{:}\,50\ (vol)$ as a solvent. The extraction is performed employing a closed-vessel system (*CEM Corporation, Mars Xpress*) and two different microwave tubes, each containing $1\ g$ of sample and $40\ mL$ of solvent. So, the sample was weighted twice ($1.0057 g$ and $1.0022\ g$). After the tubes were filled, they were put in the microwave with the magnetic stirrer. The equipment always has to work with polar solvents, $10\ to\ 20\ °C$ above the boiling temperature. For this extraction, a pre-existing method, labelled $EX\ WE105$, was used, reaching a maximum temperature of $105\ °C$, with a ramp of temperature of four minutes, mixing, and a total duration of 30 minutes.

After extraction, the solution is cooled down to room temperature and filtered. A first separation was made by pouring carefully the liquid fraction inside a beaker, and moving the solid particles onto a paper filter, to recover some extract drops. In order to quicken the filtration step, the liquid portion is separated with a syringe equipped with a $1\ \mu m$ filter. The tubes are washed twice, with $20\ mL$ of ethanol and $20\ mL$ of water each, then filtered again with the syringe. The solution in the flask is brought to volume with water, then it is transferred to a dark bottle, sealed with parafilm, and stored in the fridge for further analyses.

The same procedure was repeated for all the other samples, which are yellow corn cob, mix corn cob (red and yellow), and corn leaves. One gram of each is weighted twice, as reported in Table 5.

Table 5: *Amounts of corn weighted analytes*

Sample	Weight #1	Weight #2
	g	g
Mixed corn cobs	1.0012	1.0002
Yellow corn cobs	1.0000	1.0019
Corn leaves	1.0028	1.0029

2.1.2. Soxhlet extraction method

2.1.2.1. Description of the method[30]

The Soxhlet extraction technique is thought to be invented by Franz Ritter von Soxhlet (Brünn, 1848 – Munich, 1926). This method was a noticeable advance in the isolation of solutes from solid samples that were uneasy to extract. In fact, Soxhlet extraction has been considered the most advanced and useful extraction technique for more than 100 years. While still being used, due to its low application costs, it is being replaced by a number of other advanced extraction techniques, such as ultrasound-assisted extraction, microwave-assisted extraction, and pressurised solvent extraction.

The Soxhlet extractor is defined as a continuous-discontinuous device: continuous in the sense that solvent is continuously evaporated from the solvent reservoir flask and condensed, and discontinuous since it relies on a number of siphon cycles. This process is able to minimise channelling of solvent through the sample, as may occur with continuous methods. Given this, Soxhlet process can be more precisely defined as a batch process.

The first scientific paper[31] reporting Soxhlet application concerned with the determination of milk fat, but nowadays this extraction technique is used for fats, oils and mostly nonpolar solutes, from solid and semi-solid matrices. Because of its wide acceptance, Soxhlet technique has been used for some regulatory methods, mostly regarding semi-volatiles organics in solids, fats and oils content, and solvent-soluble materials in wood and pulp.

The Soxhlet apparatus is shown in Figure 24, with the extractor being the central section. The solid sample is placed into a porous extraction thimble, generally made of cellulose, positioned in the Soxhlet extractor before assembling the device.

[30] https://www.chromatographyonline.com/view/looking-past-understand-future-soxhlet-extraction

[31] Soxhlet, F. (1879) 'Die gewichtsanalytische Bestimmung des Milchfettes', *Dingler's Polytechnisches Journal*, 232, pp. 461-465.

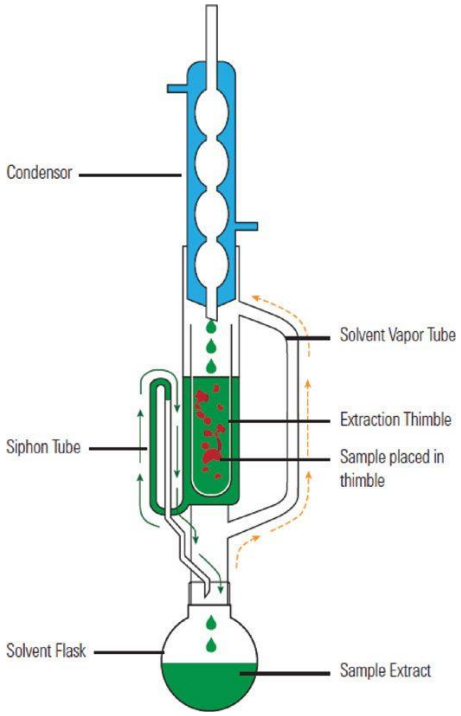

Figure 24: *Soxhlet apparatus*

The solvent, represented in green colour, is added to the reservoir flask, and mounted onto a heating plate or mantle. As it boils, the solvent vapours rise through the lateral tube and enter in contact with the condenser section, where cool water keeps running. The vapours liquify again and flow down onto the sample, where they may permeate into the matrix and dissolve the targeted analytes. When the solvent reaches the top of the siphon, the mechanism is activated, and the solvent-solute mixture flows back into the solvent flask. This is defined as one extraction cycle, and many of these are performed during one complete extraction process. As the extraction cycles keep going, the solvent re-evaporates, and the solutes concentrate as they are left behind in the solvent flask.

The performance of a Soxhlet extractor depends on many different parameters:

a) particle size, since solid samples should be grinded to a flowable powder, with size generally no larger than sand. For fine particles, better results are obtained by mixing them with an inert material to hone their dispersion;
b) solvent selection, for which general solubility guidelines, such as “like dissolves like” principle, should be considered. Equally important are considerations of human health and environmental impact. Often, mixed solvents provide better results than a single solvent.

Another important consideration regards the fact that, in many instances, solvent evaporation and extract clean-up are needed after the extraction;

c) sample moisture, which generally should be lower than 10% water content. For wet samples, up to about 30% of moisture, the sample can be mixed with a suitable adsorbent, such as silica gel, alumina, or sodium sulphate. The extraction of moist samples can be enhanced by the addition of a miscible, polar solvent;
d) extraction cycles, the rate of which is predominantly governed by the rate of heating of the solvent in the reservoir flask. The heating mantle should be adjusted so that four to six cycles per hour are performed. A more frequent extraction rate increases the risk of channelling and inefficient extraction, so the solvent siphoning must occur as a separate event. The solvent should be able to diffuse into the sample matrix, for a more complete extraction;
e) extraction time, for which there are no precise guidelines, so generally the apparatus is left running for six to eight hours. If that time is not sufficient, the extraction can be continued over one night (24-hours approach) or two (48 hours).

The most important advantage of the Soxhlet technique is its history legacy. Not only newly developed methods are typically compared to Soxhlet, but regulatory agencies and industrial laboratories have over a century of data collected on the basis of Soxhlet technique, with subsequent decisions being made depending on these data. Procedurally, the sample is continuously exposed to fresh solvent through the reflux, at some elevated temperatures, which are still lower than the normal boiling point. Increasing the solvent temperature generally increases the solubility of the sample, accelerating the diffusion into the matrix. The Soxhlet apparatus is quite inexpensive, with a total price of about $\$ 200 - 300$. The cellulose thimble acts as a filter to separate the extract from the solid residue, and, with a wide variety of sizes, it is able to accommodate many different samples. In conclusion, the technique is quite simple to be performed.

Despite having plenty of advantages, the Soxhlet extraction method has a few limiting drawbacks. It can easily take 6 to 48 hours and the technique is manual, though the procedure runs mostly unattended. Even more important are the disadvantages related to the solvent: depending on the sample size, up to hundreds of millilitres of solvent may be used in a Soxhlet extraction, and this magnifies safety, environmental and human health concerns of the solvent itself. This results in the mandatory setup under a fume hood, as well as an increased water disposal.

The relevant solvent consumption carries a significant cost. In fact, despite the low cost of the apparatus, the solvent-related expenses boost the cost per extraction up to the double of alternative method, such as supercritical fluid extraction, microwave-assisted extraction, and ultrasound-assisted extraction. The large amounts of solvent also require evaporation, costing time and energy, to retrieve the desired extract concentration. Moreover, the selectivity is solely related to the solvent used. Consequently, some clean-up processes are always required. Another concern regards the thermolability of analytes: if, on one hand, higher temperature enhances the solubility of the sample, on the other hand the extremization of this advantage may result in thermal degradation of the analytes themselves, making them no longer viable for analyses.

With the significant solvent and time disadvantages, new methods have been assessed to address these concerns, while maintaining Soxhlet advantages. One of these is the high-pressure approach, initially used as a screening tool in the development of supercritical fluid extraction method. In this approach, the entire apparatus is mounted in a high-pressure vessel. A volatile solvent is used, mostly carbon dioxide, usually under supercritical conditions.

Another development is the so-called *automated Soxhlet*: in this technique, during the initial portion of the extraction, the thimble is directly immersed into the boiling solvent. Then the conventional approach is used with a rinse function. With this approach, the solvent content is highly reduced, passing from hundreds of millilitres to about $50\,mL$, as well as the time is reduced to $30-60$ minutes.

Other approaches take advantage of more intense energy sources, such as ultrasound or microwave, to enhance the extraction. There are two main reasons why these techniques have yet to completely catch the attention at industrial level: the first is that, especially with ultrasonic, the loss of energy intensity as it is transferred to the sample is quite noticeable, and the second is the advent of other modern instrumental methods, such as Microwave-Assisted Extraction (MAE), Ultrasound-Assisted Extraction (UAE), Supercritical Fluid Extraction (SFE) and Pressurised Solvent Extraction (PSE).

2.1.2.2. Soxhlet extraction of corn by-products

Corn by-products were treated following an adapted Soxhlet procedure described by Monroy *et al.*[32], in which the extraction of purple corn cobs was performed with different mixtures of water – ethanol and for a total duration of three hours. Given that, the solvent was prepared in order to have the same conditions as for the microwave extraction, so $500\ mL$ of water and $500\ mL$ of ethanol have been mixed, to obtain a $50{:}\,50\ v/v$ solvent ratio. To represent as closely as possible the conditions in the MAE, a similar proportion between the sample and the solvent was used. To this aim, since the cellulose thimble for the Soxhlet fits almost $7\ g$ of sample, $300\ mL$ of solvent were used to perform the extraction.

The temperature was first set to $150\ °C$, to let the boiling begin, then, after the first complete cycle, it was decreased to $130\ °C$ to have one drop of solvent in the thimble per second. The first two extractions were performed on yellow corn cobs and red corn cobs, but since the cycle time was very low for the red cobs, the temperature was increased to $145\ °C$. The total duration of the extraction was supposed to be three hours, as reported in literature but, to have comparable results, red cobs sample was kept for a longer time, about four hours, to achieve the same number of cycles as the yellow corn cobs. After the extraction was finished, the liquid was filtered with a syringe to reduce filtration time.

The same procedure was repeated with mixed corn cobs and corn leaves, but for the latter only $2\ g$ were used, since leaves are much lighter, and the thimble was already almost full. Also in this case, the temperature was initially brought to $150\ °C$, then decreased to $135\ °C$ for the mixed cobs and $140\ °C$ for the leaves, since their cycle was slower. For these samples, the same number of cycles was used: three hours for the mixed cobs and about four for the leaves, similarly to what happened with the first two samples. Also in this case the liquid obtained was filtered with a syringe.

Table 6 reports the total number of cycles and the average cycle time for each sample analysed.

Table 6: *Soxhlet extraction number of cycles and average length*

Sample	Number of cycles	Average cycle length min:sec
Yellow corn cob	14	12:52
Red corn cob	14	18:15
Mixed corn cob	14	14:43
Corn leaves	14	17:51

[32] Monroy, Y. M. *et al.* (2016) 'Extraction of bioactive compounds from cob and pericarp of purple corn (Zea mays L.) by sequential extraction in fixed bed extractor using supercritical CO2, ethanol, and water as solvents', *Journal of Supercritical Fluids*, 107 (September 2015), pp. 250–259.

2.1.3. Room temperature extraction method

This method, described by Sultana *et al.* [33], was taken into account since the authors reported that the amount of antioxidants extracted was able to inhibit more than 50% of the DPPH solution.

The first step requires the removal of moisture, so yellow and red corn cobs were dried in the oven at $45\ °C$, for about four hours. Then, a sample consisting of $10\ g$ of yellow cobs and another one containing $5\ g$ of yellow and $5\ g$ of red cobs were prepared. Each sample was soaked in $100\ mL$ of pure ethanol and stirred overnight.

The extracts were filtered, and the liquid fraction was stored in the refrigerator, while the solid fraction was extracted again, adding $100\ mL$ of fresh ethanol. After 24 hours in ethanol, the second extract was filtered, and the liquid fraction was added to the previous one.

The solutions were poured into $250\ mL$ flasks and brought to volume with ethanol, in order to have a known volume and thus a known concentration.

$20\ mL$ of each extract were employed for the Folin-Ciocalteu test, while the rest was concentrated via *Rotavapor* at $45\ °C$.

2.1.4. Microwave-Assisted Extraction with methanol

In order to analyse the antioxidant activity of corn cobs as thoroughly as possible, new extractions were performed, using methanol as main solvent. This alcohol must be handled in a much safer way with respect to ethanol, due to its high flammability, toxicity via inhalation and possible damaging of internal organs. Since methanol is a polar solvent, the extraction was performed with the microwave-assisted method.

To obtain comparable results as those retrieved with ethanol, the same solid-liquid ratio was used. In particular a mixture of water and methanol in the ratio $1{:}\,1\ v{:}\,v$ was used, and $1\ g$ of grinded corn cobs was introduced in the microwave tube, with $40\ mL$ of solvent. Two different samples were analysed, one consisting of yellow cobs and one of red cobs.

The extraction in the microwave was performed with the same MAE protocol used with ethanol, since boiling temperatures of the two liquids are similar ($64.7\ °C$ for methanol, $78.2\ °C$ for ethanol).

[33] Sultana, B., Anwar, F. and Przybylski, R. (2007) 'Antioxidant potential of corncob extracts for stabilization of corn oil subjected to microwave heating', *Food Chemistry*, 104 (3), pp. 997–1005.

At the end of the procedure, the content of the two tubes was mixed and the tubes were washed with 40 mL of fresh solvent twice. Then, the solution was filtered with 1 μm syringe filters, brought to 250 mL to obtain the same concentration in both extracts and stored in the fridge for further analyses.

2.1.5. Extraction with nonpolar solvent using the Ultrasound-Assisted Extraction method and limonene

Limonene, shown in Figure 25, is a natural cyclic monoterpene with a molar mass equal to 136.24 g/mol, and it represents the major component of the oil extracted from citrus rind. It is a clear to light yellow liquid, characterised by a strong citrusy scent.

With a density of 0.842 kg/m^3, limonene is lighter than water, in which it is insoluble, and it shows a boiling point of 176 $°C$ at atmospheric pressure.

Limonene has been used as an alternative to the already mentioned polar solvents, such as methanol and ethanol, and it has been preferred to other substances, such as benzene, hexane and cyclohexane due to its lower toxicity and its natural derivation.

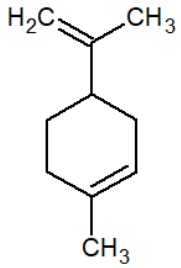

Figure 25: *Limonene structure*

2.1.5.1. Ultrasound-Assisted Extraction (UAE)[34]

Ultrasound technology has continuously increased its appealing in natural products extraction processes, becoming a very active field of research. There are two different approaches:

- high-frequency, low-intensity ultrasound, which is specifically focused on quality monitoring of products (measurement of ultrasound velocity, analysis of frequency spectra)
- low-frequency, high-power ultrasound, applied to improve maceration, fermentation and extraction processes.

[34] Esclapez, M. D. *et al.* (2011) 'Ultrasound-Assisted Extraction of Natural Products', *Food Engineering Reviews*, 3 (2), pp. 108–120.

This technique is mostly applied in solid/liquid systems, where the main beneficial effect is the enhancement of mass transfer given by the acoustic-induced cavitation in a liquid medium. When mechanical waves are transmitted through a fluid, the average distance within molecules is modified: during the compresion cycle, the intermolecular distance is decreased, and it increases again in the rarefaction cycle. In this step, when the pressure drop is enough to exceed the critical distance between molecules, cavities may appear in the bulk of the liquid. These bubbles keep increasing in size until the system reaches its minimal pressure, corresponding to the beginning of a new compression cycle. At the end of this, cavities can start another rarefaction cycle, increasing in diameter, or collapse adiabatically, resulting in a violent implosion which yields shock waves at hundreds of atmpospheres and at a temperature of around $5000\ K$. The potential energy of the expanded bubble is thus converted into kinetic energy, forming a liquid jet travelling at hundreds of metres per second and penetrating the opposite bubble wall.

As abrupt as they may seem, the timescale of these microreactions is so low that the macroscopic system is barely affected, leaving the parameters of the medium (temperature and pressure) unaltered. However, they could affect the cellular structure and enhance mass transport processes, such as the extraction of bioactive compounds.

Different applied power may affect different mechanisms:

- at low intensities, the external and, with lower impact, internal mass transfer are affected;
- at intermediate intensities the product structure is affected, increasing the effect on the internal mass transfer resistance;
- at high intensities cell disintegration may take place.

Sonication has many beneficial effects related to the extraction of natural compounds from solid natural matrices, such as an increase in the efficiency and extraction rate, a decrease in temperatures (very important effect, since most bioactive compounds are thermolabile), lower quantity of solvent needed, and easier solubilisation of targeted compounds.

More in detail, the local increase of temperature enhances the solubility of the analytes in the solvent and allows their diffusion from the solid matrix to the liquid medium, while the increased local pressure facilitates both the penetration of the solvent in the matrix and the transfer of compounds. Moreover, the implosion of cavitation bubbles can hit the surface of the solid matrix, disintegrating the cell wall.

As a consequence of these effects, less extraction time is required, with respect to conventional solid/liquid extraction techniques.

UAE is influenced by many process variables, which need to be considered to estimate the reliability and the reprocducibility of results.

Ultrasonic Power

The actual acoustic energy applied to sonication processes is not easy to be evaluated. Some of the methods used rely on physical measurements, such as the estimation of acoustic pressure through hydrophones or optical microscope, and a calorimetric technique. Other applications regard chemical methods, based on the indirect estimation of $OH^{\cdot}$ radical formed by cavitation measuring the sonoluminesence.

More comparable results are obtained indicating the power density Π $[W/cm^3]$, especially for the case of ultrasonic baths, where the volume of the total bath needs to be considered.

As stated above, an increased power affects different mass transfer resistances, but the extraction yield usually increases with the power intensity applied, as declared in Zou *et al.* article[35].

Ultrasonic Frequency

A lower frequency in the sonication process provokes the formation of larger bubbles, which give rise to more violent implosions and, consequently, increase the efficiency of the extraction.

Temperature

This parameter affects both physical and chemical characteristics of a product, so temperature is a key variable especially for volatile or sensible compounds. In fact, for some natural compounds a decrease in extraction yield is observed at higher temperatures, probably related to thermal degradation or polymerisation reactions. In general, however, the increase in extraction temperature enhances the mass transfer thanks to a higher solvent diffusivity into the cell.

Nonetheless, the use of higher temperatures could accelerate the volatilisation of the solvent, bringing higher energy cost and a more relevant possibility of impurities extraction.

In conclusion, the higher boiling point of some solvents allows the use of higher temperatures (still limited by the stability of the product), increasing the efficiency of the extraction.

[35] Zou, Y. *et al.* (2010) 'Optimization of ultrasound-assisted extraction of melanin from Auricularia auricula fruit bodies', *Innovative Food Science and Emerging Technologies*, 11 (4), pp. 611–615.

Solvent-Sample Interaction

The choice of an appropriate solvent is always a critical factor for extractions, since the optimal fluid for traditional processes may differ from the one for UAE.

The selection is generally made to achieve high molecular affinity between the solvent and the solute, but factors affecting cavitation, such as solvent vapour pressure and surface tension, should be considered as well. In fact, higher vapour pressures consent an easier penetration of cavitation bubbles from the volatilised solvent, cushioning their collapse. In this way, cheaper solvents, such as water mixtures, could work better than traditional pure solvents, employed for conventional extractions.

Considering a fixed amount of solid matrix, a higher solvent volume gives a more relevant concentration gradient effect, obtaining a faster extraction rate. However, for large solvent/matrix ratios, the improvement in extraction is negligible, since the increase in the gradient is negligible as well, and more time and energy are needed for post-treatment concentration.

The extraction yield may also be linked to particle size, since the process is influenced by the amount of exposed surface and the length of path that the molecules should move along. Comparable results of different natural matrices suggest that when the particle is small enough, most of cell walls are broken by the application of ultrasound, and diffusion would not be a significant step in the extraction of such small particles. Moreover, a further decrease in the size does not result in a corresponding increase in the extraction rate.

2.1.5.2. Description of the Ultrasound-Assisted Extraction method

Limonene, being a nonpolar solvent, thus not suitable for the microwave-assisted extraction, was employed in the present research project with the UAE method described by Dong *et al*[36].

In particular, $2\ g$ of each analyte (yellow corn cob, red corn cob, mixed corn cob) were left soaking in $100\ mL$ of pure limonene for 24 hours, then the samples were extracted in an ultrasonic cleaner (*BPAC-04SK-180D*) at $40\ °C$ for 30 minutes, with an ultrasonic frequency of $40\ kHz$ and a power of $180\ W$. The obtained solutions were filtered with $0.45\ \mu m$ syringe filters, then brough to a volume of $250\ mL$ with fresh limonene, to obtain a known concentration.

The extracts were poured into glass bottles and stored in the fridge for further analyses.

[36] Dong, J. *et al.* (2014) 'Antioxidant activities and phenolic compounds of cornhusk, corncob and stigma maydis', *Journal of the Brazilian Chemical Society*, 25 (11), pp. 1956–1964.

2.2. Characterisations performed

2.2.1. Evaluation of the Total Phenolic Content (TPC)

The most used method to measure the content of phenolic compounds is the *Folin-Ciocalteu* test. It relies on the Folin-Ciocalteu reagent, made by a mixture of phosphomolybdate and phosphotungstate, and can be utilised in one of the forms showed in Scheme 14.

$$3\ H_2O \cdot P_2O_5 \cdot 13\ WO_3 \cdot 5\ MoO_3 \cdot 10\ H_2O$$
$$3\ H_2O \cdot P_2O_5 \cdot 14\ WO_3 \cdot 4\ MoO_3 \cdot 10\ H_2O$$

Scheme 14: *Folin-Ciocalteu Reagent forms*

The reagent is reduced in alkaline conditions, leading to the formation of anions like $(PMoW_{11}O_{40})^{4-}$, blue coloured, which can be read by a spectrophotometer (*Shimadzu – UVmini 1240*) at $\lambda_{MAX} = 765\ nm$.

The first step of the test is to create a calibration curve of a known phenolic compound, to be used as a reference. So, a gallic acid stock solution was prepared, with a concentration of $1\ mg/mL$, mixing $50\ mg$ of gallic acid with $5\ mL$ of ethanol and bringing to volume ($50\ mL$) with *milli-Q* water. From this, standard solutions are prepared, with a concentration ranging from $0\ \mu g/mL$ to $250\ \mu g/mL$. An alkaline condition is required for the test, so a solution of $75\ g/L$ of Na_2CO_3 is prepared, by mixing $3.75g$ of sodium carbonate in $50\ mL$ of *Milli-Q* water.

To read the absorbance, $0.5\ mL$ of the different gallic acid solutions are poured in a vial, with $2\ mL$ of Folin – Ciocalteu reagent and $2.5\ mL$ of sodium carbonate. The samples are then left in the dark at $25\ °C$ for 30 minutes, to let the colouration develop. After that, the absorbance can be measured. Pure water is used as a blank.

The absorbance read for the $250\ \mu g/mL$ solution was not stable, oscillating between two quite different values. This was probably due to the fact that for absorbances higher than $1/1.5$ the correlation is no longer linear, therefore both values were taken into account, and the most suitable with the calibration curve was used. The results are shown in Table 7.

Table 7: *Gallic acid absorbances*

GALLIC ACID STOCK SOLUTION (1 mg/mL)		
Gallic acid mass (mg)	Solution volume (mL)	Gallic acid concentration (µg/mL)
50.2	50	1004

GALLIC ACID CALIBRATION CURVE				
Gallic acid concentration (theoretical) µg/mL	Gallic acid concentration (experimental) µg/mL	Absorbance (first reading)	Absorbance (second reading)	Absorbance (mean values)
0	0.0	0.014	0.014	0.014
25	25.1	0.318	0.315	0.317
50	50.2	0.626	0.596	0.611
100	100.4	1.133	1.130	1.131
150	150.6	1.615	1.630	1.622
200	200.8	2.128	2.129	2.128
250	251.0	2.607	2.607	2.607

After the creation of the calibration curve, which resulted to be linear (Figure 26), all the different extracts were analysed. The same concentration as for the gallic acid was used: 0.5 mL of the sample, 2 mL of Folin – Ciocalteu reagent and 2.5 mL of sodium carbonate. After 30 seconds the blue colour developed and then the test tubes were left in the dark at 25 °C for 30 minutes. They were analysed at the wavelength of $\lambda_{MAX} = 765\ nm$ and the absorbance value was taken.

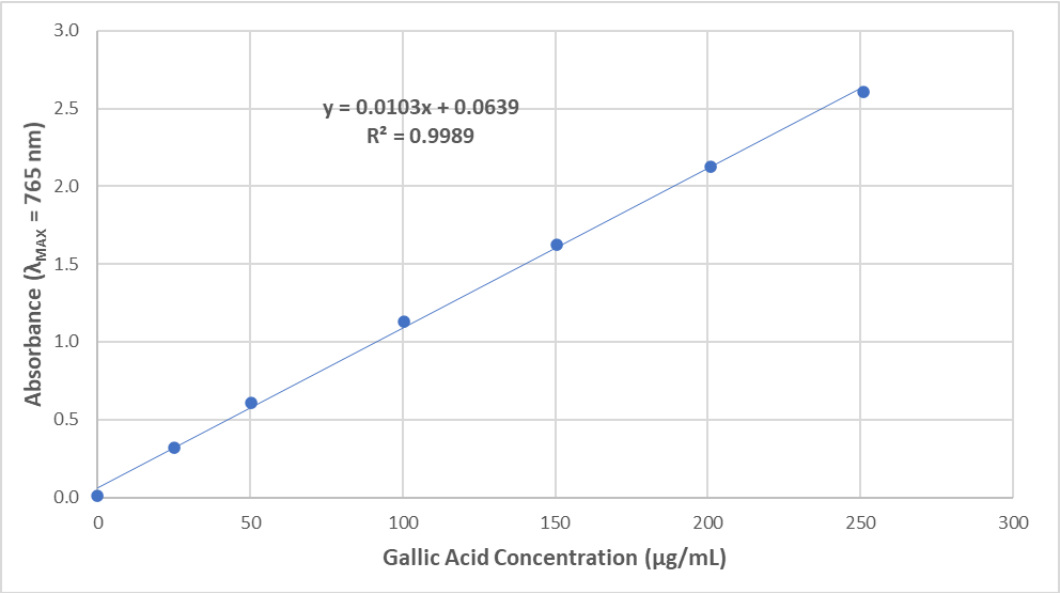

Figure 26: *Gallic acid calibration curve*

2.2.2. Evaluation of the antioxidant capacity

The selected method to evaluate the content on antioxidant molecules is the DPPH assay, which relies on the neutralisation of a $2{,}2-diphenyl-1-picrylhydrazyl$ (DPPH) radical solution.

The test must be conducted on solid samples, so the solvent in which the analytes are dissolved must be removed. This procedure, described in the next paragraphs, may require one or two steps, depending on the solvent.

2.2.2.1. Removal of the organic solvent through rotary evaporator

The removal of the organic fraction of the solution is obtained through a rotary evaporator, commonly known as *Rotavapor* (Figure 27) and composed by the four following parts:

- evaporation section, where the balloon containing the sample and the solvent rotates, while immersed in a water bath at a fixed, chosen temperature;
- vacuum pump, which removes gases from the sealed environment to leave behind a partial vacuum, able to create a continuous feed and to keep the purity of extracted solvent;
- condensing section, which brings back the vapourised solvent to a liquid state;
- receiving section, where a flask or a balloon collects the condensed solvent.

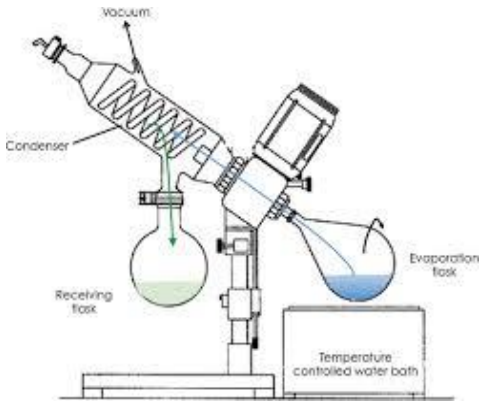

Figure 27: *Rotavapor apparatus*

The conditions used differ depending on the solvent. The temperature of the water bath was roughly the same for all samples, ranging between $40\ °C$ and $60\ °C$, but the vacuum pressure was lower for solvents which boil at higher temperatures. Pressure values are reported in Table 8.

Table 8: *Conditions used for Rotavapor concentration*

Organic solvent	Pressure mbar
Ethanol	175
Methanol	337
Limonene	106

An estimation of the pressure to be used may be done considering the polynomial equation from *Table 2-8* of *Perry's Chemical Engineers' Handbook 8th Edition* (Equation 4), where parameters $C1 - C5$, found in the same table, are peculiar of each solvent, and T is the temperature expressed in Kelvin.

$$P_{VAP}\ (Pa) = \exp\left(C1 + \frac{C2}{T} + C3\ ln\ T + C4 \times T^{C5}\right)$$

Equation 4: *Polynomial equation for vapour pressure evaluation*

The *Rotavapor* apparatus was left running in the selected conditions until all the organic solvent fraction was evaporated, which is crucial for a positive outcome of the eventual subsequent lyophilisation.

The content in the round flask was weighted before and after the procedure, to evaluate the fraction of the total vapourised solution.

Limonene is characterised by a quite high boiling point, equal to $176\ °C$ at room pressure, so a strong vacuum must be applied to consent the evaporation at a much lower temperature. However, the presence of an azeotrope with water[37] consents to strongly decrease the boiling point of the solution, up to $\sim 76\ °C$.

The reduction in boiling point is achieved for a molar fraction of water equal to 0.7636, so its content must be precisely evaluated.

In Equation 5, the moles of limonene in the solution are evaluated.

[37] Barrera Zapata, R. *et al.*, (2012) 'Modeling and simulation of a batch distillation column for recovering limonene epoxide', *Revista EIA*, 9 (18), pp. 131–141.

$$Limonene\ volume: 230\ mL \rightarrow Limonene\ mass = 0.230\ L \times 841 \frac{g}{L} = 193.43\ g$$

$$Limonene\ moles = \frac{193.43\ g}{136.24 \frac{g}{mol}} = 1.4198\ mol$$

Equation 5: *Evaluation of limonene moles*

Followingly, the moles of water which give the needed molar fraction are evaluated, as reported in Equation 6.

$$Molar\ fraction\ H_2O = 0.7636$$

$$moles\ H_2O = \ moles\ Limonene \times \frac{0.7636}{1 - 0.7636} = 1.4198\ mol \times \frac{0.7636}{0.2364} = 4.586\ mol\ H_2O$$

Equation 6: *Calculation of needed moles of water*

Having this, the mass and the needed volume of water can be calculated, as shown in Equation 7.

$$mass\ H_2O = 4.586\ mol \times 18.015 \frac{g}{mol} = 82.6175\ g$$

$$volume\ H_2O = \frac{82.6175\ g}{997.05 \frac{g}{L}} = 0.08286\ L = 82.86\ mL$$

Equation 7: *Evaluation of water mass and volume*

So, for $230\ mL$ of limonene, the azeotrope is formed by adding $82.86\ mL$ of water.

The mixture is then removed via rotary evaporator, considering a pressure of $80\ mmHg$ (corresponding to $106\ mbar$) and a starting temperature of $40\ °C$.

The temperature of the water bath was progressively increased, up to $65\ °C$, but the solution was not boiling. This was probably due to the fact that the azeotrope did not form. In fact, when reaching $70\ °C$, the underneath aqueous phase started boiling and at the end the evaporation flask was still containing the limonene fraction, which could not boil.

Therefore, to facilitate the azeotrope formation, smaller quantities were used, mixing $50\ mL$ of limonene and $18.01\ mL$ of water, but the layering of the different phases brought to the same abrupt boiling.

2.2.2.2. Removal of aqueous phase via lyophilisation

The extracts that were partially concentrated via *Rotavapor* apparatus were subjected to lyophilisation (*LABCONCO FreeZone Triad*), to remove all the water and obtain solid samples. The total volume of liquid extract is poured into a crystalliser, after measuring the weights, and sealed with holed parafilm, to consent the sublimation of water. Then, crystallisers are introduced into the lyophilisation machine.

The process consists in a first freezing of the sample, then adding heat in a vacuum environment to allow frozen water in the material to sublimate.

The first step is achieved by decreasing the temperature in the equipment up to $-50\ °C$, for about two hours. When the sample reached a temperature lower than $-20\ °C$, vacuum is gradually applied until $0.01\ mbar$. Then the temperature is increased up to $20\ °C$, to consent a rapid sublimation of water. Samples are left in the lyophilisation apparatus for 24 hours, then they are removed and weighted, to evaluate the yield of the extraction and stored in the fridge for further analyses.

2.2.2.3. DPPH assay

All the lyophilised samples were analysed through the DPPH assay. DPPH is the common abbreviation for $2{,}2-diphenyl-1-picrylhydrazyl$. This molecule is a radical, as well as a trap for other radicals, therefore the rate of reduction of a chemical reaction upon DPPH addition is an indicator of the antioxidant power of the analyte.

DPPH shows a strong absorption band around $\lambda_{MAX} = 520\ nm$, forming a deep violet colour in solution. When the DPPH is neutralised, it switches to a pale-yellow colour, as shown in Figure 28. In this way, the decrease in the read absorbance can be related to the content of antioxidants in the analyte.

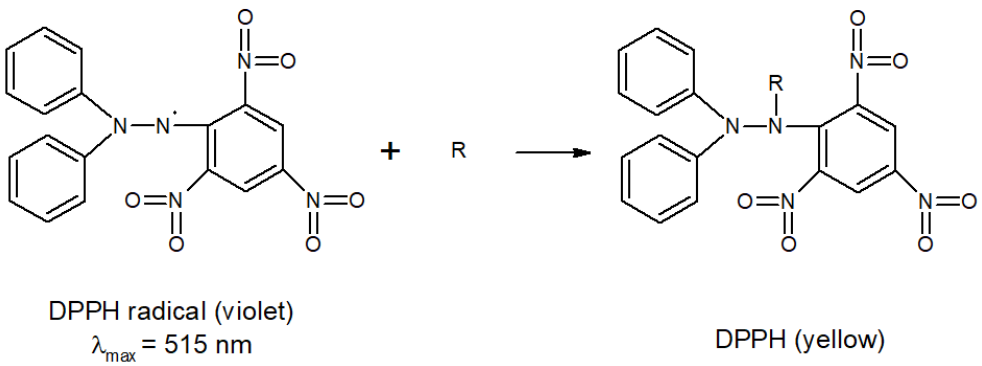

Figure 28: *DPPH radical neutralisation reaction*

The assay is generally conducted with the aim of finding the concentration of the sample that reduces the absorbance to 50% ($EC50$) of the initial value. The lower is the concentration needed, the higher will be the content of antioxidants in the analysed sample.

In order to obtain a comparative result, ascorbic acid, which structure is shown in Figure 29, is used as reference.

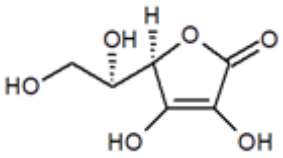

Figure 29: *Ascorbic acid*

A fresh 60 μM solution of DPPH must be prepared daily. The molar mass of DPPH is 394.32 g/mol, so the stock solution is prepared as shown in Equation 8.

$$Molar\ concentration = 60\ \mu M = 6 \times 10^{-5}\frac{mol}{L}$$

$$Concentration = 394.32\frac{g}{mol} \times\ 6 \times 10^{-5}\frac{mol}{L} = 0.02366\frac{g}{L}$$

Equation 8: *Evaluation of DPPH concentration*

Considering a 100 mL flask, a weight of 2.366 mg of pure DPPH is needed.

A stock solution of each extract must be prepared as well. A concentration of 1 mg/mL is required, so 10 mg of each sample are weighted and inserted into a 10 mL flask (or 25 mg in 25 mL, depending on the yield of the lyophilisation). From this, standard solutions at different concentrations are prepared, ranging from 0 $\mu g/mL$ to 1000 $\mu g/mL$. Then, in a vial, 0.1 mL of each standard solution are mixed with 3.9 mL of DPPH. The vials are incubated in the dark for 30 minutes at 25 °C, to develop the colour, then their absorbance is measured in the UV-Vis spectrophotometer (*Shimadzu – UVmini 1240*) at $\lambda_{MAX} = 515\ nm$, using pure ethanol as blank.

2.3. Extrusions and material characterisations

2.3.1. Differential Scanning Calorimetry (DSC)

DSC is a calorimetric technique in which the sample and a reference inert material are placed in two different crucibles and their behaviour is analysed as temperature is increased. The main feature of the DSC is the presence of two separated heating sourced: in this way, the applied heating energy can be directly measured.

Measurement of oxidative induction time (OIT)[38]

The oxidative induction time is a relative measure of the resistance of a material to oxidative decomposition. This parameter is measured by performing an isothermal DSC, with generally three steps: at the beginning, the sample is placed in the equipment and undergoes heating in nitrogen environment, following a constant ramp of temperature. Then, once the set temperature is reached, the sample is kept in isothermal conditions for a few minutes, to consent stabilisation. Finally, nitrogen is removed, and an oxygen flow is activated, to evaluate the oxidative decomposition of the sample. The OIT is then determined by the time interval between oxygen insertion and the onset point of the exothermal oxidation, evaluated by a positive change in slope, as shown in Figure 30[39].

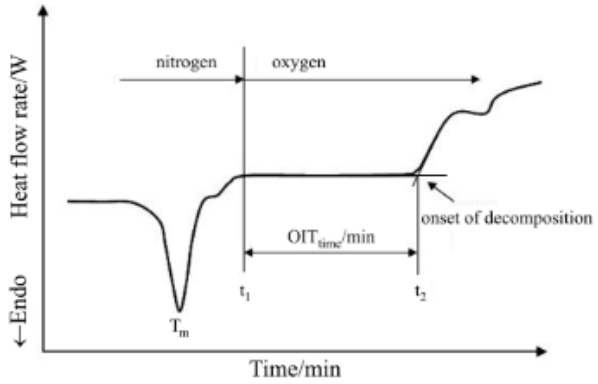

Figure 30: *Evaluation of oxidative induction time*

[38] https://www.netzsch-thermal-analysis.com/en/contract-testing/glossary/oxidative-induction-time-oit-and-oxidative-onset-temperature-oot/

[39] Schmid, M. *et al.* (2006) 'Determination of oxidation induction time and temperature by DSC', *Journal of Thermal Analysis and Calorimetry*, 83 (2), pp. 367–371.

2.3.2. Extrusion of extracts with polymeric matrices

2.3.2.1. Selection of polymeric matrices

Two polymer matrices were taken into account: low-density polyethylene (LDPE), which is a polyolefin and thus hydrophobic, and poly (butylene succinate – co – adipate) (PBSA), which is a polyester and thus less hydrophobic with respect to LDPE.

To evaluate the exploitability of polyethylene as a matrix for corn cob extracts, its oxidative induction time was measured: $10.2\ mg$ of neat LDPE were introduced in the DSC equipment, setting a maximum temperature of $180\ °C$. A ramp of temperature of $20\ °C/min$ was selected, with a flow of nitrogen equal to $50\ mL/min$. The isothermal condition was kept for five minutes, then the flow was switched to oxygen with the same rate. The sample was kept at $180\ °C$ for one hour, and as seen in Figure 31 the oxidative decomposition starts immediately after oxygen insertion. This makes LDPE a good matrix to study the effect of corn cob extracts, in order to evaluate the eventual shift in time of the decomposition onset.

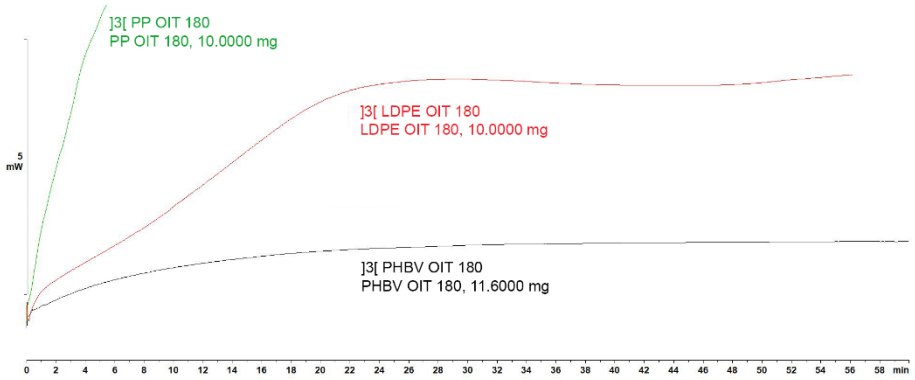

Figure 31: *DSC outcome of different polymeric matrices*

The graph in Figure 31 displays the behaviour of three polymeric materials: poly (3 – hydroxybutyrate – *co* – 3 – hydroxyvalerate) (PHBV), low-density polyethylene (LDPE), and polypropylene (PP), which show an increasing rate of oxidative degradation.

2.3.2.2. Preparation of extracts of corn cobs

Concerning the results of antioxidant extractions exposed in Paragraph 3.3, methanolic extract were selected, being those with the higher yield and higher content in antioxidants. So, $6\ g$ of mixed corn cobs and $6\ g$ of red corn cobs were extracted with microwave-assisted extraction, using a solution $50/50\ v/v$ of methanol and water as a solvent, following the method reported in Paragraph 2.1.4.

After the extraction, both samples were subjected to *Rotavapor* concentration, to remove methanol, and lyophilisation, to remove water.

In Table 9, the yield of the extraction is reported.

Table 9: *Yield of methanolic extraction*

Extract	Initial weight	Final weight	Yield
	g	mg	%
Mixed corn cobs	6.0	257.9	4.30
Red corn cobs	6.0	307.3	5.12

For the extrusion, perfectly dried samples are required, so both extracts were subjected to drying in a vacuum oven, employing a temperature of $60\ °C$ and a pressure of $50\ mbar$.

2.3.2.3. Production of polymer – additive extrudates

The production of polymeric samples was performed through extrusion (*Haake MiniLab Rheomex CTW5)*, considering a $2\ wt.\%$ concentration of additive in a total of $6\ g$ of sample introduced. For each polymer, four extrusions were realised:

- neat polymer
- polymer and *Irganox*
- polymer and mixed corn cobs
- polymer and red corn cobs.

Irganox is a class of antioxidants produced by BASF[40], useful to prevent oxidation of polymers from heat exposure. *Irganox* family is made up of sterically hindered phenols and thioethers, and an example is displayed in Figure 32.

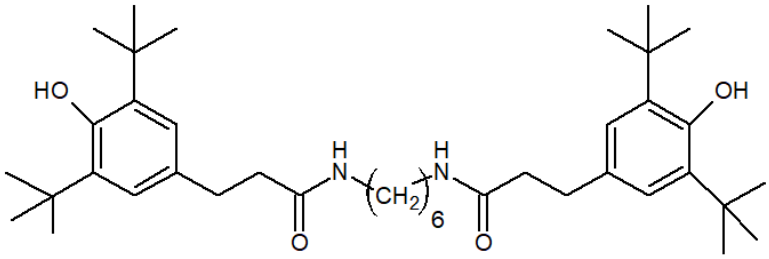

Figure 32: *Irganox 1098 structure*

[40] https://www.basf.com/us/en/products/General-Business-Topics/dispersions/Products/irganox-.html

Values of additives content are reported in Table 10.

Table 10: *Additives content in LDPE extrudates*

NEAT LDPE				LDPE + IRGANOX			
LDPE weight	Additive weight	Total weight	Additive percentage	LDPE weight	Additive weight	Total weight	Additive percentage
g	g	g	%	g	g	g	%
6.0021	0	6.0021	0	5.8813	0.1196	6.0009	1.993

LDPE + MIXED CORN COB				LDPE + RED CORN COB			
LDPE weight	Additive weight	Total weight	Additive percentage	LDPE weight	Additive weight	Total weight	Additive percentage
g	g	g	%	g	g	g	%
5.8803	0.12	6.0003	2.000	5.8803	0.1201	6.0004	2.002

LDPE extrusions were realised at $140\ °C$, which corresponds to $10\ °C$ higher with respect to its melting temperature, and $100\ rpm$.

Once all the powdered sample was introduced, the machine was left on recirculation for five minutes, during which the torque ($M\ [N \cdot cm]$) and the pressure difference ($\Delta P\ [bar]$) were evaluated. Results for all the analytes are reported in Table 11.

Table 11: *Torque and pressure difference of the analytes*

NEAT LDPE							LDPE + IRGANOX						
Time (min)	0	1	2	3	4	5	Time (min)	0	1	2	3	4	5
M (N·cm)	70	70	68	68.5	67.5	-	M (N·cm)	61	64	62	61	61.5	62
ΔP (bar)	29	29	29.5	29.5	29	-	ΔP (bar)	30	30.5	29.5	29.5	29.5	28.5

LDPE + MIXED CORN COB							LDPE + RED CORN COB						
Time (min)	0	1	2	3	4	5	Time (min)	0	1	2	3	4	5
M (N·cm)	89	79	77	77	76	76	M (N·cm)	85	78.5	79	77	76.5	78
ΔP (bar)	28	28	27.5	28	27.5	27.5	ΔP (bar)	28	28	28	27	27.5	27

As highlighted in Table 11, a slight decrease in torque and pressure difference was present throughout the extrusions, demonstrating that the samples may have undergone minor degradation.

PBSA was dried overnight in the vacuum oven before extruding, at $60\ °C$ and $50\ mbar$. Then, the sample was extruded at $130\ °C$ and $100\ rpm$.

Additives contents are displayed in Table 12, while extrusion parameters are shown in Table 13.

Table 12: *Additives content in PBSA extrudates*

NEAT PBSA				PBSA + IRGANOX			
PBSA weight	Additive weight	Total weight	Additive percentage	PBSA weight	Additive weight	Total weight	Additive percentage
g	g	g	%	g	g	g	%
6.0084	0	6.0084	0	5.8840	0.1212	6.0052	2.018

PBSA + MIXED CORN COB				PBSA + RED CORN COB			
PBSA weight	Additive weight	Total weight	Additive percentage	PBSA weight	Additive weight	Total weight	Additive percentage
g	g	g	%	g	g	g	%
5.3946	0.1056	5.5002	1.920	5.8792	0.1200	5.9992	2.000

Table 13: *Torque and pressure difference of the analytes*

NEAT PBSA							PBSA + IRGANOX						
Time (min)	0	1	2	3	4	5	Time (min)	0	1	2	3	4	5
M (N·cm)	33	32	32	31.5	32	32.5	M (N·cm)	33	32	32	32	31.5	31
ΔP (bar)	21	21	21	21	21	21	ΔP (bar)	21	21	21	21	20.2	20.5

PBSA + MIXED CORN COB							PBSA + RED CORN COB						
Time (min)	0	1	2	3	4	5	Time (min)	0	1	2	3	4	5
M (N·cm)	26	26	26	26	26	26	M (N·cm)	33.5	33	33	32.5	32.5	32.5
ΔP (bar)	19.5	19.5	19	19	19	19	ΔP (bar)	21.5	21.5	21.5	21	21	21

For PBSA, Table 13 shows an even minor decrease in torque and pressure difference, demonstrating a higher stability of the polymer during extrusion.

Figure 33 shows extrudates of neat LDPE and LDPE with mixed corn cobs, while Figure 34 shows extrudates of neat PBSA and PBSA with mixed corn cobs.

Figure 33: *Extrudates of neat LDPE (left) and LDPE with mixed corn cobs (right)*

Figure 34: *Extrudates of neat PBSA (left) and PBSA with mixed corn cobs (right)*

2.3.3. Measurement of Oxidative Induction Time (OIT)

2.3.3.1. Low-Density Polyethylene extrudates

The first test performed on extrudates regards the measurement of the oxidative induction time, as described in Paragraph 2.3.1. In order to have reliable results, a suitable temperature must be chosen. The initial part of the temperature path was set with a ramp of $20\ °C/min$, starting from $30\ °C$ to $180\ °C$ in nitrogen environment ($50\ mL/min$), then, to consent stabilisation, the sample was left at $180\ °C$ for five minutes. Finally, nitrogen flow was replaced with oxygen, with the same rate of $50\ mL/min$, for a total duration of one hour. However, the exothermic peak due to oxidative degradation was not steep enough to consent an easy evaluation of the onset point, so the temperature was increased to $200\ °C$, keeping the same ramp of temperature but increasing the stabilisation time to 10 minutes. The three steps of the evaluation are reported in Table 14.

Table 14: *Parameters for OIT measurement of LDPE extrudates*

Parameters	Step 1	Step 2	Step 3
Temperature (°C)	30 - 200 (20 °C/min)	200	200
Time (min:sec)	-	10	60
Flow	N_2 - 50 mL/min	N_2 - 50 mL/min	O_2 - 50 mL/min

As displayed in Figure 35, the oxidation peak resulted to be steeper, and easier to be evaluated.

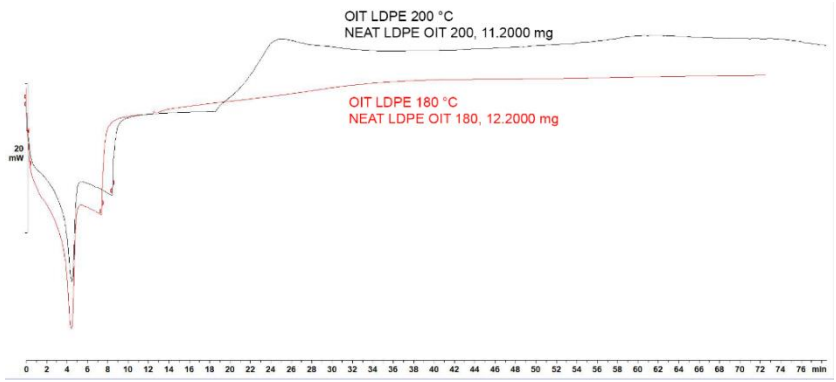

Figure 35: *DSC results of neat LDPE at* $180\ °C$ *and* $200\ °C$

So, the same parameters were considered for all the samples, in order to compare the behaviours of the polymer with the different extracts.

2.3.3.2. Poly (butylene succinate – co – adipate) extrudates

The measurement of oxidative induction time was repeated for PBSA samples, in order to analyse the behaviour of the different additives. As for LDPE, a suitable temperature must be chosen for the experiment, to have a well-visible degradation curve. Three different tests were performed, gradually increasing the final temperature from $180\ °C$ to $230\ °C$.

Results of the DSC are reported in Figure 36.

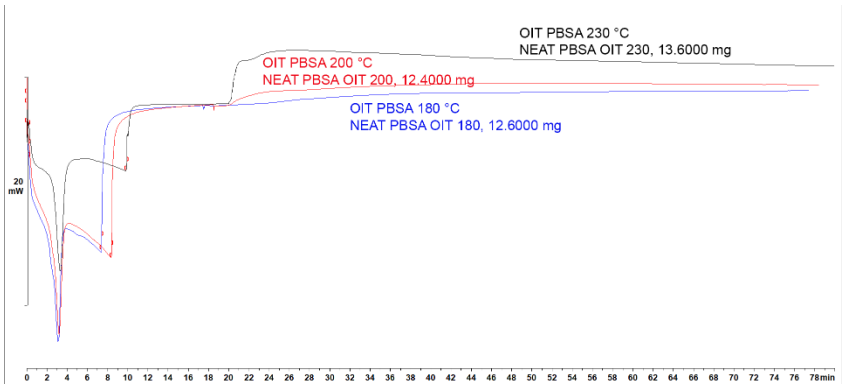

Figure 36: *DSC outcomes for neat PBSA samples*

The chosen parameters for the measurement of OIT are reported in Table 15.

Table 15: *Parameters for OIT measurement of PBSA analytes*

Parameters	Step 1	Step 2	Step 3
Temperature (°C)	30 - 230 (20 °C/min)	230	230
Time (min:sec)	-	10	60
Flow	N_2 - 50 mL/min	N_2 - 50 mL/min	O_2 - 50 mL/min

2.3.4. Rheology measurements and principles[41]

The rheometer used for materials characterisation (*Ares SN:4X621108*) is an oscillating rotational rheometer with a parallel plate geometry. In this equipment, the polymer under analysis is placed between the plates, one fixed and one rotating, and different types of experiment can be performed. The four essential parameters of the rheometer are strain, frequency of rotation, temperature, and time, so three of them can be kept constant while the fourth is changed.

For example, performing a *frequency sweep* test, the behaviour of the analyte is evaluated at a constant temperature and strain, with the aim to evaluate many different parameters, such as the storage modulus (G'), the loss modulus (G''), the tangent to the phase shift angle ($\tan\delta$), and the complex viscosity (η^*).

G' and G'' represent, respectively, the elastic portion of the viscoelastic behaviour and the viscous portion of the viscoelastic behaviour of the polymer. They both derive from the complex shear modulus G^*, defined in Equation 9, where τ_A represents the shear stress amplitude and γ_A represents the strain amplitude.

$$G^* = \frac{\tau_A}{\gamma_A}$$

Equation 9: *Definition of complex shear modulus*

The application of a sinusoidal shear strain produces a sinusoidal stress phase, shifted by a certain amount δ. This value differs depending on the behaviour of the polymer:

- if the material is ideally elastic, there is no shift in time between the stress applied and the response, giving a value of $\delta = 0°$ ($\tan\delta = 0$);
- if the material is ideally viscous, the response is out of phase with the stress applied, giving a value of $\delta = 90°$ ($\tan\delta \rightarrow \infty$);
- if the material is viscoelastic, as for the vast majority of polymers, the value of the phase shift is comprised between $\delta = 0°$ and $\delta = 90°$.

From the decomposition of the stress in an elastic and a viscous portion, the tangent to the phase shift angle can be defined as described in Equation 10.

[41] Macosko, C. W. (1996) *Rheology: Principles, Measurements and Applications*, *Powder Technology*, Wiley-VCH, chap. 3, pp 121-124.

$$\tan\delta = \frac{G''}{G'}$$

Equation 10: *Definition of the phase shift angle*

The decomposition of the stress also arises a decomposition of the complex viscosity (η^*), giving a dynamic viscosity (η'), defined in Equation 11, and an elastic part of the complex viscosity (η''), defined in Equation 12, where ω represents the frequency.

$$\eta' = \frac{G''}{\omega}$$

Equation 11: *Definition of dynamic viscosity*

$$\eta'' = \frac{G'}{\omega}$$

Equation 12: *Definition of the elastic part of the complex viscosity*

Coupling Equations 11 and 12, the magnitude of the complex viscosity is obtained, as shown in Equation 13.

$$|\eta^*| = (\eta'^2 + \eta''^2)^{\frac{1}{2}} = \left[\left(\frac{G''}{\omega}\right)^2 + \left(\frac{G'}{\omega}\right)^2\right]^{\frac{1}{2}} = \frac{1}{\omega}|G^*|$$

Equation 13: *Evaluation of the magnitude of complex viscosity*

Typical results from sinusoidal experiments on a polymer melt are exposed in Figure 37.

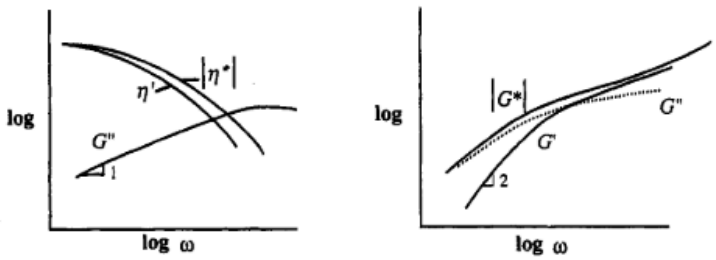

Figure 37: *Typical outcomes of sinusoidal experiments on polymer melt*

The first samples to be analysed were the low-density polyethylene extrudates: a frequency sweep test was performed, to evaluate the effect of the different additives on polymer characteristics as the rotation speed increases. The parameters of the test are reported in Table 16.

Table 16: *Parameters of LDPE analytes frequency sweep test*

Temperature (°C)	Strain (%)	Frequency range (rad/s)
140	5	0.1 - 100

In particular, the temperature was taken equal to the extrusion one, and the value of strain percentage was taken from previous tests.

The same frequency sweep test was repeated for PBSA analytes, with a slight variation in parameters, as reported in Table 17.

Table 17: *Parameters of PBSA analytes frequency sweep test*

Temperature (°C)	Strain (%)	Frequency range (rad/s)
130	3	0.1 - 100

Also in this case, the chosen temperature is equal to the extrusion one and the strain percentage derives from previous analyses

2.3.5. Thermal ageing

Thermal ageing is a technique which consents to accelerate the degradation of the polymer, in order to study the effect of the additives for a long-term application.

To achieve this, samples of LDPE and PBSA with *Irganox* and corn cobs extracts are placed in an oven at $85\ °C$, and analysed through the rheometer after 3 and 7 days.

To compare the characteristics of the thermally degraded polymers with those of the undegraded one, all the samples underwent rheology measurements, with the same parameters displayed in Paragraph 2.3.4.

2.3.6. Photo ageing

2.3.6.1. Photo-Oxidative degradation in polymers

Photochemical reactions are defined as those occurring in a polymer which is exposed to UV light, and which are connected with changing chemical structure of the system. A typical photochemical sequence is divided in three stages:

i. the absorption of radiations, which induces an electronically excited state;
ii. the primary photochemical process, involving electronically excited states;
iii. the secondary, or “dark” reactions of the radicals, radical ions, ions, and electrons produced by the primary process.

Photodegradation of a polymer is generally considered a combined result of primary and secondary reactions, which change the primary structure of the material by chain scission, crosslinking and oxidative processes.

These different processes take place in different parts of the polymer: while degradation and crosslinking reside predominantly in the amorphous part of the material, the other radiation-induced processes start at specifical radiation sensitive sites (chromophoric groups). It is also generally accepted that photo-oxidation reactions are initiated at the surface, giving rise to a gradient of degraded material across the thickness of the analyte[42].

Photodegradation of polymers depends on different physical factors, as displayed in the following paragraphs[43].

Effect of free volume

The free volume of a polymer matrix, defined in Equation 14, represents the difference between the total volume of the matrix (V_T) at a temperature T and the theoretical molecular volume of the most dense packing of the matrix molecules at $T = 0\ K$ (V_0).

$$V_f = V_T - V_0$$

Equation 14: *Definition of free volume*

As represented in Figure 38, the amount of free volume increases with temperature, with a consistent change in slope occurring at the glass transition temperature.

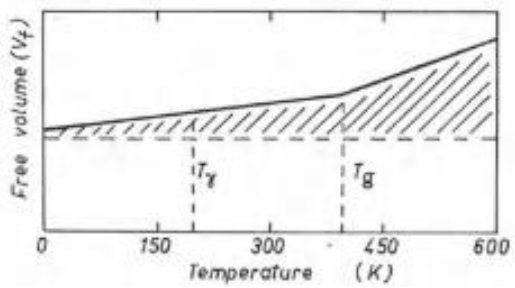

Figure 38: *Dependence of free volume on temperature*

[42] Rabek, J. F. (1975) *Photodegradation of Polymers, Physical Characteristics and Applications,* Springer, chap. 4, p. 51.

[43] Rabek, J. F. (1975) *Photodegradation of Polymers, Physical Characteristics and Applications,* Springer, chap. 5, pp. 98 – 107.

Breaking of polymer bonds due to irradiation causes fragments to occupy more volume than the reactant, giving the formation of strains and stresses which are responsible for the development of micro cracking and degradation of irradiated material.

Effect of glass transition temperature

The glass transition temperature (T_g) is one of the three fundamental transitions occurring in a semicrystalline polymer upon change in temperature, together with the crystalline melting temperature (T_m) and the decomposition temperature (T_C). Below the glass transition temperature, chain segments are in a disordered, fixed position. Some small molecular movements are still possible, such as vibrations about a fixed position, but a diffusional rearrangement is less probable. With increasing temperature, the amplitude of vibration rises, and chain segments and loops may perform rotational and transitional motions. Above the glass transition temperature, the slip of the entire molecule is predominant, and the polymer chain gains a conformational freedom comparable to that of a solution. Concerning the photo-oxidation, in amorphous and semicrystalline polymers T_g plays a fundamental role, since the mobility of the chains and radicals increases above the transition point and, simultaneously, oxygen diffusion occurs more rapidly.

Effect of crystallinity

The majority of polymers shows a partially crystalline structure, with these regions affecting the chemical and physical properties of the macromolecule. Crystallinity also imposes certain constraints on the photo-oxidative degradation of polymers: while the absorption of UV irradiation and the formation of excited states is generally unaltered, these constraints apply to secondary reactions, such as the stability of radicals and the diffusion of oxygen towards them.

Therefore, oxidation of semicrystalline polymers (PE, PP, …) is considered to occur within the amorphous region, treating the neighbouring crystalline fraction as a boundary for these reactions.

Effect of molecular weight

The molecular weight of the polymer can affect the photoreactions occurring in a solid matrix, since they are diffusion controlled and much more efficient in low molecular weight compounds. Longer chains are then more subjected to oxidative attack and chain rupture than shorter chains.

Moreover, the rate of formation of oxidation products is generally faster in crosslinked polymers.

Effect of the formation of hydrogen bonds

Hydrogen bonding is an electrostatic type of interaction which occurs since hydrogen is able to form a link between two atoms, most strongly with fluorine, oxygen and nitrogen.

The increase in the amount of photo-oxidation products can be accompanied with the reduction of free volume, since the oxidation products that are being formed interact through dipole-dipole interactions, and specifically through hydrogen bonding between acidic hydrogen and basic oxygen groups.

Although the energies of hydrogen bonds are weak ($4 - 12\ kcal/mol$) in comparison to covalent bonds ($\sim 90\ kcal/mol$), this kind of interaction is sufficient to produce appreciable frequency and intensity variation in the vibrational IR spectra. In fact, IR spectroscopy is the most used informative source to establish the presence of hydrogen bonds.

2.3.6.2. Evaluation of photo ageing on polymeric matrices

In this experiment, three samples for each polymer were subjected to accelerated artificial photo ageing chambers in anhydrous conditions, utilising the *SEPAP 12.24*. From the results of OIT in Paragraph 3.4, the mixed corn cob extract was selected as the best one and analysed together with the neat polymer and the polymer with *Irganox*.

The excitation light in the *SEPAP* is provided by four $400\ W$ mercury vapour lamps arranged at the four corners of a parallelepiped. These lamps have their shorter wavelength removed by a borosilicate glass envelope and this, together with the controlled environmental temperature, creates an optimal compromise between photochemical excitation and thermal excitation.

Prior to the insertion in the *SEPAP* equipment, a film of each analyte was realised through a manual press, considering a temperature of $130\ °C$ for PBSA samples and of $140\ °C$ for LDPE samples.

The mean thickness of films was measured, as displayed in Table 18, then the controlled degradation was started. Polymeric samples were taken after 24 and 48 hours, to be analysed through rheology measurements.

Table 18: *Mean thickness of polymeric films*

Sample	LDPE	LDPE + IRGANOX	LDPE + MCC	PBSA	PBSA + IRGANOX	PBSA + MCC
Mean Thickness (µm)	117.9	118.8	120.8	66.4	95.8	92.9

3. Results and discussion

3.1. Total Phenolic Content (TPC)

3.1.1. Ethanolic extracts – MAE and Soxhlet extraction methods

The analysis of the Total Phenolic Content (TPC) follows the Folin-Ciocalteu method, relying on the creation of a calibration curve with a known phenolic compound, gallic acid was selected, and the subsequent evaluation of the absorbance of the samples, to calculate the TPC as Gallic Acid Equivalents (GAE). The wavelength set in the UV-Vis spectrophotometer was $\lambda_{MAX} = 765\ nm$.
The obtained absorbance values are reported in Table 19, where *(S)* represents samples from Soxhlet extraction and *(M)* represents samples from MAE.

Table 19: *UV analysis results*

Extract	Mass	Solution Volume	Concentration	Absorbance
	g	mL	g/L	(λ = 765 nm)
Red Corn Cob (S)	7.0046	500	14.01	0.469
Red Corn Cob (M)	2.0079	250	8.03	0.465
Yellow Corn Cob (S)	7.0077	500	14.02	0.518
Yellow Corn Cob (M)	2.0019	250	8.01	0.474
Mixed Corn Cob (S)	7.001	500	14.00	0.658
Mixed Corn Cob (M)	2.0014	250	8.01	0.613
Corn Leaves (S)	2.0077	500	4.02	0.223
Corn Leaves (M)	2.0057	250	8.02	0.373

Once all the absorbances were obtained, the concentration in gallic acid equivalents was evaluated, as well as the total phenolic content. The calculations in Equations 15 and 16 are reported only for the red corn cob from Soxhlet extraction, while for the other samples only the results are shown.

$$Calibration\ curve\ equation \rightarrow ABS = 0.0103 \times concentration + 0.0639$$

$$Concentration\ \left[\frac{mg_{GAE}}{L}\right] = \frac{ABS - 0.0639}{0.0103} = \frac{0.469 - 0.0639}{0.0103} = 39.33\,\frac{mg_{GAE}}{L}$$

Equation 15: *Evaluation of Total Phenolic Content (TPC) in* mg_{GAE}/L

From the result of Equation 15, the TPC expressed as mg_{GAE}/g_{SAMPLE} can be obtained as displayed in Equation 16.

$$TPC\ \left[\frac{mg_{GAE}}{g_{SAMPLE}}\right] = \frac{Concentration\ \left[\frac{mg_{GAE}}{L}\right]}{Concentration\ \left[\frac{g_{SAMPLE}}{L}\right]} = \frac{39.33}{14.01} = 2.81\,\frac{mg_{GAE}}{g_{SAMPLE}}$$

Equation 16: *Evaluation of the TPC in* mg_{GAE}/g_{SAMPLE}

The same calculations are repeated for all the analytes, and the results shown in Table 20 and Figure 39.

Table 20: *TPC of all the extracts*

Extract	Concentration - Gallic Acid Equivalents	Total Phenolic Content
	mg_{GAE}/L	mg_{GAE}/g_{SAMPLE}
Red Corn Cob (S)	39.33	2.81
Red Corn Cob (M)	38.94	4.85
Yellow Corn Cob (S)	44.09	3.15
Yellow Corn Cob (M)	39.82	4.97
Mixed Corn Cob (S)	57.68	4.12
Mixed Corn Cob (M)	53.31	6.66
Corn Leaves (S)	15.45	3.85
Corn Leaves (M)	30.01	3.74

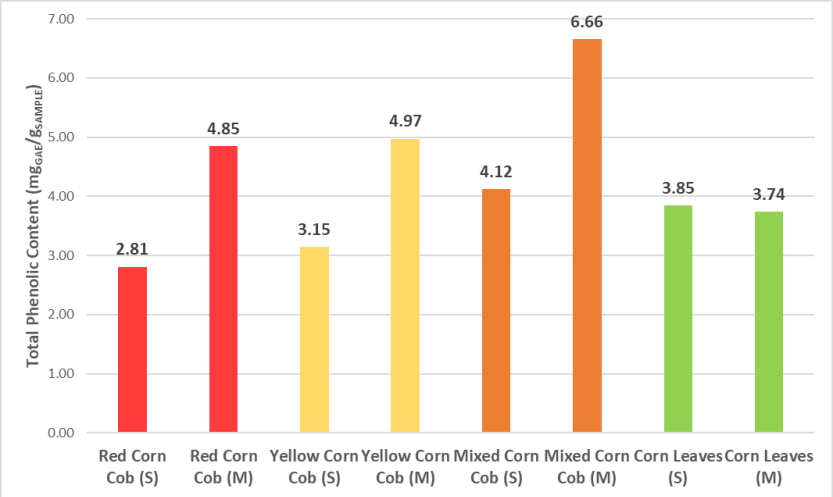

Figure 39: *TPC of the different extracts*

As displayed, MAE gives a higher content in terms of phenolic compounds with respect to Soxhlet extraction, having the highest value from mixed corn cob equal to 6.66 mg_{GAE}/g_{SAMPLE}.
In order to obtain more valuable results, the test was repeated a second time, with the outcomes shown in Table 21 and Figure 40.

Table 21: *TPC of the different extracts from the second Folin-Ciocalteu test*

Extract	Concentration - Gallic Acid Equivalents	Total Phenolic Content
	mg_{GAE}/L	mg_{GAE}/g_{SAMPLE}
Red Corn Cob (S)	36.51	2.61
Red Corn Cob (M)	38.94	4.85
Yellow Corn Cob (S)	44.86	3.20
Yellow Corn Cob (M)	-	-
Mixed Corn Cob (S)	72.05	5.15
Mixed Corn Cob (M)	55.64	6.95
Corn Leaves (S)	21.95	5.47
Corn Leaves (M)	30.69	3.83

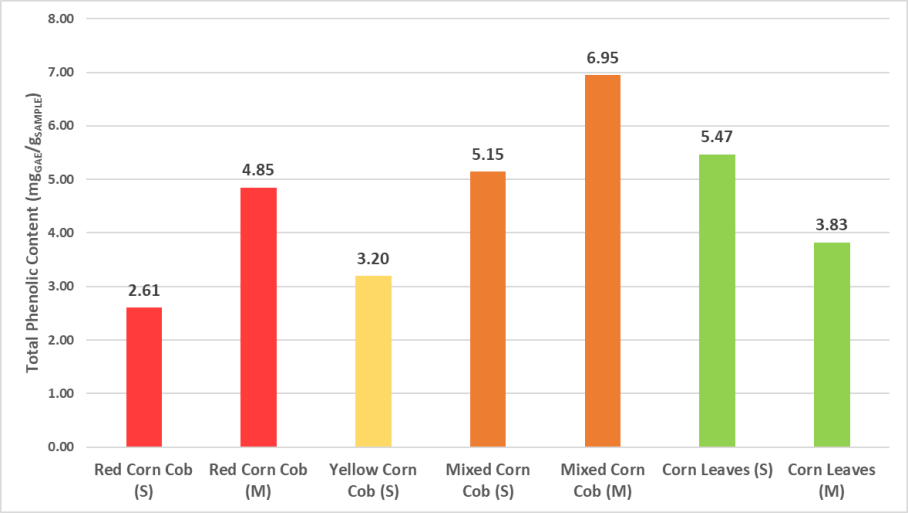

Figure 40: *TPC of the different extracts from the second Folin-Ciocalteu test*

The results from both assays may now be compared, as shown in Figure 41.

Extract	Total Phenolic Content (1)	Total Phenolic Content (2)
	mg_{GAE}/g_{SAMPLE}	mg_{GAE}/g_{SAMPLE}
Red Corn Cob (S)	2.81	2.61
Red Corn Cob (M)	4.85	4.85
Yellow Corn Cob (S)	3.15	3.20
Yellow Corn Cob (M)	4.97	-
Mixed Corn Cob (S)	4.12	5.15
Mixed Corn Cob (M)	6.66	6.95
Corn Leaves (S)	3.85	5.47
Corn Leaves (M)	3.74	3.83

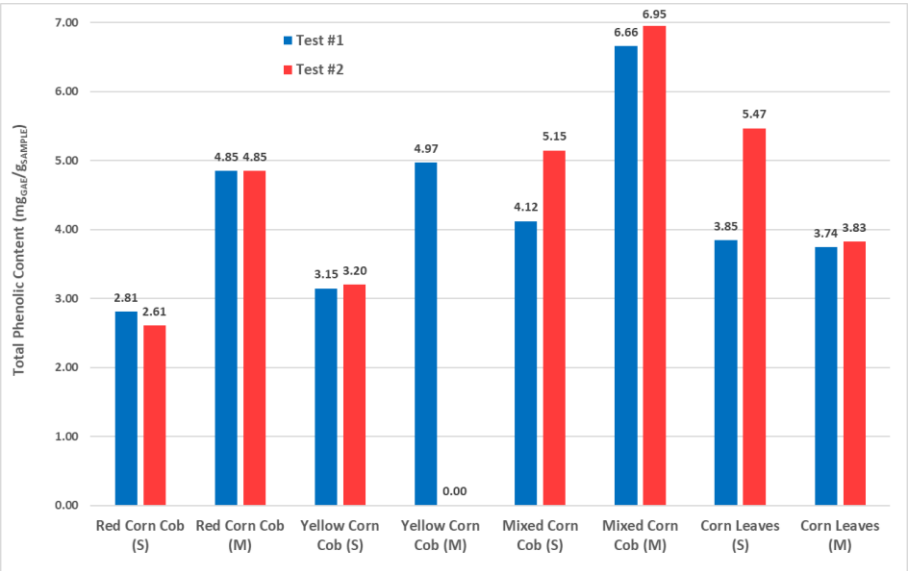

Figure 41: *Comparison between first and second TPC results*

It is possible to see how most of the values are similar to each other, showing a good reproducibility of the assay. Also the trend between the different samples is respected, with mixed corn cob demonstrating a higher TPC with respect to separate yellow and red corn cobs, probably due to a synergy of the two species.

To obtain a final value for each sample, the mean one was calculated. The two underlined values in Table 22 represent the maximum (green-coloured, from mixed corn cob extracted with MAE) and the minimum one (red-coloured, from red corn cob extracted with Soxhlet apparatus).

Table 22: *Mean TPC results for all the extracts*

Extract	Total Phenolic Content (mean) mg_{GAE}/g_{SAMPLE}
Red Corn Cob (S)	2.71
Red Corn Cob (M)	4.85
Yellow Corn Cob (S)	3.17
Yellow Corn Cob (M)	4.97
Mixed Corn Cob (S)	4.63
Mixed Corn Cob (M)	6.80
Corn Leaves (S)	4.66
Corn Leaves (M)	3.78

3.1.2. Ethanolic extracts – room temperature extraction method

The same calculations of paragraph *3.1.1* were used to evaluate the total phenolic content of the two analytes extracted with this procedure, in particular yellow corn cob and mixed corn cob.

Results are shown in Table 23.

Table 23: *Results from Folin-Ciocalteu test on yellow and mixed corn cobs*

Extract	Mass g	Solution Volume mL	Concentration g/L	Absorbance First Reading	Absorbance Second Reading	Mean Absorbance
Yellow Corn Cob	10	250	40.00	0.439	0.473	0.456
Mix Corn Cob	10	250	40.00	0.447	0.465	0.456

FOLIN-CIOCALTEU TEST		
Extract	Concentration - Gallic Acid Equivalents mg_{GAE}/L	Total Phenolic Content mg_{GAE}/g_{SAMPLE}
Yellow Corn Cob	38.07	0.95
Mix Corn Cob	38.07	0.95

Despite the extraction method at room temperature, the final TPC of the samples resulted to be lower than those obtained with MAE and Soxhlet.

3.1.3. Methanolic extracts

As for the previous analyses, the total phenolic content was analysed through the Folin-Ciocalteu technique, evaluating the content in the extracts as milligrams of gallic acid equivalents (GAE) per gram of solid sample. The test was performed on samples extracted with MAE and repeated twice. Results reported in Table 24.

Table 24: *Results of Folin-Ciocalteu tests on yellow and red corn cobs methanolic extracts*

Extract	Mass	Solution Volume	Concentration	Absorbance	Absorbance	Mean
	g	mL	g/L	First Reading	Second Reading	Absorbance
Yellow Corn Cob	2	250	8.00	0.384	0.408	0.396
Red Corn Cob	2	250	8.00	0.437	0.447	0.442

FOLIN-CIOCALTEU TEST		
Extract	Concentration - Gallic Acid Equivalents	Total Phenolic Content
	mg_{GAE}/L	mg_{GAE}/g_{SAMPLE}
Yellow Corn Cob	32.24	4.03
Red Corn Cob	36.71	4.59

As reported in Table 22 for the ethanolic extracts and Table 24 for the methanolic extracts, the content in phenolic compounds is very similar between the samples analysed, showing that the difference between the two solvents is minimal, as long as the analytes are extracted via MAE.

3.1.4. Limonene UAE extracts

The evaluation of the TPC is carried out with the same analytical procedure as for the other extracts, with the main difference being the extraction method. Limonene is nonpolar, so it cannot be utilised in the microwave. Consequently, an extraction technique assisted with ultrasound (UAE) is taken into account. Results are reported in Table 25.

Table 25: *TPC results of yellow, red, and mixed corn cobs limonene extracts*

Extract	Mass	Solution Volume	Concentration	Absorbance	Absorbance	Mean
	g	mL	g/L	First Reading	Second Reading	Absorbance
Yellow Corn Cob	2.0043	250	8.02	0.214	0.318	0.266
Red Corn Cob	2.0237	250	8.09	0.340	0.150	0.245
Mix Corn Cob	1.0015	250	4.01	0.261	0.156	0.209

FOLIN-CIOCALTEU TEST		
Extract	Concentration - Gallic Acid Equivalents	Total Phenolic Content
	mg_{GAE}/L	mg_{GAE}/g_{SAMPLE}
Yellow Corn Cob	19.62	2.45
Red Corn Cob	17.58	2.17
Mix Corn Cob	14.04	3.50

From Table 25 it is possible to see how the trend of the mixed corn cob showing a synergy is respected, but also how the TPC is lower with respect to the same samples extracted with ethanol and methanol.

The best TPC results obtained with the different extraction methods are summarised in Table 26.

Table 26: *Summarising table of TPC analyses*

FOLIN - CIOCALTEU RESULTS		
Extraction Technique	**Best analyte**	**TPC (mg_{GAE}/g_{SAMPLE})**
Ethanol - MAE	Mixed corn cobs	6.80
Ethanol - Soxhlet	Corn leaves	4.66
Ethanol - Ambient T	Mixed corn cobs	0.95
Methanol - MAE	Red corn cobs	4.59
Limonene - UAE	Mixed corn cobs	3.50

3.2. Removal of the solvent

As described in section 2, the extract antioxidant properties have to be evaluated on solid samples. For this reason, the extracts solutions were subjected to *Rotavapor* and lyophilisation in case of water presence. In the following paragraphs the specific solvent removal treatment for each type of extract and the amount of solid obtained are reported.

3.2.1. Ethanolic extracts – MAE and Soxhlet extraction methods

This first extraction method deals with a solvent made by a mixture of ethanol and water, 50% in volume. Given this, the solvent is removed in two steps: the organic fraction is evaporated via rotary evaporator, while the aqueous phase is removed via lyophilisation.

Conditions used are summarised in Table 27.

Table 27: *Conditions used for ethanol vaporisation*

Solvent	Temperature	Pressure
	°C	mbar
Ethanol	45 - 60	175

The content in the evaporation flask is weighted before and after the evaporation, in order to evaluate the yield, and results are reported in Tables 28 and 29.

Table 28: *Ethanol removed from MAE samples*

SAMPLES FROM MICROWAVE-ASSISTED EXTRACTION					
Extract	Extract weight (before RV)	Extract weight (after RV)	Weight difference	Volume difference	Total duration
	g	g	g	mL	h:min
Yellow CC	233.3	123.5	109.8	139.72	03:55
Red CC	213.9	89.6	124.3	158.17	01:20
Mix CC	214.4	116.7	97.7	124.32	01:30
Corn leaves	214.7	103.9	110.8	140.99	01:20

Table 29: *Ethanol removed from Soxhlet extracts*

SAMPLES FROM SOXHLET EXTRACTION					
Extract	Extract weight (before RV)	Extract weight (after RV)	Weight difference	Volume difference	Total duration
	g	g	g	mL	h:min
Yellow CC (1)	223	166	57	72.53	02:34
Yellow CC (2)	219.5	155.4	64.1	81.56	01:30
Yellow CC (tot)	442.5	321.4	121.1	154.10	-
Red CC	441.2	285.4	155.8	198.25	02:08
Mix CC	441.5	279.3	162.2	206.39	01:53
Corn leaves	441.3	270.9	170.4	216.83	02:07

To evaluate the volume of ethanol removed, the density must be accounted. It was calculated from the polynomial equation (Equation 17) at *Table 2-32* of *Perry's Chemical Engineers' Handbook 8th Edition*.

$$\rho\left(\frac{mol}{dm^3}\right) = \frac{C1}{C2^{1+\left(1-\frac{T}{C3}\right)^{C4}}}$$

Equation 17: *Formula for molar density evaluation*

Where T is the temperature in Kelvin and $C1 - C4$ are found in the same table, and for ethanol are shown in Table 30.

Table 30: *Ethanol parameters for density evaluation*

C1	C2	C3	C4
1.6288	0.27469	514	0.23178

Therefore, the molar density of ethanol was calculated by substituting $C1 - C4$ values as shown in Equation 18.

$$\rho\left(\frac{mol}{dm^3}\right) = \frac{1.6288}{0.27469^{1+\left(1-\frac{298.15}{514}\right)^{0.23178}}} = 17.059\,\frac{mol}{dm^3}$$

Equation 18: *Calculation of ethanol molar density*

To obtain the mass density, the molar density must be multiplied by the molar mass of ethanol (Equation 19).

$$MW = 46.068\,\frac{g}{mol} \rightarrow \rho\left(\frac{g}{dm^3}\right) = 17.059\,\frac{mol}{dm^3} \times 46.068\,\frac{g}{mol} = 785.88\,\frac{g}{dm^3}$$

Equation 19: *Calculation of ethanol mass density*

Given this, the amount of removed ethanol can be evaluated as shown in Equation 20.

$$V = \frac{weight\ difference}{density} = \frac{109.8\ g}{785.88\,\frac{g}{dm^3}} = 0.13972\ dm^3 = 139.72\ mL$$

Equation 20: *Calculation of the volume of ethanol removed*

The remaining liquid volume of extracts was subjected to lyophilisation, in order to completely remove water by sublimation and obtain solid samples, on which the DPPH assay can be performed. The amounts of solid analytes are shown in Table 31.

Table 31: *Results of lyophilisation of extracts from MAE and Soxhlet*

EXTRACTS FROM MAE			
Extract	Total final weight	Initial weight	Yield
	mg	g	%
Yellow CC	40.3	2.0019	2.01
Red CC	15.1	2.0079	0.75
Mix CC	105.6	2.0014	5.28
Corn leaves	25.1	2.0057	1.25

EXTRACTS FROM SOXHLET			
Extract	Total final weight	Initial weight	Yield
	mg	g	%
Mix CC	535.4	7.001	7.65
Corn leaves	29.9	2.0077	1.49

The amount of solid obtained differs highly from analyte to analyte, mostly due to their physical aspect once removed from the lyophilising equipment. In fact, a very low amount ($\sim 15 - 30\ mg$) is obtained from red corn cob and corn leaves, since they formed a solid with wax-like consistency, very difficult to be scratched from the crystalliser and stored in bottles. On the other hand, mixed corn cob, both from MAE and Soxhlet, presented a flakes-like structure, much easier to be removed and stored.

3.2.2. Ethanolic extracts – room temperature extraction method

In this procedure, the solvent was pure ethanol, so that only the *Rotavapor* step was necessary to obtain solid samples. Extracts were poured into the evaporation flask, and weighted before and after the vaporisation procedure, to evaluate the yield.

Conditions in the equipment were selected equal to those reported in Table 8, since the solvent is the same. Results of the evaporation are reported in Table 32.

Table 32: *Weights and yield of concentrated analytes*

Extract	Final solid weight	Initial weight	Yield
	mg	g	%
Yellow Corn Cob	94.3	10	0.943
Mixed Corn Cob	66.2	10	0.662

Also in this case, as for mixed corn cob from MAE and Soxhlet, solid analytes were obtained in the form of large flakes. Thus, a noticeable amount of solid extracts could be retrieved from both samples. The yield is evaluated considering the initial amount of corn cob equal to $10\ g$.

3.2.3. Methanolic extracts

Being a 50% mixture of water and methanol, the solvent for this extraction technique was removed with a two-step process.

The organic fraction was evaporated in the *Rotavapor* equipment, considering the conditions reported in Table 33. Results of weightings preceding and antecedent to the process are displayed in Table 34.

Table 33: *Conditions used for methanol evaporation*

Solvent	Temperature	Pressure
	°C	mbar
Methanol	45 - 60	337

Table 34: *Methanol removed from extracts*

CONCENTRATION OF THE SOLUTIONS WITH ROTAVAPOR					
Extract	Bottle weight	Initial weight	Final weight	Weight difference	Volume difference
	g	g	g	g	mL
Yellow corn cobs	156.0	215.3	166.6	48.7	61.31
Red corn cobs	157.0	216.2	183.8	32.4	40.79

The molar density for the evaluation of the volume difference was calculated with the same formula as Equation 17, but with different parameters (Table 35). The result for yellow corn cob is shown in Equation 21.

Table 35: *Parameters for methanol molar density evaluation*

DENSITY EVALUATION				
Compound	**C1**	**C2**	**C3**	**C4**
Methanol	2.3267	0.27073	512.5	0.24713

$$\rho_{mol}(T = 293.15\ K) = 24.792\frac{mol}{dm^3}$$

$$MW = 32.042\frac{g}{mol} \rightarrow \rho_{mass}(T = 293.15\ K) = \rho_{mol} \times MW = 794.38\frac{g}{dm^3}$$

$$Removed\ volume = \frac{Removed\ mass}{\rho_{mass}} = \frac{48.7\ g}{794.38\frac{g}{dm^3}} = 0.0613\ dm^3 = 61.3\ mL$$

Equation 21: *Calculation of removed methanol volume*

The remaining liquid was poured into a crystalliser, to be subjected to lyophilisation. The container was weighted, left in the equipment for 24 hours, and weighted again, to evaluate the yield. Results are shown in Table 36.

Table 36: *Yield evaluation*

Extract	**Solid weight**	**Initial weight**	**Yield**
	mg	**g**	**%**
Yellow corn cobs	97.3	2	4.865
Red corn cobs	103.3	2	5.165

These extracts showed a noticeable amount of solid extracts, reaching a yield close to 5%. This was mainly due to the appearance of the solid after lyophilisation, which allowed an easy removal from crystallisers and storage in plastic bottles.

3.2.4. Limonene extracts

As displayed in Paragraph 2.2.2.1, limonene mixtures were unable to boil, since the azeotrope with water could not form. Thus, the DPPH assay could not have been performed.

3.3. Evaluation of antioxidant activity – DPPH assay

3.3.1. Ethanolic extracts – MAE and Soxhlet extraction methods

For this assay, a stock solution of each extract must be prepared, with a concentration of $1\ mg/mL$. So, depending on the yield of solid sample retrieval, 10 or $25\ mg$ of each sample are weighted, and diluted in the correspondent amount of pure ethanol ($10 - 25\ mL$). From these stock solutions, which concentrations are reported in Table 37, standard solution at different concentrations are prepared, in a range from $0\ \mu g/mL$ to $1000\ \mu g/mL$. The absorbances obtained from UV-Vis spectrophotometer analysis are reported in Tables 38 and 39.

Table 37: *MAE and Soxhlet extracts stock solutions*

EXTRACTS STOCK SOLUTIONS			
Extracts	**Weight**	**Volume**	**Concentration**
	mg	**mL**	**mg/mL**
Yellow CC (MAE)	10.3	10	1.03
Red CC (MAE)	10	10	1
Mix CC (MAE)	24.9	25	0.996
Ascorbic Acid (ref)	25.4	25	1.016

EXTRACTS STOCK SOLUTIONS			
Extracts	**Weight**	**Volume**	**Concentration**
	mg	**mL**	**mg/mL**
Mix CC (S)	25	25	1
Corn Leaves (S)	25.2	25	1.008

Table 38: *Absorbances of standard solutions of MAE samples*

ABSORBANCES (λ_{MAX} = 515 nm) AT DIFFERENT CONCENTRATIONS									
Extracts	0	5	10	25	50	125	250	500	1000
	µg/mL	µg/mL	µg/mL	µg/mL	µg/mL	µg/mL	µg/mL	µg/mL	µg/mL
Yellow CC (MAE)	0.518	-	-	0.515	0.52	0.516	0.508	0.493	-
Red CC (MAE)	0.587	-	-	0.582	0.579	0.570	0.560	0.534	-
Mix CC (MAE)	0.584	-	-	0.584	0.582	0.575	0.564	0.548	0.494
Ascorbic Acid (ref)	0.703	0.682	0.685	0.618	0.539	0.300	0.030		

Table 39: *Absorbances of standard solutions of Soxhlet samples*

ABSORBANCES (λ_{MAX} = 515 nm) AT DIFFERENT CONCENTRATIONS									
Extracts	0	5	10	25	50	125	250	500	1000
	µg/mL	µg/mL	µg/mL	µg/mL	µg/mL	µg/mL	µg/mL	µg/mL	µg/mL
Mix CC (S)	0.705	-	-	0.715	0.713	0.710	0.699	0.682	0.640
Corn Leaves (S)	0.794	-	-	0.769	0.765	0.761	0.754	0.742	0.710

Once all the absorbances were measured, the percentage of DPPH inhibition could be calculated, as shown in Equation 22, where ABS_0 is the absorbance of the solution with pure ethanol ($0\ \mu g/mL$) and ABS_i the absorbance of the referring concentration.

$$DPPH\ inhibition\ (\%) = \frac{ABS_0 - ABS_i}{ABS_0} \times 100$$

Equation 22: *DPPH inhibition percentage calculation*

The obtained values are reported in Tables 40 and 41.

Table 40: *DPPH inhibition of MAE samples*

DPPH INHIBITION (%)									
Extracts	0 µg/mL	5 µg/mL	10 µg/mL	25 µg/mL	50 µg/mL	125 µg/mL	250 µg/mL	500 µg/mL	1000 µg/mL
Yellow CC (MAE)	0.00	-	-	0.58	-0.39	0.39	1.93	4.83	-
Red CC (MAE)	0.00	-	-	0.85	1.36	2.90	4.60	9.03	-
Mix CC (MAE)	0.00	-	-	0.00	0.34	1.54	3.42	6.16	15.41
Ascorbic Acid (ref)	0.00	2.99	2.56	12.09	23.33	57.33	95.73		

Table 41: *DPPH inhibition of Soxhlet samples*

DPPH INHIBITION (%)									
Extracts	0 µg/mL	5 µg/mL	10 µg/mL	25 µg/mL	50 µg/mL	125 µg/mL	250 µg/mL	500 µg/mL	1000 µg/mL
Mix CC (S)	0.00	-	-	-1.42	-1.13	-0.71	0.85	3.26	9.22
Corn Leaves (S)	0.00	-	-	3.15	3.65	4.16	5.04	6.55	10.58

The trend in DPPH inhibition with respect to extract concentration is displayed in Figure 42.

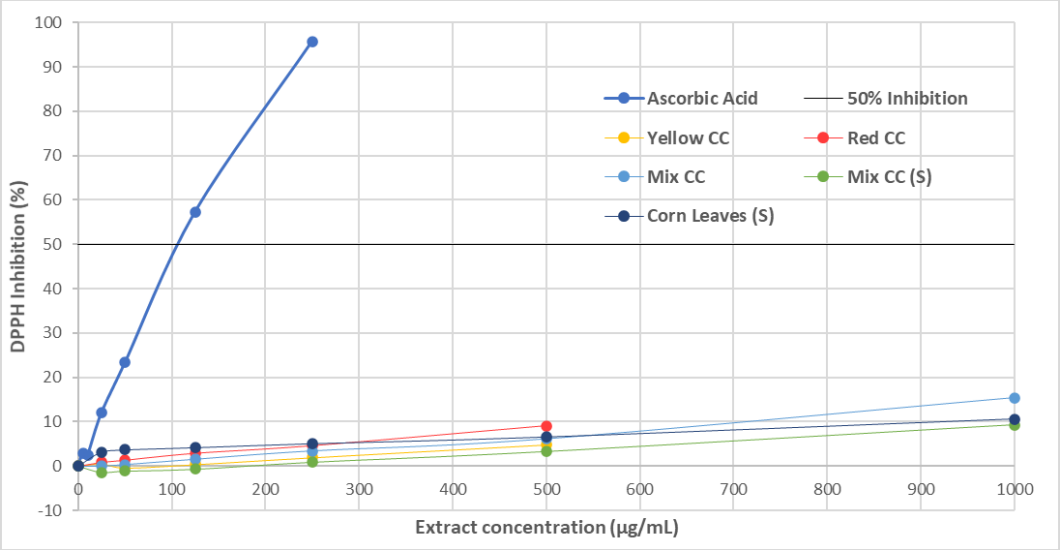

Figure 42: *Trend of DPPH inhibition with increasing extract concentration*

From Figure 42 it is possible to see how none of the extracts is able to reach the threshold limit of 50% inhibition, achieving a highest value of only 15.41% (mixed corn cob from MAE). As a comparison, ascorbic acid, a known antioxidant, is able to reach the needed value of inhibition with a concentration slightly higher than $100\ \mu g/mL$.

One of the main reasons for this very low concentration could be the high temperatures reached both in the microwave ($\sim 105\ °C$) and the Soxhlet extractor ($\sim 130 - 140\ °C$), which could have degraded the eventually present antioxidants.

3.3.2. Ethanolic extracts – room temperature extraction method

Stock and standard solutions of different samples are prepared with the same procedure illustrated in Paragraph *3.3.1*, as shown in Table 42. Then, the analysis at $\lambda_{MAX} = 515\ nm$ was performed, as well as the calculation of the inhibition percentage. Results are displayed in Table 43 and Figure 43.

Table 42: *Stock solutions of different extracts*

EXTRACTS STOCK SOLUTIONS			
Extracts	**Weight**	**Volume**	**Concentration**
	mg	**mL**	**mg/mL**
Yellow Corn Cobs	25.1	25	1.004
Mix Corn Cobs	25.9	25	1.036
Ascorbic Acid (ref)	25.4	25	1.016

Table 43: *Absorbances and DPPH inhibition percentage of extracts standard solutions*

ABSORBANCES (λ_{MAX} = 515 nm) AT DIFFERENT CONCENTRATIONS									
Extracts	0	5	10	25	50	125	250	500	1000
	µg/mL	µg/mL	µg/mL	µg/mL	µg/mL	µg/mL	µg/mL	µg/mL	µg/mL
Yellow Corn Cob	0.614	-	-	0.609	0.613	0.602	0.6	0.592	0.566
Mix Corn Cob	0.731	-	-	0.733	0.722	0.719	0.721	0.699	0.675
Ascorbic Acid (ref)	0.703	0.682	0.685	0.618	0.539	0.300	0.030		

DPPH INHIBITION (%)									
Extracts	0	5	10	25	50	125	250	500	1000
	µg/mL	µg/mL	µg/mL	µg/mL	µg/mL	µg/mL	µg/mL	µg/mL	µg/mL
Yellow Corn Cob	0.00	-	-	0.81	0.16	1.95	2.28	3.58	7.82
Mix Corn Cob	0.00	-	-	-0.27	1.23	1.64	1.37	4.38	7.66
Ascorbic Acid (ref)	0.00	2.99	2.56	12.09	23.33	57.33	95.73	-	-

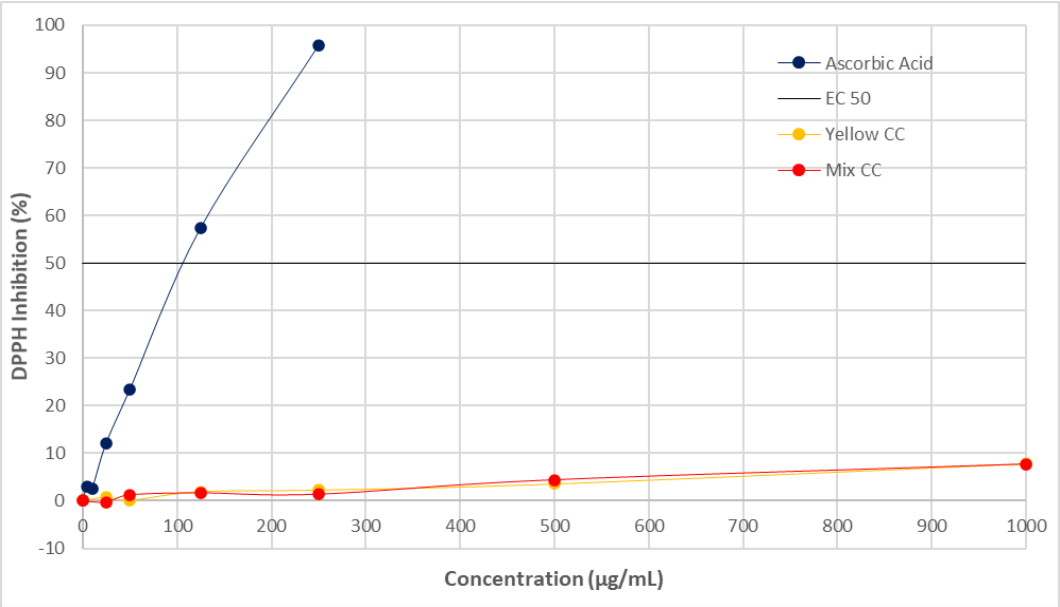

Figure 43: *Trend of DPPH inhibition with increasing concentration*

As displayed in the graph from Figure 43, not even the samples obtained with this extraction method are able to reach the threshold value. In fact, the maximum inhibition value (7.82%) is lower than the one obtained with MAE and Soxhlet methods, confirming once again that these procedures consent a better extraction of natural compounds, despite the relevant temperatures reached during the process.

3.3.3. Methanolic extracts

As for the previous tests, the DPPH assay is conducted on stock (Table 44) and standard solutions obtained from each extract. Values from UV-Vis analysis and DPPH inhibition calculation are reported in Table 45 and Figure 44.

Table 44: *Stock solutions of different extracts*

EXTRACTS STOCK SOLUTIONS			
Extracts	**Weight**	**Volume**	**Concentration**
	mg	**mL**	**mg/mL**
Yellow Corn Cob	25.3	25	1.012
Red Corn Cob	24.9	25	0.996
Ascorbic Acid (ref)	25.4	25	1.016

Table 45: *Absorbances and DPPH inhibition percentages of extracts standard solutions*

ABSORBANCES (λ_{MAX} = 515 nm) AT DIFFERENT CONCENTRATIONS									
Extracts	0	5	10	25	50	125	250	500	1000
	µg/mL	µg/mL	µg/mL	µg/mL	µg/mL	µg/mL	µg/mL	µg/mL	µg/mL
Yellow Corn Cob	0.600	-	-	0.604	0.534	0.504	0.495	0.485	0.440
Red Corn Cob	0.793	-	-	0.740	0.700	0.696	0.663	0.650	0.615
Ascorbic Acid (ref)	0.703	0.682	0.685	0.618	0.539	0.300	0.030		

DPPH INHIBITION (%)									
Extracts	0	5	10	25	50	125	250	500	1000
	µg/mL	µg/mL	µg/mL	µg/mL	µg/mL	µg/mL	µg/mL	µg/mL	µg/mL
Yellow Corn Cob	0.00	-	-	-0.67	11.00	16.00	17.50	19.17	26.67
Red Corn Cob	0.00	-	-	6.68	11.73	12.23	16.39	18.03	22.45
Ascorbic Acid (ref)	0.00	2.99	2.56	12.09	23.33	57.33	95.73	-	-

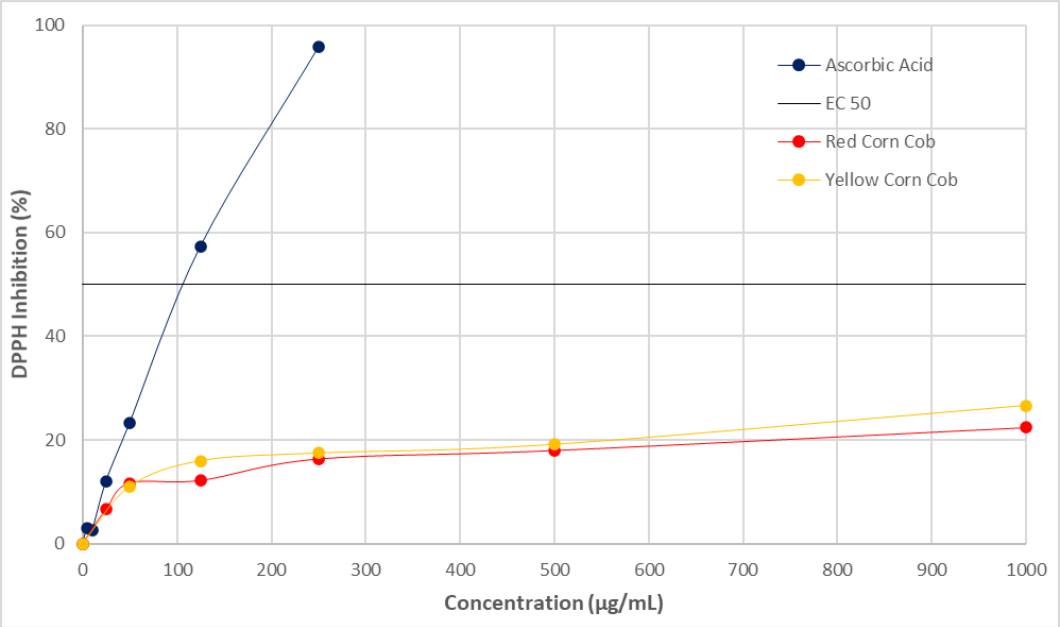

Figure 44: *Trend of DPPH inhibition with increasing extract concentration*

As demonstrated in the graph from Figure 44, even in this case the maximum value of inhibition reached from samples is not high enough to overcome the threshold of 50%.

But, as shown in Table 46, samples from methanolic extracts display the highest value of DPPH inhibition percentage. This difference may be due to higher value of methanol dielectric constant ($\varepsilon'' = 33.05, T = 298.15\ K$)[44] with respect to ethanol ($\varepsilon'' = 25.08, T = 298.15\ K$)[45], which gives a higher efficiency in microwave-assisted extractions, as reported in Paragraph 2.1.1.1.

Table 46: *Summary of DPPH inhibition percentages*

DPPH ASSAY RESULTS			
Extraction Technique	**Best analyte**	**Concentration**	**DPPH Inhibition**
		µg/mL	**%**
Ethanol - MAE	Mixed corn cob	1000	15.41
Ethanol - Soxhlet	Corn leaves	1000	10.58
Ethanol - Ambient T	Yellow corn cob	1000	7.82
Methanol - MAE	Yellow corn cob	1000	26.67

[44] http://www.ddbst.com/en/EED/PCP/DEC_C110.php

[45] http://www.ddbst.com/en/EED/PCP/DEC_C11.php

3.4. Material Characterisations – Low-Density Polyethylene

3.4.1. Measurement of Oxidative Induction Time (OIT)

Employing the same parameters reported in Table 14, all the four extrudates were analysed in the DSC equipment, in order to evaluate the different effects of the additives inserted during extrusion. So, the same procedure displayed in Paragraph 2.3.3. was taken into account for LDPE with *Irganox*, LDPE with mixed corn cobs, and LDPE with red corn cobs.

The results are shown in Figures 45 and 46.

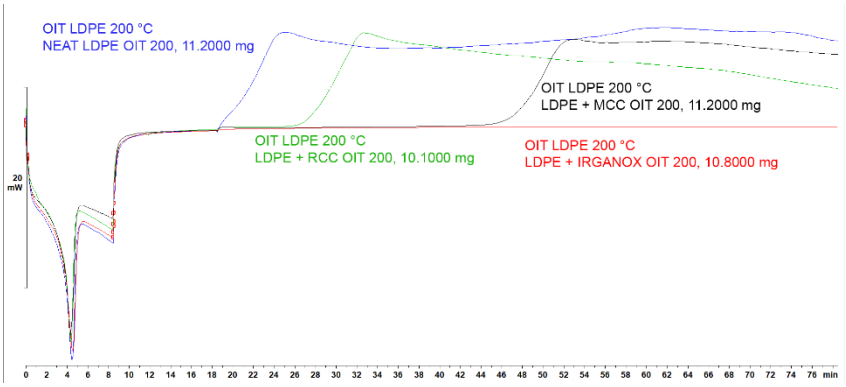

Figure 45: *DSC outcomes of LDPE extrudates*

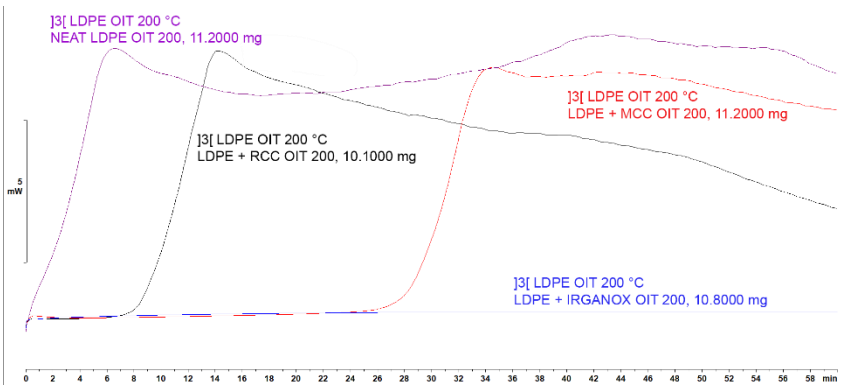

Figure 46: *Third step of DSC analysis of LDPE extrudates*

As displayed in the graphs in Figures 45 and 46, the samples show different behaviours: the extrudate of neat LDPE suffers an immediate degradation when the flow is switched to oxygen, while the sample containing 2 *wt*. % of *Irganox* does not undergo any oxidation. The samples with added corn cobs have an intermediate behaviour, with red cobs and mixed cobs reporting a lag of, respectively, ~ 8 and ~ 28 minutes between the insertion of oxidative atmosphere and the beginning of degradation. This experiment demonstrates that, even if with lower effectiveness than *Irganox*, corn cobs are able to delay the oxidative degradation of LDPE.

3.4.2. Rheology measurements

The analysis of physical properties of LDPE samples was obtained exploiting the rheometer, as reported in Paragraph 2.3.4. The main matter of comparison is the difference in viscosity among the different samples, which is able to show whether the introduction of the additive is sufficient to delay degradation of the polymer. Figure 47 displays the comparison of η^* in all extrudates, in order to analyse more efficiently any possible deviation.

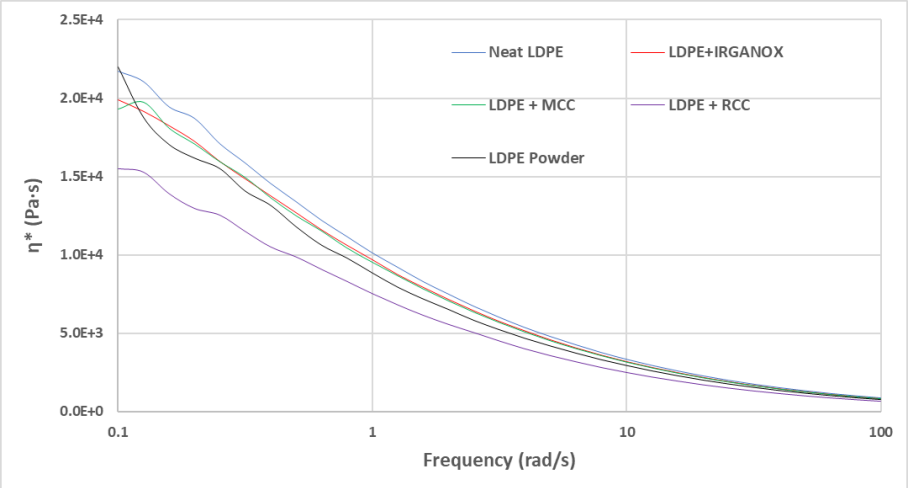

Figure 47: *Comparison of complex viscosity of LDPE samples*

As seen in Figure 47, after a first increase in viscosity due to the extrusion process, a decrease occurs at low frequency upon addition of the additives. Values of complex viscosity for a frequency of $1\ rad/s$ are reported in Table 47.

Table 47: *Values of complex viscosity of LDPE samples for* $\omega = 1\ rad/s$

Sample	LDPE Powder	Neat LDPE	LDPE + *Irganox*	LDPE + MCC	LDPE + RCC
Viscosity (Pa·s)	8.862×10^3	1.012×10^4	9.708×10^3	9.526×10^3	7.530×10^3

3.4.3. Thermal ageing

Samples which have been degraded in the oven are analysed again in the rheometer, to verify how the temperature has affected their physical properties. Extrudates were analysed after 3 and 7 days of ageing. Figure 48 displays the comparison of the complex viscosity among the different samples, while Table 48 reports the values of η^* at a frequency of $1\ rad/s$.

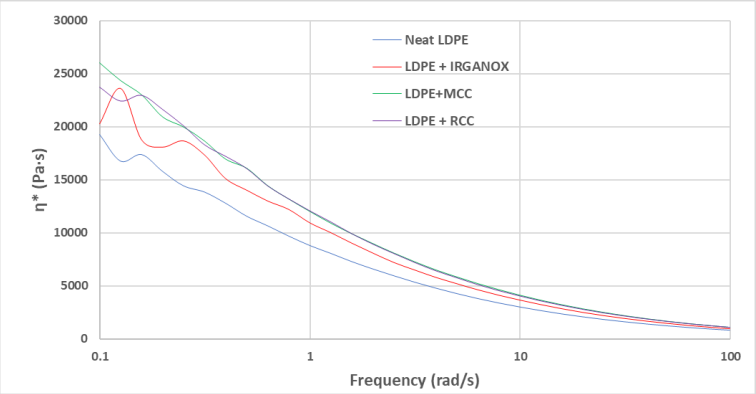

Figure 48: *Comparison of the complex viscosity of LDPE samples after three days of ageing*

Table 48: *Values of complex viscosity of LDPE samples for* $\omega = 1\ rad/s$

Sample	Neat LDPE	LDPE + *Irganox*	LDPE + MCC	LDPE + RCC
Viscosity (Pa·s)	8.798×10^3	1.096×10^4	1.202×10^4	1.209×10^4

As demonstrated from the complex viscosity, for low values of frequency the addition of additives brings an increase in η^*, which is found to be the opposite behaviour with respect to the same samples not subjected to the thermal treatment.

In fact, comparing values from Tables 47 and 48 it is possible to highlight two different degradation mechanisms: the sample of neat polymer shows a decrease in viscosity, symbol of a chain scission mechanism. On the other hand, samples with additives display an increase in viscosity, which could be related to a recombination mechanism of degradation.

Figure 49 shows the comparison of the complex viscosity among all the samples after one week of ageing.

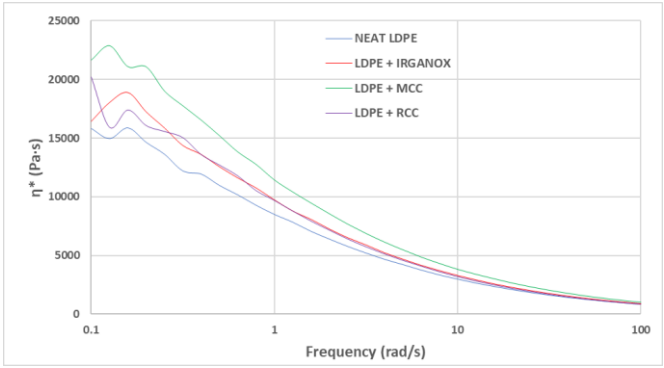

Figure 49: *Comparison of the complex viscosity of LDPE samples after seven days of ageing*

Table 49 reports the values of complex viscosity of seven-days-aged LDPE samples, for a frequency of $1\ rad/s$.

Table 49: *Values of η^* of LDPE samples for $\omega = 1\ rad/s$*

Sample	Neat LDPE	LDPE + *Irganox*	LDPE + MCC	LDPE + RCC
Viscosity (Pa·s)	8.500×10^3	9.715×10^3	1.144×10^4	9.698×10^3

In order to assess the trend in viscosity, and thus the prevailing degradation mechanism, Figure 50 displays the comparison of complex viscosity of the samples for different thermal ageing.

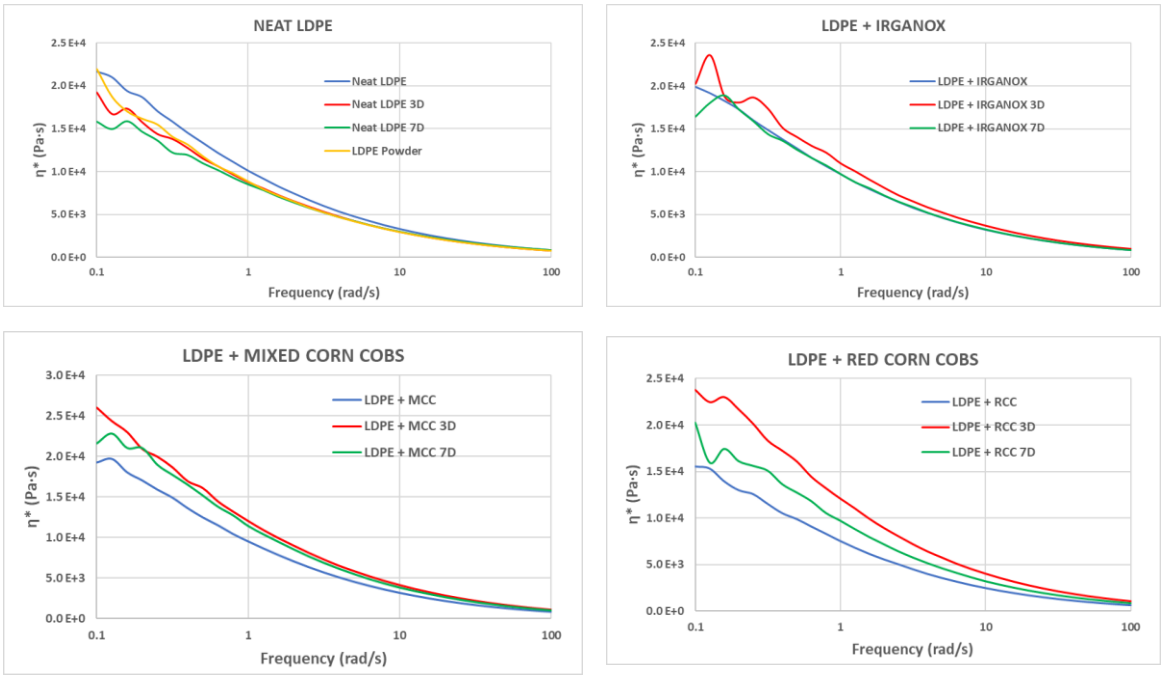

Figure 50: *Comparison of η^* of LDPE samples for different ageing time*

The graphs in Figure 50 show different behaviours for the different samples: the neat polymer displays a chain recombination consequent to extrusion, then degrades mainly by a chain scission mechanism, with the viscosity decreasing as the ageing time increases. For the other samples, however, a first recombination mechanism is followed by the chain scission, which is found to be the predominant degradation process for longer times.

This behaviour is confirmed by plotting the *col-col* graphs (Figure 51) which relate η' with η''. From these graphs, η_0 is calculated by selecting three points in the curve and building the circumference which crosses those points. Then, from the equation of the curve, it is possible to estimate the value of η_0 for $\eta'' = 0$.

Figure 51 displays the graphs of the different samples, while Table 50 reports the values of η_0.

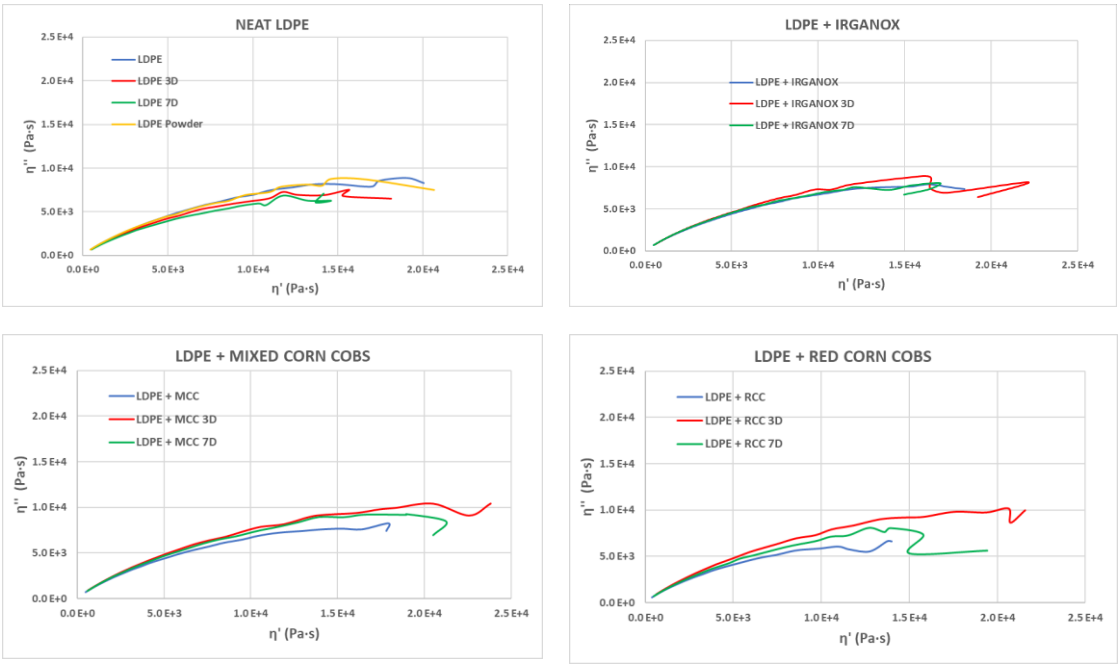

Figure 51: *Comparison of η' and η'' of LDPE samples*

Table 50: *Values of η_0 of LDPE samples*

SAMPLE	η_0 (Pa·s)
LDPE Powder	32061
LDPE	32921
LDPE 3D	29355
LDPE 7D	26948

SAMPLE	η_0 (Pa·s)
LDPE+IRG	33017
LDPE+IRG 3D	33967
LDPE+IRG 7D	30603

SAMPLE	η_0 (Pa·s)
LDPE+MCC	31334
LDPE+MCC 3D	34758
LDPE+MCC 7D	34206

SAMPLE	η_0 (Pa·s)
LDPE+RCC	27215
LDPE+RCC 3D	37658
LDPE+RCC 7D	32912

As displayed in the charts, and confirmed by the values in Table 50, the different samples show different behaviours:

- neat LDPE shows a decreasing slope in the curve of increasingly degraded samples, as well as lower values of η_0. This could be explained by a chain scission degradation mechanism of the polymer;
- LDPE with *Irganox* shows a first constant slope in the curve and a second decrease, which demonstrates a delay in the degradation process;
- LDPE with mixed corn cobs shows, differently from other samples, an increase in the slope of the curves and in the values of η_0 for more degraded samples. This may be explained by a partial recombination of polymer chains, induced by the presence of the additive, which increases its viscosity;

- LDPE with red corn cobs has a behaviour similar to the previous sample, with the main difference that a first increase in the curve is followed by a degradation, which still gives a final value higher than the initial one. This demonstrates a prevalence in recombination for short-term ageing and in chain scission for long-term ageing.

To better compare all the samples, a normalisation of the viscosity was evaluated. It is obtained by dividing the value of η_0 at each time reference by the η_0 at $t = 0$. Results are reported in Figure 52.

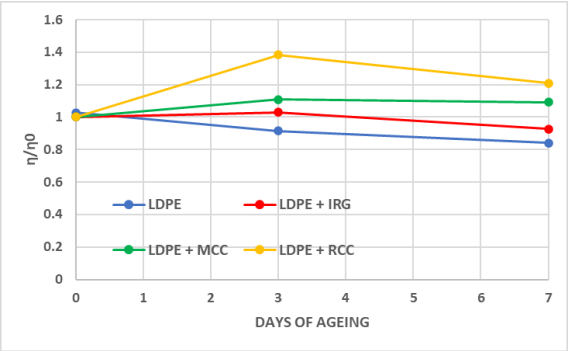

Figure 52: *Values of normalised viscosity for LDPE samples*

As displayed in the graph, the samples with mixed corn cobs and *Irganox* show a trend able to keep the value of normalised viscosity close to one, which demonstrates a very low degradation. This behaviour is confirmed by analysing the results from DSC in Paragraph 3.4, which assess these two additives as those with the highest stabilising capacity.

3.4.4. Photo ageing

As illustrated in Paragraph 2.3.6.2, films were prepared from polymeric samples in order to be analysed after 24 and 48 hours of photo ageing, exploiting rheometric analyses.

Figure 53 displays the comparison of complex viscosities after 24 hours of ageing, while Table 51 reports the values of η^* for a frequency of 1 rad/s.

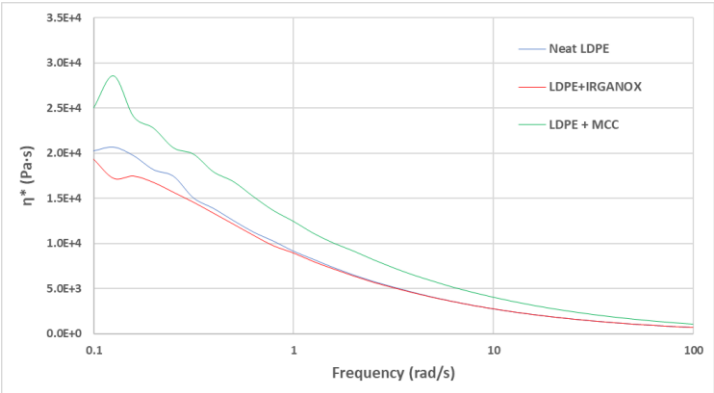

Figure 53: *Comparison of LDPE samples complex viscosity after 24 hours of ageing*

Table 51: *Values of* η^* *for* $\omega = 1\ rad/s$

Sample	Neat LDPE	LDPE + *Irganox*	LDPE + MCC
Viscosity (Pa·s)	9.175 x 10^3	8.970 x 10^3	1.244x10^4

The same comparisons are reported in Figure 54 and Table 52, concerning a photo ageing of 48 hours.

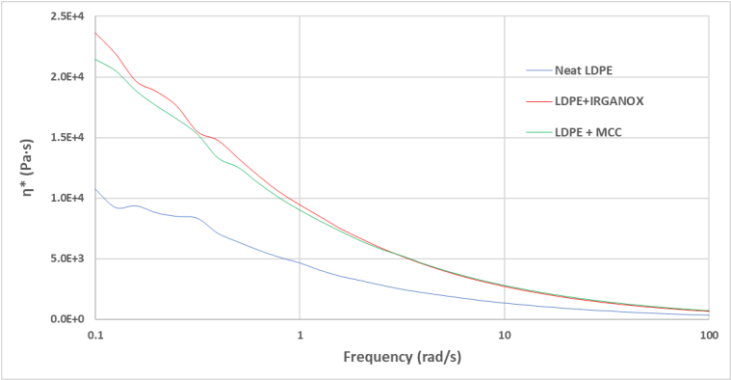

Figure 54: *Comparison of LDPE samples complex viscosity after 48 hours of ageing*

Table 52: *Values of* η^* *for* $\omega = 1\ rad/s$

Sample	Neat LDPE	LDPE + *Irganox*	LDPE + MCC
Viscosity (Pa·s)	4.655 x 10^3	9.454 x 10^3	9.027 x 10^3

To better understand the occurring degradation mechanism, Figure 55 reports the comparison of complex viscosities for different ageing times.

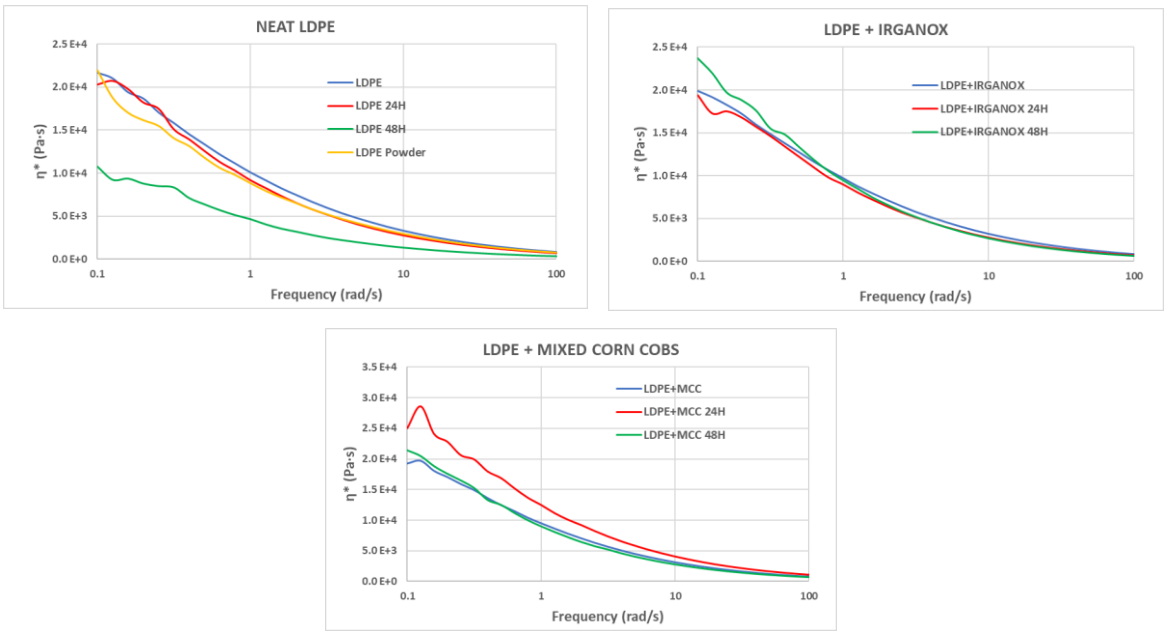

Figure 55: *Comparison of complex viscosities of photo aged LDPE samples*

As demonstrated in the graphs, the neat polymer undergoes the most important degradation, showing a noticeable decrease in viscosity, due to chain scission, after the first 24 hours of ageing. On the other hand, the sample with added corn cobs shows a first recombination, seen with an increase in viscosity, and a subsequent chain scission mechanism, confirming the behaviour already seen for thermal ageing. The best results are obtained with added *Irganox*, which shows only a brief degradation of polymeric chains.

These behaviours are confirmed by building the *col-col* graphs and evaluating η_0 for each sample, as shown in Figure 56 and Table 53.

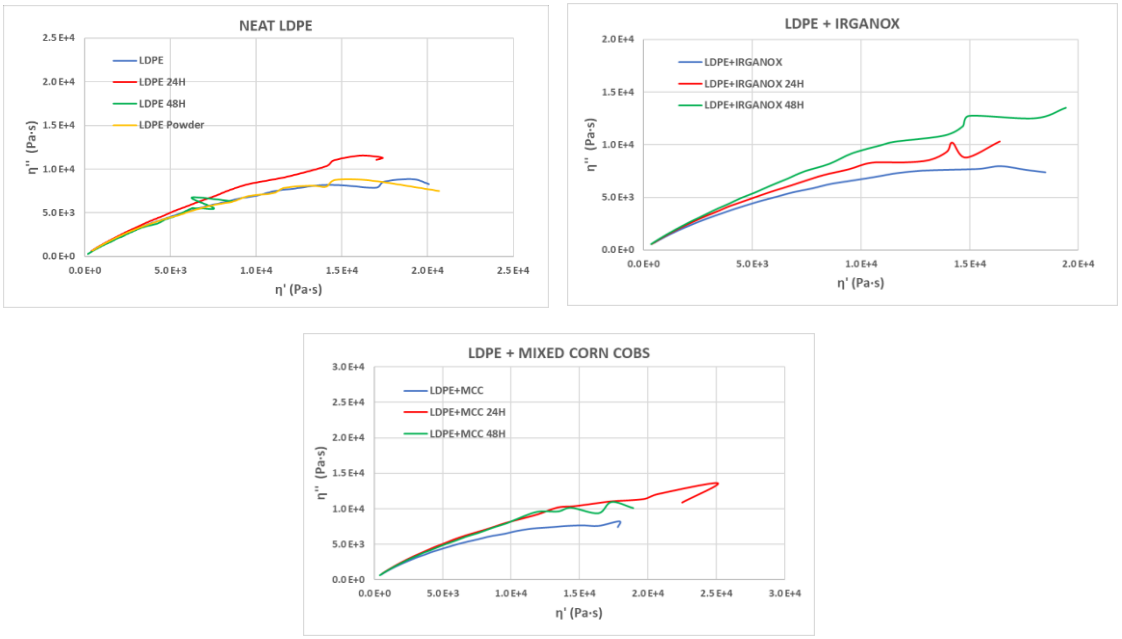

Figure 56: *Col-col graphs of LDPE samples*

Table 53: *Extrapolated values of η_0 for LDPE samples*

SAMPLE	η_0 (Pa·s)
LDPE Powder	39061
LDPE	38326
LDPE 24H	50968
LDPE 48H	41651

SAMPLE	η_0 (Pa·s)
LDPE+IRG	35051
LDPE+IRG 24H	46018
LDPE+IRG 48H	76438

SAMPLE	η_0 (Pa·s)
LDPE+MCC	34967
LDPE+MCC 24H	79308
LDPE+MCC 48H	70865

From the charts in Figure 56 it is possible to better estimate the degradation mechanism in *Irganox* samples, which demonstrate a successive increase in the slope of the curve as well as in η_0 value, assessing the prevalence of a recombination mechanism.

3.5. Material Characterisations – Poly (butylene succinate – co – adipate)

3.5.1. Measurement of Oxidative Induction Time (OIT)

Selecting experimental parameters as in Table 15, the four extrudates were analysed through DSC, to evaluate their oxidative induction time and the effect of the additives in the polymer.

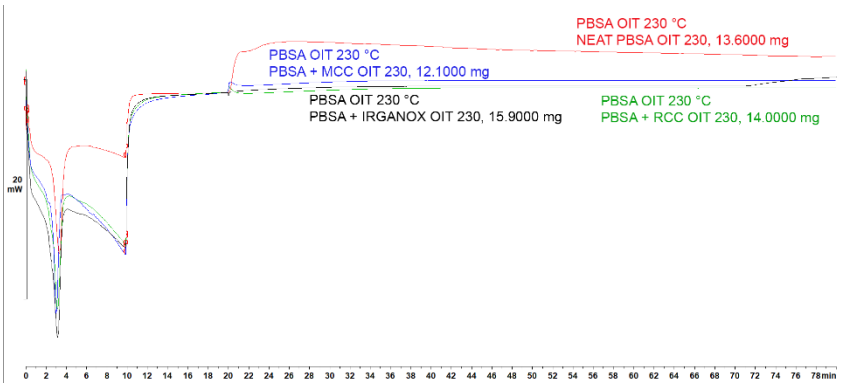

Figure 57: *DSC outcomes of PBSA extrudates*

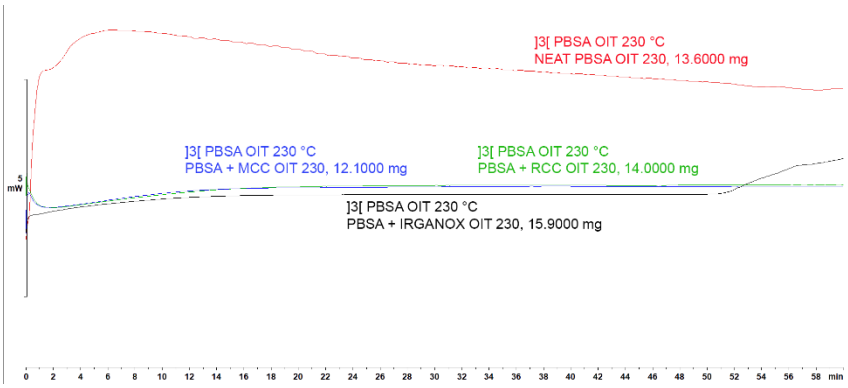

Figure 58: *Third step of DSC analysis of PBSA extrudates*

As shown in the graphs in Figures 57 and 58, the addition of corn cobs brings a substantial delay of the polymer degradation, demonstrating the same antioxidant property of *Irganox*.

3.5.2. Rheology measurements

PBSA samples show strong oscillations in all the measured parameters at low frequency, probably due to the low viscosity of the polymer, which may provoke this kind of instability. However, as frequency increases, all parameters stabilise.

Figure 59 shows the comparison of the complex viscosity amongst PBSA samples.

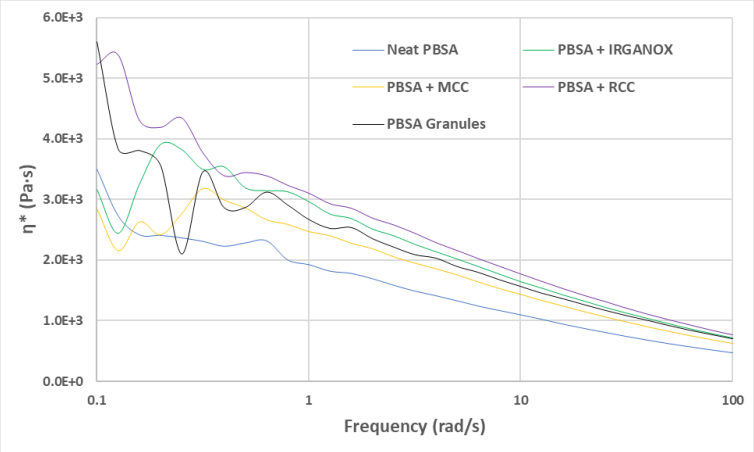

Figure 59: *Comparison of complex viscosity of PBSA analytes*

As displayed in Figure 59, despite the initial oscillations in the value, a pattern can be seen in the complex viscosity of PBSA samples. Considering the viscosity for a frequency of $1\ rad/s$, which values are reported in Table 54, the extrusion process brings a decrease in the value. Then, the samples of neat polymer are those with the lowest values, increased upon the insertion of the additives.

Table 54: *Values of complex viscosity of PBSA samples at* $\omega = 1\ rad/s$

Samples	PBSA Granules	Neat PBSA	PBSA + Irganox	PBSA + MCC	PBSA+RCC
Viscosity (Pa·s)	2.67×10^3	1.93×10^3	2.96×10^3	2.47×10^3	3.10×10^3

3.5.3. Thermal ageing

Rheological analyses were performed also on PBSA samples after three and seven days of ageing in the oven. Figure 60 reports the comparison of complex viscosity for PBSA samples after three days of ageing, while Table 55 shows the values of η^* for a frequency of 1 rad/s.

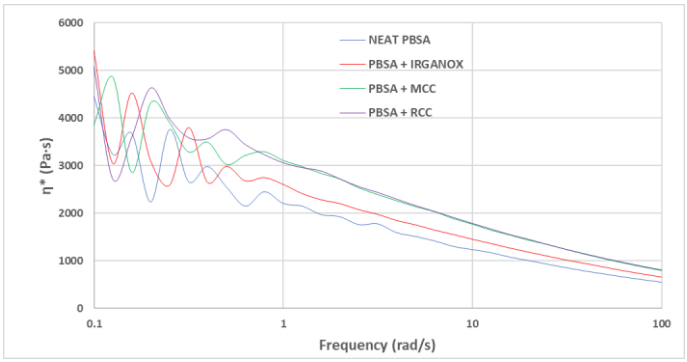

Figure 60: *Comparison of complex viscosity of PBSA samples after three days of ageing*

Table 55: *Values of η^* for $\omega = 1\ rad/s$*

Sample	Neat PBSA	PBSA + Irganox	PBSA + MCC	PBSA + RCC
Viscosity (Pa·s)	2.203 x 10^3	2.609 x 10^3	3.113 x 10^3	3.058 x 10^3

Concerning the viscosity comparison, the sample demonstrating the lower viscosity is still found to be the neat polymer, with values increasing upon additives addition.

Figure 61 displays the comparison after seven days of ageing, while Table 56 reports the values for a frequency of 1 rad/s.

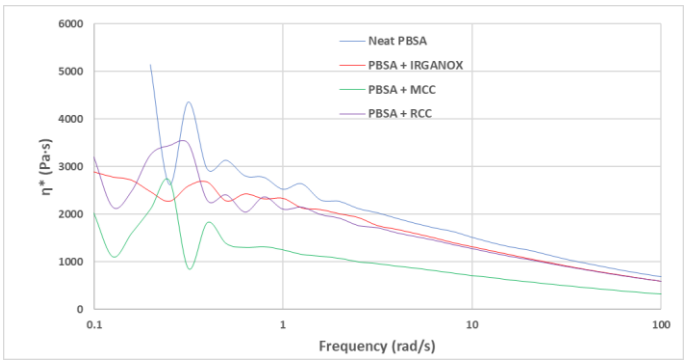

Figure 61: *Comparison of complex viscosity of PBSA samples after seven days of ageing*

Table 56: *Values of η^* for $\omega = 1\ rad/s$*

Sample	Neat PBSA	PBSA + Irganox	PBSA + MCC	PBSA + RCC
Viscosity (Pa·s)	2.527 x 10^3	2.339 x 10^3	1.156 x 10^3	2.102 x 10^3

Comparing the values of viscosity between three-days-aged and seven-days-aged samples, the difference for the mixed corn cobs stands out the most: an important decrease is shown, demonstrating a strong degradation by chain scission mechanism. Also the sample with red cobs decreases in viscosity, but in a lower manner.

A better total overlook is given by Figure 62, which reports the comparison in complex viscosity for different ageing times.

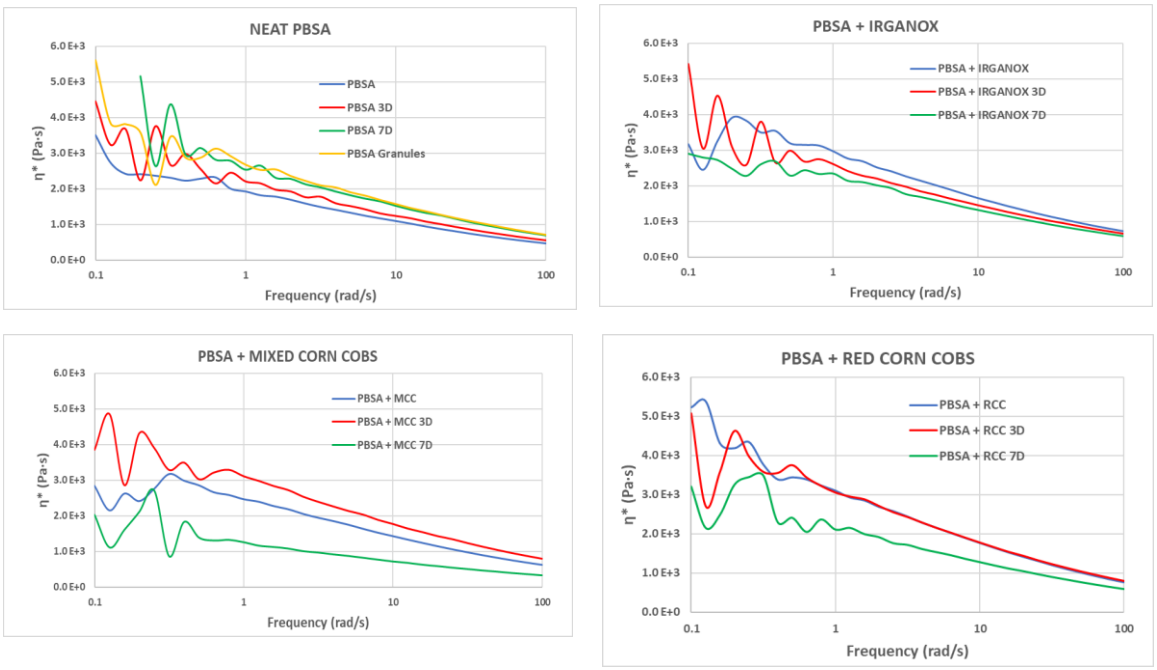

Figure 62: *Comparison of complex viscosities of thermally aged PBSA samples*

As displayed in the charts, different samples have different behaviours:

- neat PBSA demonstrates a first chain scission process due to the extrusion procedure, then it shows continuous degradation by chain recombination, which gives an increase in viscosity both after three and seven days of ageing;
- PBSA with added *Irganox* is characterised by a chain scission mechanism, which progressively decreases the value of complex viscosity;
- PBSA with added mixed corn cobs is found to be the most degraded sample, showing a first recombination after three days and a noticeable decrease in viscosity after one week, given by a relevant chain scission degradation;
- PBSA with red corn cobs has a behaviour similar to the sample with mixed cobs, characterised by a first stabilisation of the viscosity and a subsequent important decrease of η^*.

A confirmation of these behaviours is brought out in Figure 63, with the graphics displaying the relation between η' and η'' as the ageing of the sample increases. Extrapolated values of η_0 are then reported in Table 57.

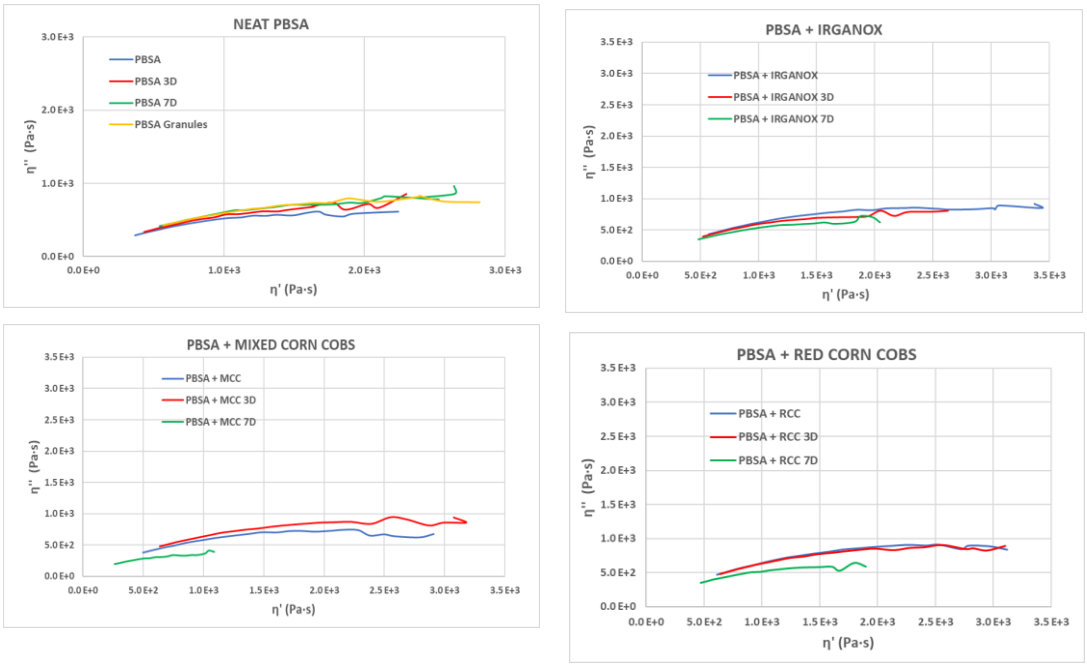

Figure 63: *Col-col graphs of PBSA samples*

Table 57: *Extrapolated η_0 values of PBSA samples*

SAMPLE	η_0 (Pa·s)
PBSA Granules	3299
PBSA	2859
PBSA 3D	2911
PBSA 7D	3203.64

SAMPLE	η_0 (Pa·s)
PBSA+IRG	4647
PBSA+IRG 3D	4013
PBSA+IRG 7D	3581

SAMPLE	η_0 (Pa·s)
PBSA+MCC	4163
PBSA+MCC 3D	4429
PBSA+MCC 7D	1721

SAMPLE	η_0 (Pa·s)
PBSA+RCC	4986
PBSA+RCC 3D	4334
PBSA+RCC 7D	3835

The normalised viscosity of PBSA samples was evaluated, and its trend is displayed in Figure 64.

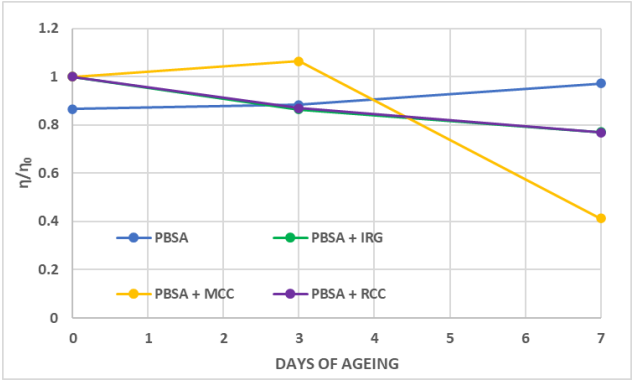

Figure 64: *Values of normalised viscosity of PBSA samples*

The graph in Figure 64 shows a superimposed trend between the extrudates with *Irganox* and red corn cobs, demonstrating an analogous behaviour to thermal degradation. The worst result is obtained with mixed cobs, which demonstrate an abrupt chain scission after seven days of ageing.

3.5.4. Photo ageing

PBSA films were subjected to photo ageing in the SEPAP equipment, as discussed in Paragraph 2.3.6.2, and subsequently analysed at the rheometer after 24 and 48 hours of degradation.

Figure 65 reports the comparison of complex viscosity among different samples after 24 hours in the equipment, while Table 58 displays the values of η^* for a frequency of 1 rad/s.

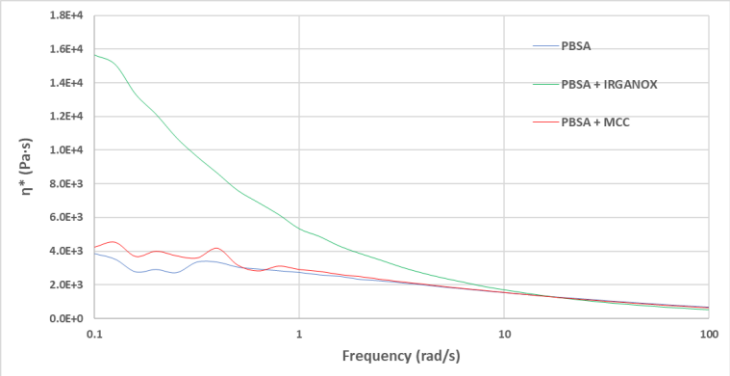

Figure 65: *Comparison of complex viscosity of PBSA samples after 24 hours of ageing*

Table 58: *Values of* η^* *for* $\omega = 1\ rad/s$

Sample	Neat PBSA	PBSA + Irganox	PBSA + MCC
Viscosity (Pa·s)	2.739×10^3	5.331×10^3	2.920×10^3

The chart in Figure 65 displays an interesting behaviour of the *Irganox*-added sample, which has a sudden increase in viscosity, much higher with respect to the other samples. This could be given by a reticulation of the chain, confirmed by the comparison of $\tan\delta$ in Figure 66, which is almost constant and equal to 1.

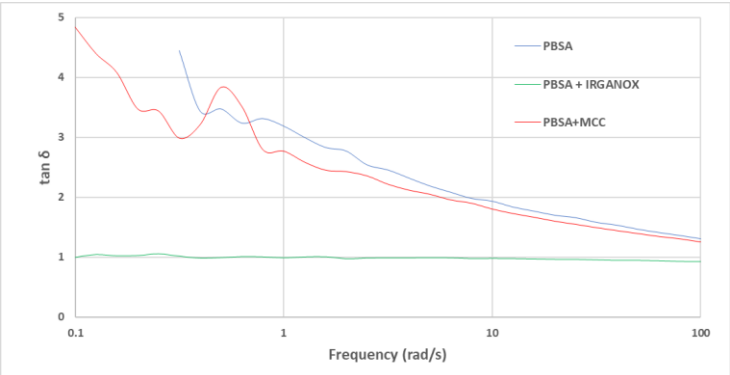

Figure 66: *Comparison of* $\tan\delta$ *of PBSA samples after 24 hours of ageing*

Figure 67 reports the comparison of the complex viscosity among PBSA samples after 48 hours of photo ageing, while Table 59 displays the values of η^* for a frequency of 1 rad/s.

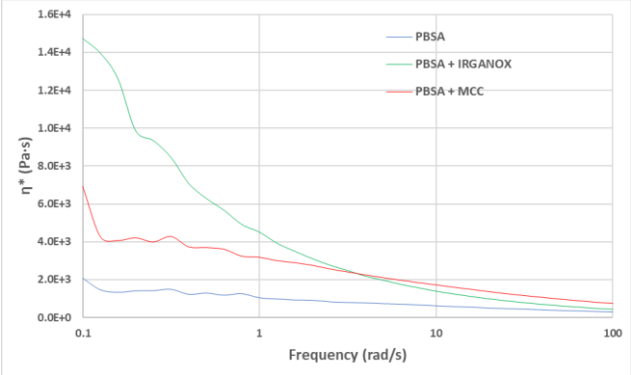

Figure 67: *Comparison of complex viscosity of PBSA samples after 48 hours of ageing*

Table 59: *Values of η^* for $\omega = 1\ rad/s$*

Sample	Neat PBSA	PBSA + Irganox	PBSA + MCC
Viscosity (Pa·s)	1.052 x 10^3	4.517 x 10^3	3.172 x 10^3

Also for two days of photo ageing, the trend of the different samples is respected: the analyte with *Irganox* shows again high values of viscosities, related to reticulation of polymeric chains, while the neat PBSA sample demonstrates a chain scission degradation mechanism, with the viscosity decreasing for longer ageing times.

Figure 68 correlates the complex viscosities of PBSA films for different ageing times.

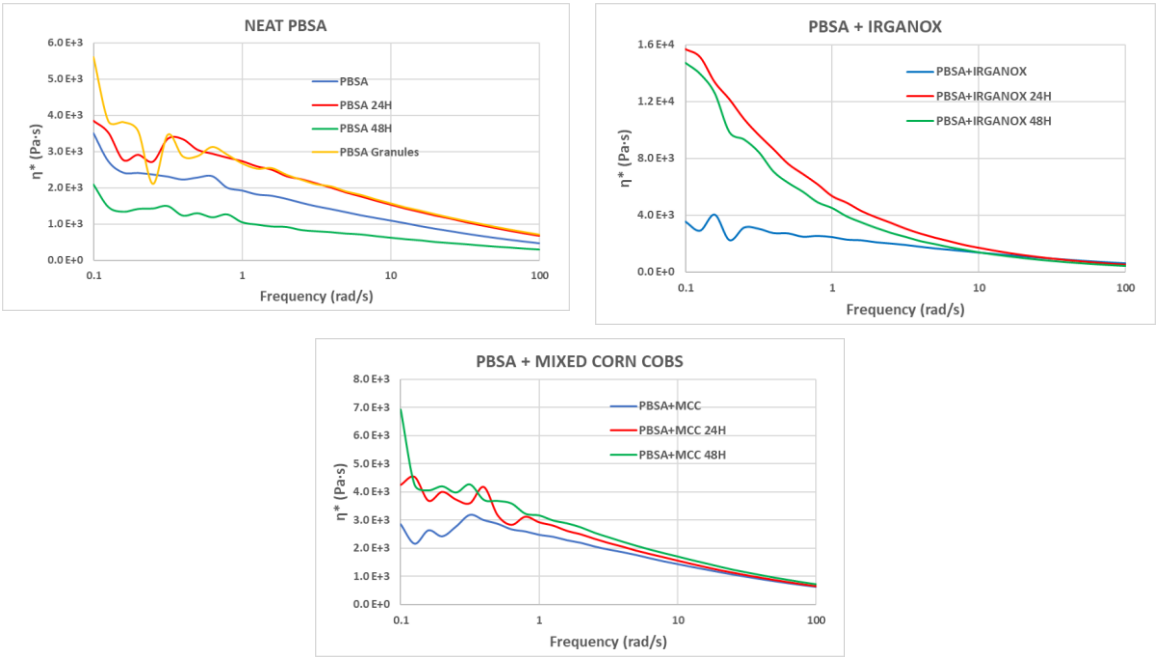

Figure 68: *Comparison of complex viscosities of photo aged PBSA samples*

The charts in Figure 68 assess different behaviours for different PBSA samples:

- neat PBSA is subjected to a prevailing recombination mechanism for short-term ageing and to chain scission for long-term degradation;
- PBSA with added *Irganox* shows high reticulation even for short periods of photo ageing, with a sudden and relevant increase in viscosity;
- PBSA with added mixed corn cobs is found to be the sample with lower degradation, still being characterised by a recombination mechanism for both three and seven days of ageing.

These trends are confirmed by the *col-col* graphs reported in Figure 69, as well as by the extrapolated values of η_0 reported in Table 60.

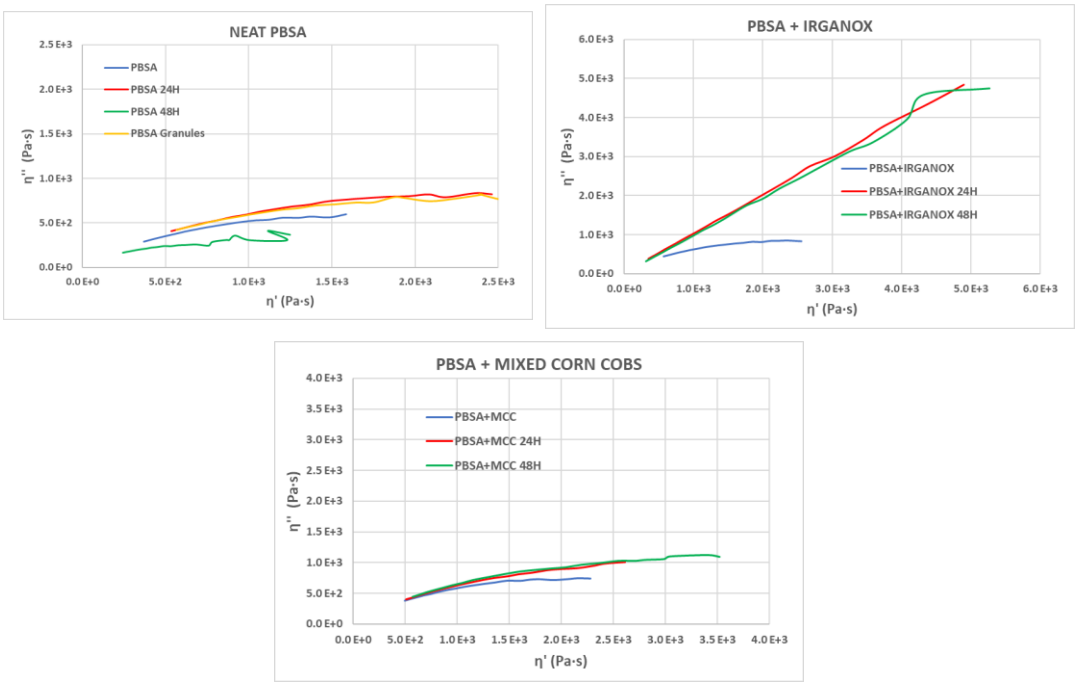

Figure 69: *Col-col graphs of photo aged PBSA samples*

Table 60: *Extrapolated η_0 values of PBSA samples*

SAMPLE	η_0 (Pa·s)
PBSA Granules	4299
PBSA	3144
PBSA 24H	4833
PBSA 48H	1220

SAMPLE	η_0 (Pa·s)
PBSA+IRG	4223
PBSA+IRG 24H	123855
PBSA+IRG 48H	123199

SAMPLE	η_0 (Pa·s)
PBSA+MCC	4237
PBSA+MCC 24H	4722
PBSA+MCC 48H	4952

Figure 70 reports the values of normalised viscosity, to finally estimate the sample which has undergone the lesser degradation. Values for PBSA with *Irganox* are out of scale, to better visualise the differences between the neat polymer and the sample with mixed corn cobs.

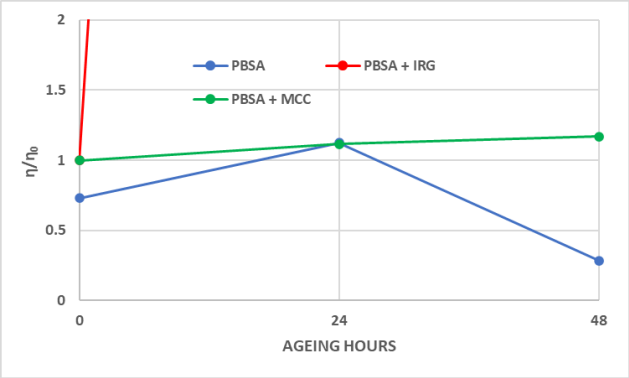

Figure 70: *Values of normalised viscosity of PBSA samples*

As already demonstrated by the values of complex viscosity and by *col-col* charts, the values of normalised viscosity prove that the sample which undergoes the lesser degradation is the extrudate with added mixed corn cobs, confirming the behaviour obtained from OIT measurements of Paragraph 3.5.1 (Figures 57 and 58).

4. Conclusions

The project of this dissertation has been conceived from the knowledge that, nowadays, almost 30% of corn by-products are discarded, making up immense amounts of unexploited material. So, a question on how to take advantage of this natural matrix rose consequently.

The first step involved a deep analysis of the vast bibliography present on the reutilisation and recycling of corn by-products, which was oriented in three main directions: the exploiting of their antimicrobial and antioxidant activities, the extraction of amorphous silica, and the production of bio-composites. The first field of study demonstrated to be the most promising, so the focus of the project was moved on the evaluation of the antioxidant content of corn by-products and on their subsequent incorporation in polymeric matrices.

The analyses could be commenced thanks to the fundamental support of *Limagrain* company, who provided the three varieties of corn by-products to work on: yellow corn cobs, red corn cobs and corn leaves.

The first issue to be overcome was the finding of the best extraction conditions, able to maximise the content of antioxidants. So, the corn by-products were subjected to a wide range of extraction techniques, comprising traditional and advanced methods as well as different categories of solvents. In particular, the natural matrices underwent a soaking procedure, at room temperature, and a Soxhlet process, both described as traditional methods, but also microwave-assisted (for polar solvents) and ultrasonic-assisted (for nonpolar solvents) extractions.

In order to pursue an analysis as thorough as possible, both polar and nonpolar solvents were taken into account. More specifically, ethanol, methanol and limonene were utilised.

After performing the extractions, the content of antioxidants and phenolic compounds had to be measured: all samples were subjected to the Folin-Ciocalteu test, to evaluate the content of phenolic compounds, and to the DPPH assay, to assess their antioxidant capacity.

Results of these analyses confirmed how advanced extraction techniques provide a higher yield with respect to traditional ones, but also gave good insights about the most efficient solvent, which was found to be methanol. In fact, samples extracted with the aid of this hydrocarbon resulted in the highest antioxidant activity, as well as the highest yield in the recovery of solid matrix from the extract ($\sim 5\%$). An interesting trend was shown by the analyses of the mixed corn cobs, formed by equal weights of red and yellow cobs, which demonstrated a synergy regardless to the chosen extraction technique and solvent.

Having stated the best extraction conditions (methanol, through microwave-assisted technique), the focus of the project could be shifted on the incorporation of the natural compounds into the polymeric matrices. The choice fell on a petrol-based polyolefin, low-density polyethylene, and a possibly bio-based polyester, poly (butylene succinate – co – adipate), to estimate the antioxidant and anti-degrading properties of corn by-products on different families of macromolecules.

From the previous steps of the experiments, the extracts which gave the optimal results were red and mixed cobs, so they were taken into account for the implementation as well. The chosen by-products were extracted through the selected conditions and subsequently extruded with the selected polymers. Four types of extrudates were realised: neat polymer, polymer with red cobs, polymer with mixed cobs, and polymer with *Irganox*, a synthetic antioxidant selected to compare the performance of natural additives. Then, the extrudates were subjected to DSC analyses, to evaluate their oxidative induction time, and rheological analyses after thermal ageing and photo ageing.

Starting with LDPE, the thermal analysis of the polyolefin shows an increasing oxidative induction time from the neat polymer, to the sample with red cobs, to that with mixed cobs and finally to the *Irganox*-added extrudate. This demonstrates how the natural additives are able to delay the thermal degradation of the polymer, even if in lower amount with respect to the synthetic one. These results are confirmed from the rheological analyses after the thermal and photo ageing: the samples with *Irganox* demonstrate the lowest amount of degradation, mostly by chain scission, while the extrudate with mixed cobs shows only slightly worse outcomes, displaying a first chain recombination mechanism and a subsequent chain scission process.

Turning to PBSA, the conducted thermal analyses show that neither extrudates with natural additives, nor those with *Irganox* present on oxidative induction time, demonstrating a noticeable performance of corn cobs. However, rheological analyses provide different results: after being subjected to seven days of thermal ageing, the sample with mixed corn cobs shows an abrupt degradation by chain scission, while the extrudates with red cobs and *Irganox* have similar behaviours, displaying only a brief chain scission. The outcomes of photo ageing are once again different: the sample with *Irganox* is characterised by a relevant reticulation, demonstrating a high effectiveness only in preventing thermal degradation, while the sample with mixed cobs shows the best results, with only a slight chain scission over the ageing period.

So, to finally draw a conclusion, this project has indubitably demonstrated that the implementation of corn by-products in polymeric matrices, whether they are petrol- or bio-based, is able to delay, or even prevent, the degradation and the oxidation of the macromolecules.
To better understand the long-term behaviour of these natural additives further analyses are needed, employing longer ageing periods, but these outcomes have surely opened the paths to a more valuable exploitation of corn by-products.

ACKNOWLEDGEMENTS

Another important chapter of my life and my academic career comes to an end. It has indubitably been long and difficult, especially through this last year, but also full of personal enrichment and satisfactions, capped off by an incredibly fortifying and gratifying Erasmus period. There, at SIGMA University of Clermont-Ferrand, I have found many kind-hearted people, who would help me whatever I happened to need, and have sailed with me through the execution of the research project. So, a first and huge thanks goes to Professor Haroutioun Askanian, my tutor and supervisor, who introduced me to the laboratory work and made the collaboration with Limagrain company possible. With him, I would like to express gratitude to all the staff at SIGMA, from the doctoral students to the laboratory team, who immensely helped me in performing the analyses and pursuing the results, as well as Mr. Tarik Ourjdal, the representative from Limagrain company, who provided the matrices and the knowledge necessary to fulfil the project.

Switching back to Italy, I will first and foremost acknowledge the support of Professors Annamaria Celli and Laura Sisti, who made this extraordinary experience possible and followed me through the preparation of the thesis, with relevant and indispensable advice, as well as inspiring insights to work on.

Last, but surely not less important, an immense credit is due to my family, my friends and my girlfriend, who supported me in every choice I have made during this period, and who made me feel home albeit being miles and miles apart. Without any of you, nothing of this could even be conceived.

Thank you!